Department of Chemistry

Causes of Growth Rate Inhibition in Lactose

Kristy Michelle Blyth

This thesis is presented for the Degree of
Doctor of Philosophy
of
Curtin University

July 2013

Declaration

To the best of my knowledge and belief this thesis contains no material previously published by any other person except where due acknowledgment has been made.

This thesis contains no material which has been accepted for the award of any other degree or diploma in any university.

Signature: …….

Date: ……...

Acknowledgements

There are so many people to thank for their invaluable assistance and patience in guiding me through this doctoral journey.

Firstly, I would like to thank my principal supervisor, Professor Mark Ogden. I greatly appreciate the guidance, assistance, patience and flexibility that Mark has afforded me. The journey to this final destination has not been without complexity and drama, it is for his belief in me to getting here, that I am truly grateful and thankful.

I must thank Dr Tuna Dincer for all of her generous assistance in the lab and guidance in the ways of microscopy. Also to Dr Amal Friej for her companionship and friendship throughout this undertaking.

I would also like to thank, Professor Gordon Parkinson for his early assistance and guidance in undertaking this research project.

Many thanks to Professor Mark Buntine, for affording me much grace in the Department of Chemistry which has enabled the completion of this work. I must also thank Geoff Chidlow, for his unwavering support and patience.

Finally, I would like to thank my husband David and my children; Hannah, Mitchell and Tyson. It has been a long process and I thank you for your patience and understanding throughout this journey.

Abstract

Lactose is a component of mammalian milk that is most commonly recovered as a by-product of dairy processing in the form α-lactose monohydrate. Application of lactose in the pharmaceutical and food industries has an important value-add for the dairy industry of Australia. The crystallization of α-lactose monohydrate is one of the most challenging aspects of any such recovery process, and is the focus of this thesis.

It has been identified in the literature that a potent inhibitor is typically present in α-lactose monohydrate, which dramatically impairs the crystal growth rate. This inhibitor has previously been identified as a mixture of α-lactose monophosphates. A range of methods were examined here to remove the contaminant so as to resolve the true growth rate of α-lactose monohydrate. Literature methods were examined along with the novel use of zirconium phosphonate modified surfaces, which proved a successful means of removing the mixture of α-lactose monophosphates.

Purified lactose exhibited growth rates well above those found for typical pharmaceutical grade lactose, as was expected. An exception to this trend was found at low pH, where the growth rate of the purified lactose was found to drop dramatically. It is proposed that this is due to a change in morphology, where the fastest growing face grows out of the crystal, leading to a reduced growth rate. This has not been reported previously, perhaps because of the difficulty in obtaining samples of highly purified lactose.

Studies were undertaken to resolve the impacts that dairy process-relevant additives have on the crystal growth of α-lactose, in the pure and impure systems. In the absence of inherent impurities, structurally similar additives such as glucose 6-phosphate and lactose 1-phosphate cause a marked reduction in the growth rate. In contrast, the impact is negligible in the impure system, which contains the inherent lactose phosphates. Inorganic salts were found to have a much smaller influence, even in the purified system. Interestingly, the addition of sodium phosphate has a significant impact on the crystal morphology, inducing the formation of a much wider tomahawk shape, under all of the conditions studied. It appears to be the ion pair, not the individual components, that is generating this change. This observation may provide a starting point to explain some of the many inconsistencies in the literature.

Table of Contents

List of Figures

List of Tables

List of Abbreviations

AAS	- Atomic Absorption Spectroscopy
AFM	- Atomic Force Microscopy
APTES	- 3-aminopropyl-triethyloxysilane
CE	- Capillary Electrophoresis
CGE	- Capillary Gel Electrophoresis
CHS	- Common History Seed
CIEF	- Capillary Isoelectric Focussing
CITP	- Capillary Isotachophoresis
CSD	- Crystal Size Distribution
CSIRO	- Commonwealth Scientific and Industrial Research Organisation
CZE	- Capillary Zone Electrophoresis
DIPEA	- diisopropylethylamine
dl	- detection limit
EOF	- Electroosmotic flow
GC	- Gas Chromatography
GR	- Growth Rate
GRD	- Growth Rate Dispersion
HPLC	- High Performance Liquid Chromatography
HySS	- Hyperquad Simulation and Speciation
ICP-OES	- Inductively Coupled Plasma – Optical Emission Spectroscopy
IEC	- Ion Exclusion Chromatography
IEL	- Ion Exclusion Lactose
MDL	- Method Detection Limit
MEKC	- Micellar Electrokinetic Capillary Chromatography
MQ	- MilliQ

NIL	- Non-ionic lactose
NF	- Nano-filtration
ppm	- parts per million
RO	- Reverse Osmosis
RSD	- Relative Standard Deviation
SE	- Standard Error
SUP	- Sigma-Aldrich, SigmaUltra α-lactose monohydrate
ss	- supersaturation
UF	- Ultra-filtration
u/s	- ultra-sound
UV	- Ultra Violet
UWS	- University of Western Sydney

1 Introduction

Lactose is a disaccharide, which occurs naturally in mammalian milk and is commonly referred to as 'milk sugar'. It is formed in the mammary gland and is synthesised by the combination of glucose and galactose. The concentration of lactose in milk varies between species. The highest concentration is found in humans and primates (approximately 7 %). The majority of commercially refined lactose is from bovine milk, which has an approximate lactose content of 4.8 % (Harper, 1992).

In Australia, lactose is crystallised from whey and permeate. Whey and permeate are the by-products of cheese manufacture. Whey is a dilute solution containing lactose, protein, minerals and traces of fat. The lactose concentration can be a high as 70% (Zall, 1992). Whey has traditionally been considered a waste product, however, with increasing environmental awareness and economic constraints its use as a co-product of dairy product manufacture has prevailed (Zadow, 2000).

Whey utilization has developed and it is now used in many consumable products; protein concentrates, whey powders, whey concentrates, etc. (Zadow, 2005). Lactose also has significant importance in both food and pharmaceutical industries. Lactose is used as an additive in a large variety of food products. It is a major component of infant formula, and it is used in food products to reduce sweetness and alter other properties so as to make food products more palatable and visually appealing. Refined lactose is used as a carrier for active pharmaceutical excipients, because of its useful flow and tableting properties. Exploiting its physical properties allows for uniform drug delivery (Nickerson, 1974).

Lactose is extracted from whey via crystallization techniques. The water is removed from the whey and permeate by evaporation under vacuum. The remaining concentrate is then seeded using α-lactose monohydrate crystals, which induces nucleation and subsequent crystallization. When the desired crystal size is achieved, the lactose crystals are removed from the liquor,

washed and dried. To increase the purity of the α-lactose monohydrate product, subsequent recrystallization is undertaken until the desired purity is achieved (Zadow, 2000).

It is via the afore-mentioned production that we can acquire the most pure commercially available α-lactose monohydrate. While it is the most pure lactose that is readily available, it actually contains an important contaminant that has a significant impact upon lactose crystal growth. That inhibitor has been determined by Visser (1984) to be a mixture of lactose monophosphates (Breg et al, 1988).

A review of the literature shows that the impact of common whey impurities (and other materials) on the crystal growth of lactose is not well understood, with a significant number of discrepancies found between different reports. Given the strong inhibition of inherent impurities (particularly lactose phosphates), comparison between studies can be difficult. Any such work requires thorough understanding of the purification methods and analytical techniques used. The aim of this project is to systematically evaluate the impact of some important impurities on lactose crystal growth, in an effort to understand the origin of some of the existing discrepancies in the literature.

2 Literature Review

2.1 Properties of Lactose

Lactose is most commonly encountered as a white crystalline powder in the form alpha-lactose monohydrate. There are, however, a number of different forms of lactose that can be isolated, and the physical properties of these materials can vary dramatically. The chemical structure of lactose is also complicated by the fact that it is a reducing sugar, and can form two different anomers. This Chapter describes the important chemical and physical properties of the various forms of lactose.

Industrially, lactose is recovered from whey. As an average, whey consists of 90 % water, 5 % lactose and 2 % protein. Historically, whey utilisation has been minimal and the focus has been on the protein fraction. The current trend is to look at the whey by-product as a whole and focus has been expanded to cover the lactose component.

Exploitation of the properties of lactose has made it a valuable resource in the food and pharmaceutical industries. Lactose is used as a base material for tablet-making and dry powder aerosols as it has a neutral taste and odour, low hygroscopicity, relatively low reactivity, and favourable flow properties. Lactose is extensively used in food manufacturing for the same reasons. Its applications cover infant formula, frozen desserts, beer, confectionary, baked goods, soft drinks and numerous others (Zadow, 1984).

2.1.1 Structural information

Chemically, lactose is a disaccharide comprising of a glucose unit joined to a galactose unit by a β-1,4-glycosidic linkage. The derived chemical name is 4-0-β-D-galactopyranosyl-D-glucopyranose and the structural formula is depicted in Figure 2-1. Upon dissolution in water, lactose exists in an equilibrium of two anomeric forms about carbon –1 on the glucose unit, alpha (α-) and beta (β-). This phenomenon is termed mutarotation.

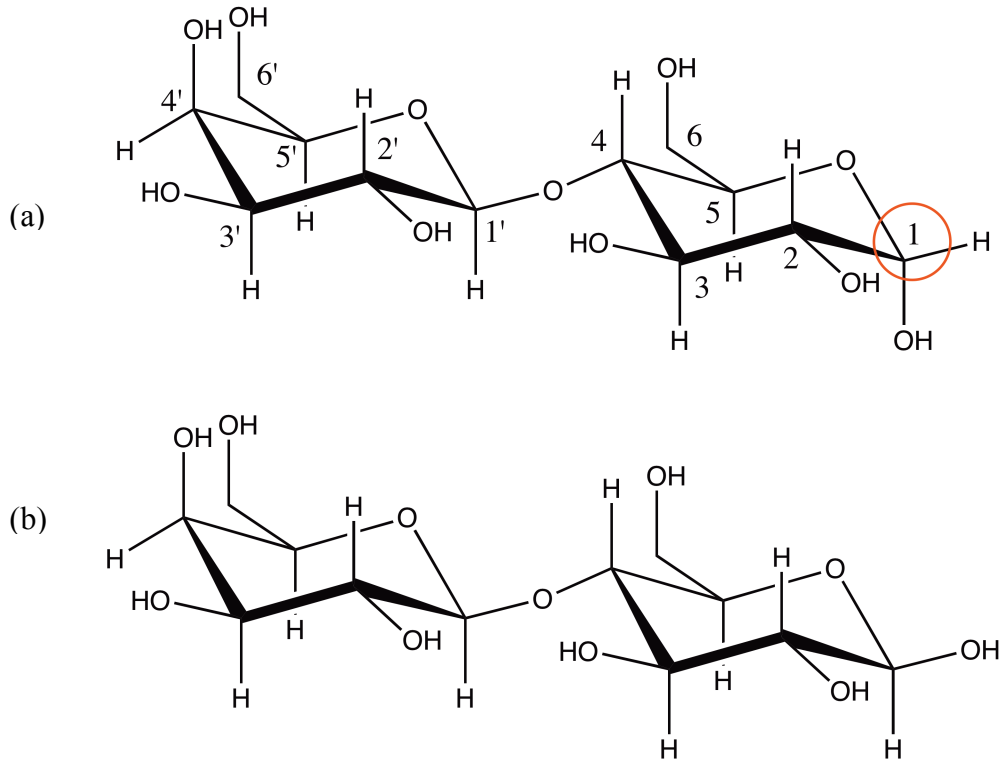

Figure 2-1 Structural formula of (a) α-lactose, with the anomeric C1 circled, and (b) β-lactose.

Mutarotation involves the opening and closing of the hemiacetal ring such that an amount of free aldehyde form will be present. As a consequence, reactions typical of aldehydes are possible and lactose is thus considered a reducing disaccharide (Walstra and Jennes, 1984).

Solubility

The two lactose anomers exhibit quite different properties to one another. α-Lactose is the more stable form (least soluble) below temperatures of 93.5 ˚C and thus determines the extent of solubility in aqueous solution. Above this temperature, β-lactose is the least soluble anomer. At equilibrium at 20 ˚C, the ratio of α to β in aqueous solution is 62.7% to 32.3% (Holsinger, 1997). The equilibrium involves two reactions as shown in Equation 2-1. The equilibrium ratio is determined as shown in Equation 2-2 and via experimentation the equilibrium ratio in dilute solutions is estimated using Equation 2-3 (Walstra

and Jennes, 1984). Temperature impacts directly on the equilibrium ratio and consequently the rate of mutarotation. The equilibrium ratio is also dependent upon lactose concentration. For higher concentrations (above 60% w/w) R is relatively independent of temperature. It takes considerable time to attain equilibrium, but is not the rate-limiting step in crystallization under typical dairy processing conditions (Walstra and Jennes, 1984).

α - lactose $\rightarrow$ β - lactose (reaction constant, k_1) Equation 2-1
β - lactose $\rightarrow$ α - lactose (reaction constant, k_2)

Equilibrium ratio, $R = k_1 / k_2$ Equation 2-2

$R = 1.64 - 0.0027T$ (˚C) Equation 2-3

The mutarotation rate is also affected by pH. The effect is minimal at pH 5.0 but significant at pH values less than 2 and greater than 9. The presence of salts in solution is also found to have an impact on the mutarotation, increasing the rate by a factor of two in the case of salts in milk compared to water (Holsinger, 1997).

At a given temperature the dissolution of lactose is dynamic as indicated by Equation 2-1. When a quantity of lactose is introduced to solution at temperatures less than 93.5 ˚C and dissolution commences, the lactose that dissolves undergoes mutarotation until equilibrium is reached between the α- and β- anomers. The solution is then unsaturated in α-lactose and more lactose can then dissolve, this continues until the final solubility is reached and the solution is saturated in α-lactose. β-Lactose is less soluble than α-lactose at temperatures above 93.5 ˚C and will preferentially crystallize.

The solubility of the α-lactose or β-lactose anomers is difficult to measure due to the immediate mutarotation upon dissolution. Several authors were able to minimize the impact of mutarotation by measuring the initial solubilities of α-lactose at low temperatures where the rate of mutarotation is decreased.

Authors Herrington (1934)) and Visser (1982) have measured the initial solubility of α-lactose at 0 ˚C to be 4.5 g α-lactose/100 g water.

2.1.2 Crystallization

2.1.2.1 Nucleation

The first step in the crystallisation process is nucleation. Nucleation is the formation of a solid crystalline phase from a supersaturated solution. There are two broad categories of nucleation mechanisms, primary and secondary.

Primary nucleation is the formation of nuclei in the absence of solute particles. This requires an energy barrier associated with the formation of a new nucleus to be overcome. Thermal or mechanical intervention can often introduce enough energy to promote nucleation. Primary nucleation can be either spontaneous, called homogenous nucleation, or induced by foreign (non-solute) particles, which is referred to as heterogeneous nucleation.

Homogeneous nucleation is rarely observed in supersaturated sugar solutions, as measurements are complicated by the difficulty of eliminating any nucleation site (Hartel and Shastry, 1991). It is generally accepted that heterogeneous nucleation is the most likely primary nucleation phenomenon in sugar solutions.

Secondary nucleation is the generation of nuclei in the presence of an existing crystalline surface. This can occur in a number of ways, but generally is caused by the physical disruption of a crystal surface. This can be occur mechanically as would happen in stirred or agitated crystallizers, or through defects, dislocations or inclusions in crystals (Mullin, 1997).

Figure 2-2 is a solubility-supersolubility diagram. Three regions define this (Mullin, 1997);

1. The stable region (not saturated), where crystallization cannot occur.

2. The metastable region (supersaturated), where spontaneous crystallization is unlikely, however if seeded α-lactose monohydrate crystals will grow.

   The boundaries are difficult to estimate and the intermediate region can be considered metastable or labile, as time and composition start to play a larger role in the likelihood of crystallization.

3. The labile or unstable region, where spontaneous crystallization is likely.

Solutions of lactose do not nucleate readily and can be easily supersaturated. In Figure 2-2 it is shown that at concentrations 2.1 times over the solubility limit spontaneous crystallization can result, possibly a consequence of homogeneous nucleation. At relative supersaturations less than 1.6 seeding is required to induce nucleation (Walstra and Jennes, 1984).

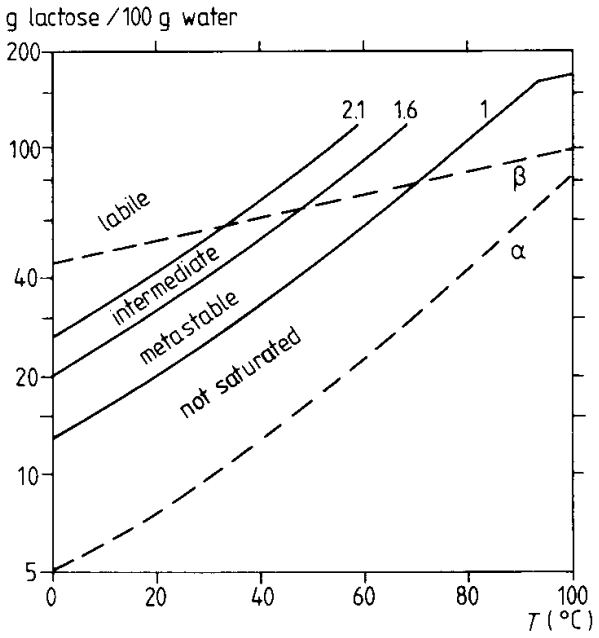

Figure 2-2 Solubility curves of lactose (Walstra and Jennes, 1984)

Nucleation rate is affected by supersaturation, temperature, rate of cooling, viscosity, energy input, pH and the presence of additives or impurities (Mullin, 1997 and Hartel and Shastry, 1991).

2.1.2.2 Crystal Growth

Once a stable nucleus has been formed in a supersaturated solution, it can grow into a detectable crystal. The growth rate of the crystal is the rate of displacement of a given face, perpendicular to that face. Different orientations have different growth rates determined by their ability to incorporate growth units, thereby determining the morphology of the crystal.

Sugar crystal growth is a combination of steps: molecular diffusion from the bulk solution to the crystal surface; mutarotation of the sugar molecules; removal of waters of hydration; counter-diffusion of water molecules; orientation of sugar molecule in the adsorption layer; diffusion of molecule to incorporation site; surface incorporation of growth unit; removal of heat generated by the phase change. Any of these steps can be the rate-limiting step of crystal growth (Hartel and Shastry, 1991 and Mullin, 1997).

As has already been discussed, lactose in solution is a mixture of the α- and β-lactose anomers. The impact of mutarotation is that neither α-lactose nor β-lactose can crystallize from a pure environment; the other anomer will always be present. α-Lactose crystallizes as α-lactose monohydrate. As α-lactose monohydrate crystallizes, some of the β-lactose will mutarotate to form α-lactose and crystallization will continue. The yield is considered to be a result of two equilibria; the conversion of β-lactose to α-lactose and the conversion of solubilised α-lactose to solid α-lactose monohydrate. Either of these can be the rate-limiting step and is directly affected by the solution and crystallizing conditions (Zadow, 1984).

The driving force of α-lactose monohydrate crystallization is the concentration of α-lactose, although the depression of solubility caused by β-lactose is also taken into consideration when determining the supersaturation ratio of α-lactose (s) (Visser, 1982), and is shown in Equation 2-4:

$$s = C / C_s - FK_M(C-C_s) \qquad \text{Equation 2-4}$$

C: total lactose concentration, g anhydrous lactose/100 g water

C_s: final solubility of lactose, g anhydrous lactose/100 g water

F: A temperature dependent factor for the depression of solubility of α-lactose by β-lactose

K_M: β/α lactose ratio at mutarotation equilibrium at the prescribed temperature

The impact of other factors on the solubility of α-lactose will be covered later.

Lactose can crystallize in four different polymorphs, each with its own unique structure and associated properties. The different polymorphs are α-hydrate, β-anhydrous, α-stable and α-unstable. The relationship between these forms is shown in Figure 2-3.

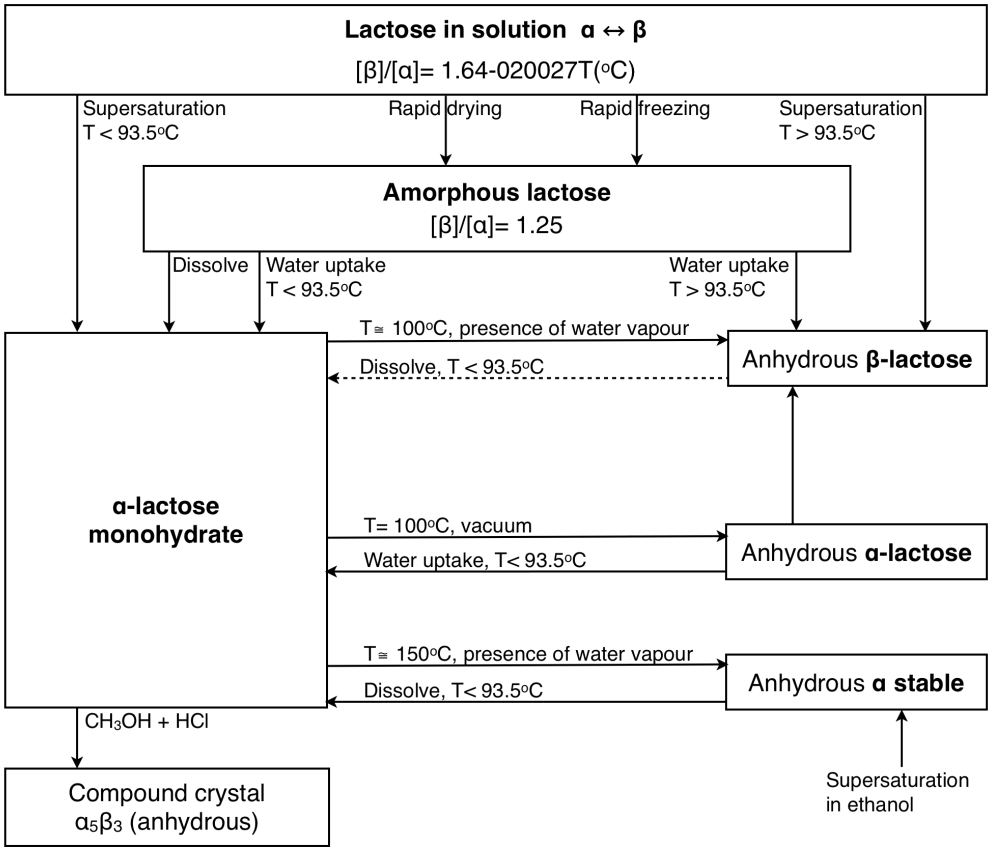

Figure 2-3 Relationships between the different crystal polymorphs of lactose (Walstra and Jennes, 1984)

2.1.2.3 α-Hydrate (or α-lactose monohydrate)

α-Lactose monohydrate is the more common crystal form of lactose and is what is typically produced commercially. α-Lactose monohydrate can form a number of crystal shapes, the most often found are those of the prism and the tomahawk. The typical progression of crystal growth, shown in Figure 2-4, generally produces the tomahawk habit shown in Figure 2-5. The varied morphologies are shown in Figure 2-6.

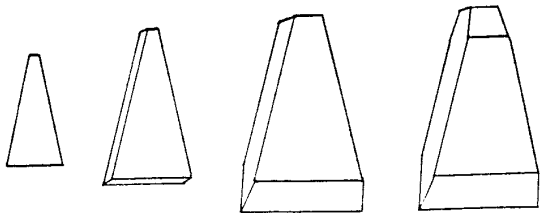

Figure 2-4 Progress of α-lactose monohydrate crystal growth in water (Hunziker and Nissen, 1924)

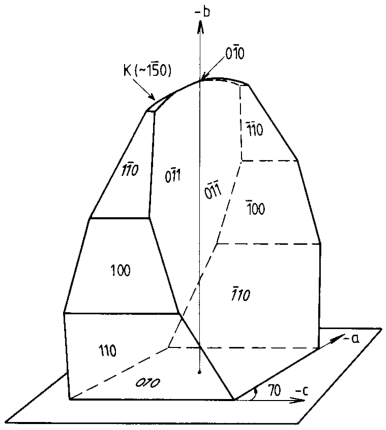

Figure 2-5 Characteristics of tomahawk crystal of α-lactose monohydrate (Walstra and Jennes, 1984)

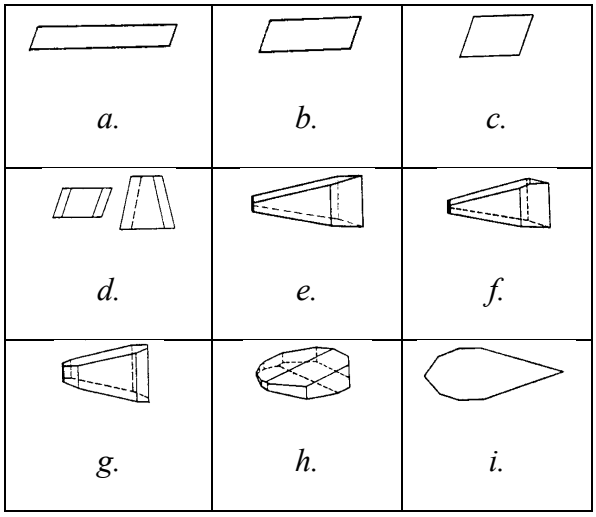

a. Prism, formed when growth velocity is high
b. Prism, formed more slowly than prism a.
c. Diamond shaped plates, transition between prism and pyramid
d. Pyramids resulting from increase of thickness of diamond
e. Tomahawk, a tall pyramid with bevel faces at base
f. Tomahawk, showing another face, which can sometimes appear
g. Fully developed tomahawk, most common
h. A crystal of 13 faces, the face shown in f. is not present
i. A profile view of h. with the tomahawk blade coming to an apex

Figure 2-6 The crystalline habit of α-lactose monohydrate (Herrington, 1934)

Most significant growth is reported (Michaels and van Kreveld, 1965) to emanate from the (010) face and the (110) face, with growth predominantly in the *b* direction with minimal growth of the $(0\bar{1}0)$ face. It is reported that if the $(0\bar{1}0)$ face is removed or damaged it does not re-grow (Jelen and Coulter 1973).

More recent Atomic Force Microscopy studies have confirmed that the growth is in the *b* direction, emanating from the (010) face (Dincer, 1999). The study by Dincer also supports the suggestion made by Visser (1982) that the unidirectional growth in the *b* direction is via a spiral dislocation mechanism (Figure 2-7). The spiral dislocations act as incorporation sites for growth units diffusing across the surface in the adsorption layer (Figure 2-8), resulting in spiral growth features on the crystal structure.

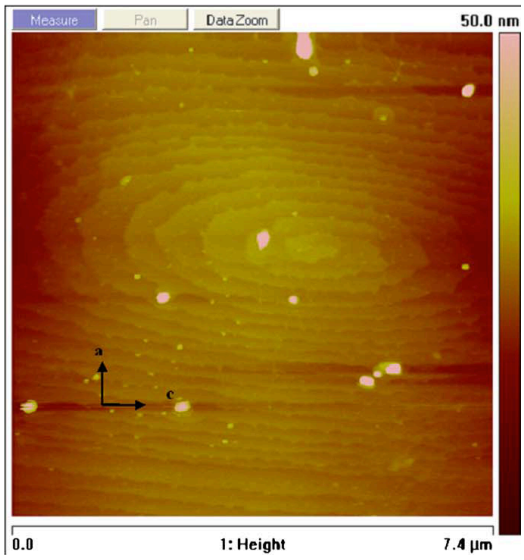

Figure 2-7 AFM images of the (010) face of α-lactose monohydrate crystals grown in (s-1) 0.55 at 30 ˚C (Dincer, 2009)

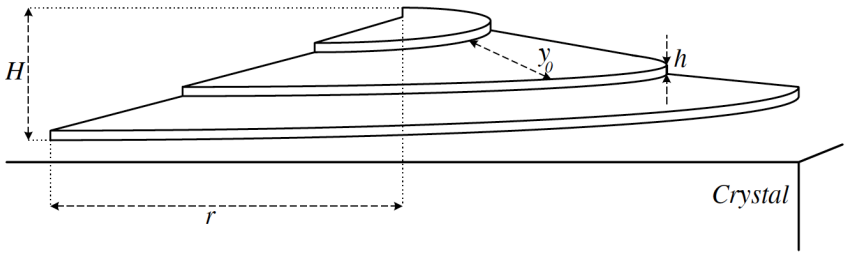

Figure 2-8 Spiral growth (Martins and Rocha, 2007)

α-Lactose monohydrate was grown in the presence of 'green fluorescent protein' and by comparing the crystal image from differential interference contrast microscopy and from the corresponding fluorescence micrograph, it was deduced by Wang et al (2001) that a sequence of once active hillocks observed through the (010) face reveal the growth history (Figure 2-9 and Figure 2-10). Supporting studies by Gurney (2001) were performed using carminic acid, a natural red dye resulting in the same conclusions.

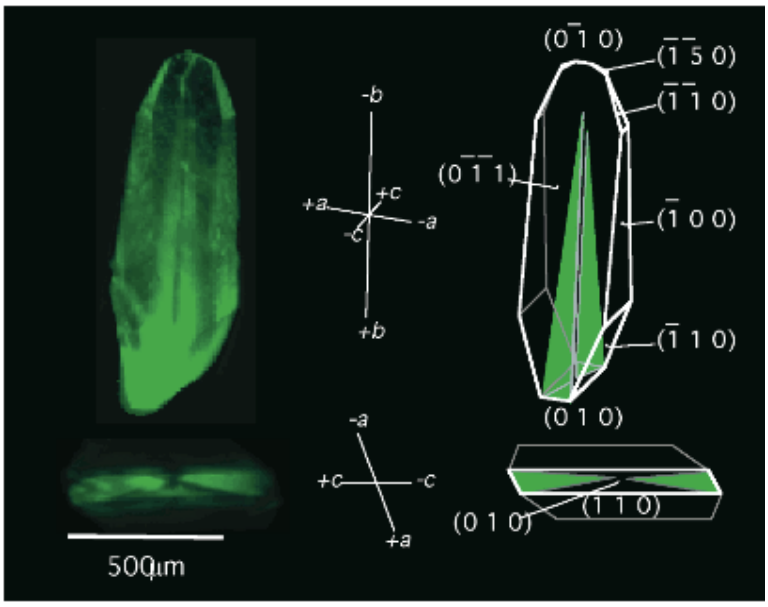

Figure 2-9 *(left)* Fluorescence micrographs of α-lactose monohydrate/green fluorescent protein ,*(right*) Idealized representations (Wang, 2001)

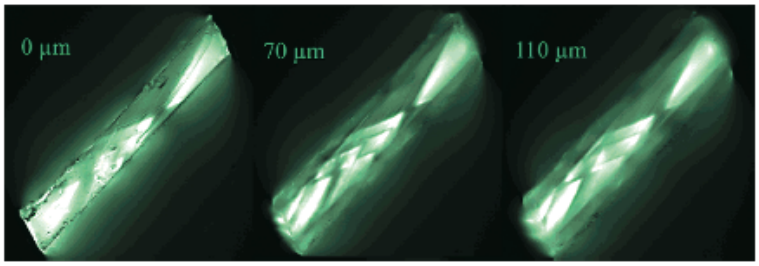

Figure 2-10 Fluorescence micrographs of α-lactose monohydrate / green fluorescent protein, (010) face at 0, 70 and 110 µ, from the surface (Wang, 2001)

Wang et al (2001) also demonstrated that α-lactose monohydrate can over-grow guest molecules which show no similarity to the host molecule. Figure 2-11 shows the interaction of six different proteins with α-lactose monohydrate identifying characteristic fluorescence from the (010) face.

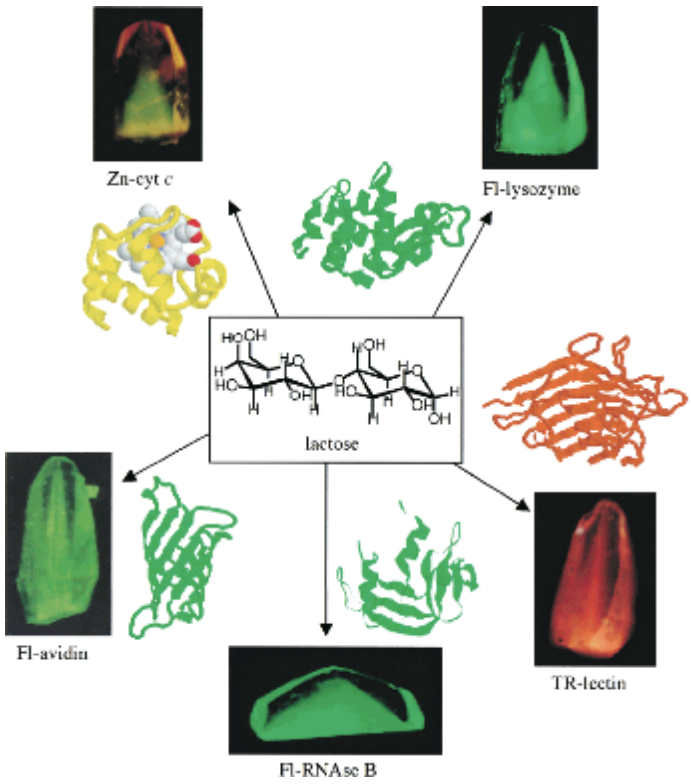

Figure 2-11 Crystals of α-lactose monohydrate containing a variety of proteins (Wang, 2001)

2.1.2.3.1 Structure of α-lactose monohydrate

A search of the Cambridge Structural Database reveals that a number of structure determination studies have been performed (see Table 2-1). There is a consensus that the unit cell of α-lactose monohydrate contains two molecules of lactose and two associated molecules of water (Figure 2-12).

Table 2-1 α-Lactose monohydrate structure determinations, found in Cambridge Structural Database (Allen, 2002)

Reference	Space Group	Cell				Temp. (K)	Density (gcm^{-3})
		a (Å)	*b* (Å)	*c* (Å)	*β* (°)		
1	P21	7.815	21.567	4.844	106.20	295	1.526
2	P21	7.98	21.68	4.836	109.78	295	1.52
3	P21	7.937	21.568	4.815	109.77	295	1.543
4	P21	7.982	21.562	4.824	109.57	295	1.53
5	P21	7.76	21.54	4.783	105.91	150	1.556

1. (Beever and Hansen 1971) *2. (Burma and Wiegers 1967)*
3. (Noordik, Beuskens et al. 1984) *4. (Fries, Rao et al. 1971)*
5. (Smith, Dann et al. 2005)

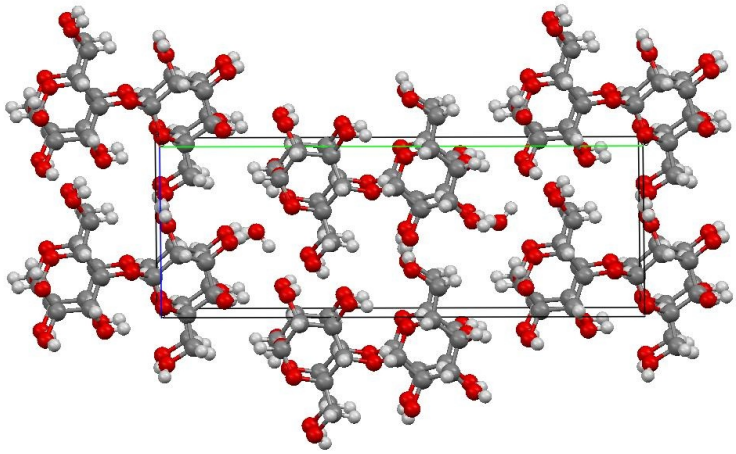

Figure 2-12 Unit cell of α-lactose monohydrate (Smith, Dann et al, 2005)

2.1.2.4 β-Anhydrous

β-Anhydrous is the next most common crystal form of lactose after α-lactose monohydrate. It crystallizes in an aqueous environment at temperatures above 93.5 ˚C and it has also been reported to crystallize at lower temperatures from alcoholic solutions (Butler, 1998). The sweetness and solubility of β-anhydrous make it more desirable than α-lactose monohydrate, however due to the complicated crystallization conditions it is not produced commercially.

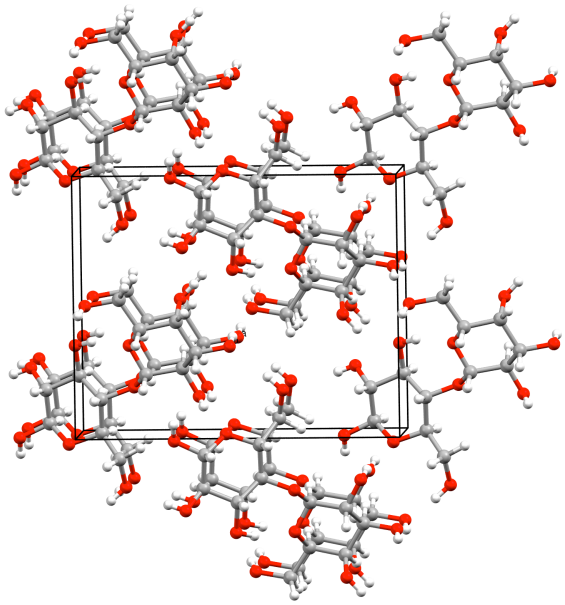

Figure 2-13 Unit cell of β-anhydrous lactose (Garnier et al, 2002)

2.1.2.5 Anhydrous α-Lactose

Dehydrating α-lactose monohydrate crystals at temperatures between 100 – 190 ˚C makes the stable form of anhydrous α-lactose. An unstable form of anhydrous α-lactose is formed, by dehydrating α-lactose monohydrate at 100 ˚C under vacuum. Unstable α-lactose is highly hygroscopic, while α-stable is denser than α-unstable and not hygroscopic, but is more soluble than the other forms (Walstra and Jennes, 1984).

2.1.3 Growth rate of α-lactose monohydrate in water

As has already been mentioned, α-lactose monohydrate is the commercially available form of lactose and this form will be the focus here.

There is significant breadth in the research that has been performed on the growth rate of α-lactose monohydrate. Three methods have been identified in the literature for measuring the growth rate; photographic methods, batch experiments and continuous crystallization experiments.

Van Kreveld and Michaels (1964) developed a photographic method for measuring the growth rate of individual faces on single crystals. Their findings were that initial growth is of the (010) face, away from the apex in the +b direction. Their studies also incorporated the effect of additives. Jelen and Coulter (1973) also used single crystals of similar shape and mass, and weighed them before and after growth. Their work showed that the growth rate increases with increasing supersaturation, particularly at higher temperatures. They assumed growth occurred only in the *b* direction and calculated growth rate of the (010) face as grams of lactose crystallized per m^2 per min.

Visser (1982) observed significant differences in growth rates amongst α-lactose monohydrate crystals. Shi et al (1989) concluded that α-lactose monohydrate crystals grow at a constant rate, however it was observed that different crystals have different growth rates. This phenomenon is called growth rate dispersion (GRD) (Shi et al, 1989). GRD is not unique to the α-lactose system; it is prevalent in a number of other crystallizing systems (Mullins, 1987).

Shi et al (1989) observed that α-lactose monohydrate crystal growth is dependant upon the growth/crystallization mechanism. With identical temperature and supersaturation, small nuclei (2 – 14 μm) produced by gentle contact nucleation gave low growth rates compared to ten times the growth rate using large seed crystals. This was explained as being due to the larger crystal bearing a number of dislocations on the surface enabling higher growth rates than the smaller crystals with smooth surfaces.

2.1.4 Growth inhibition of α-lactose monohydrate

The growth kinetics of crystallizing systems is influenced by the presence of impurities. Bhargava and Jelen (1996) suggest the reason for this is the changes in the solubility of the substance being crystallized and the absorption of impurities onto the crystal surface. Michaels and van Kreveld (1966) noted that the impurities have a much greater influence when absorbed onto the faster

growing faces. The literature suggests that the impurities affecting α-lactose monohydrate growth are β-lactose and trace levels of lactose monophosphate. Many authors have also looked at the effects individual salts present in whey have on the growth of lactose crystals.

2.1.4.1 β-Lactose

As β-lactose is always present in an α-lactose solution, it can be considered an impurity which may act as both a nucleation inhibitor or a habit modifier. It is also thought to be the determining factor for the typical α-lactose tomahawk morphology.

Michaels and van Kreveld (1966) demonstrated that a more symmetrical form of α-lactose is crystallized from solutions that contain β-lactose concentrations less than that resulting from the mutarotation equilibrium. It was suggested that β-lactose is a habit modifier because of the similar structure of the α- and β- molecules. It is thought that the β-lactose aligns its structure alongside the α- molecules of the same constituent, with the dissimilar portion pointing outward inhibiting further uptake of the α-lactose. Van Kreveld (1969) supports this by demonstrating that lactose growth in the presence of structurally similar disaccharides also inhibited growth. The concept was further elaborated upon and confirmed by Visser and Benema (1983).

Clydesdale et al (1997) used a modelling approach to further investigate these observations. They were able to predict growth from a pure solution and noted that the tomahawk morphology prevailed. Earlier work by Herrington (1934) had suggested significant changes in morphology over a range of supersaturations. Clydesdale's more recent work did not confirm such distinct variations. Raghavan et al (2000) re-examined the process of nucleation and growth of α-lactose from aqueous solution and the influence that β-lactose has on the growth process. They concluded that the tomahawk shape is due to the inhibition of growth on the $(0\bar{1}0)$ face.

Work by Herrington (1934) and Michaels and van Kreveld (1966) and Dincer et al (1999) show that a decrease in β-lactose in lactose solutions results in the formation of thin trapezoidal-shaped crystals. This is all supporting evidence that the morphology of α-lactose is a consequence of the presence of β-lactose in the crystallizing solution (see Figure 2-14).

(a)

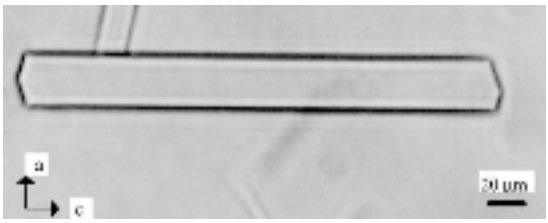

(b)

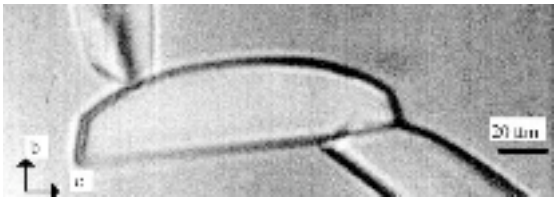

(c)

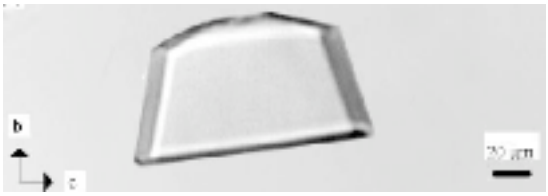

Figure 2-14 α-Lactose monohydrate crystals precipitated from DMSO solutions by the additional of ethanol in the presence of (a) 10 %, (b) 25 %, (c) 40 % β-lactose (Dincer, Parkinson et al. 1999)

2.1.4.2 Lactose monophosphate

Visser (1980) performed growth experiments on single crystals of α-lactose in supersaturated solutions. It was observed that growth rates were dependent upon the origin of the lactose material. Growth rates of the (010) face of various pharmaceutical grades of lactose were observed to vary from 3.1 μm/hour to 9.5 μm/hour.

In order to determine the true growth rate of α-lactose Visser worked toward an 'absolute blank' by purifying lactose with subsequent recrystallization.

Repeated recrystallization, however, yielded a lower pH and a slower growth rate, even upon neutralization. Michaels and van Kreveld (1966) made a similar observation, where it was first thought that the drop in growth rate was due to the removal of growth promoting substances. Visser found that fractional recrystallization slowly raised the pH until neutral lactose was obtained. Visser then used an ion exchange resin to remove the ionic impurities, which yielded a neutral product referred to as 'non-ionic lactose'. It was concluded that α-lactose contains an impurity of acidic character and that lactose itself is not acidic. The impurity seems to incorporate with high preference into the initial stages of α-lactose crystallization. Growth rate of crystals produced with the non-ionic lactose were upward of ten times higher than the original material. The acidic inhibitor was then removed from the anion exchange column and reintroduced to growing crystals and demonstrated a very strong inhibition of the lactose crystal growth.

Additional studies by Visser (1984) involved the isolation and identification of this acidic inhibitor. The inhibitor was separated by ion exchange, purified and identified using gas chromatography and nuclear magnetic resonance. This study found six isomers of a disaccharide monophosphate, all carrying the phosphate moiety on the galactose moiety. As a consequence they determined that pharmaceutical grade lactose typical of that used in this study contains approximately 60 ppm sugar-bound phosphate. The growth retarding properties were not investigated.

Further characterisation by Visser and collaborators Breg et al (1988) was performed using high performance liquid chromatography to further separate the original anion exchange residue. ^{31}P – nmr and ^{13}C – nmr analysis showed that the acidic residue contains 6-, 6'-, 3'- and 4'- lactose monophosphates (Figure 2-15).

(a)

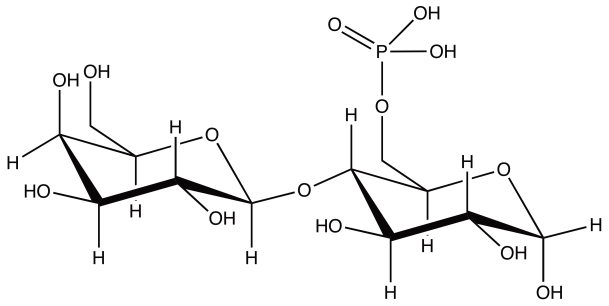

(b)

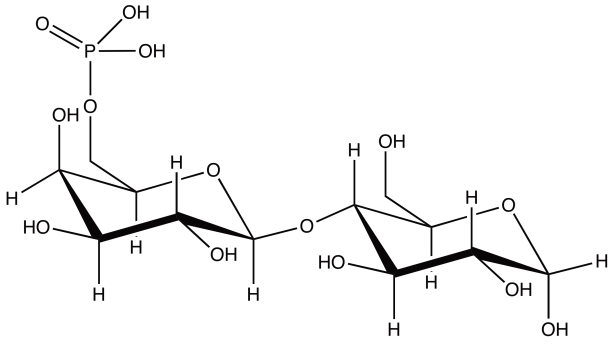

(c)

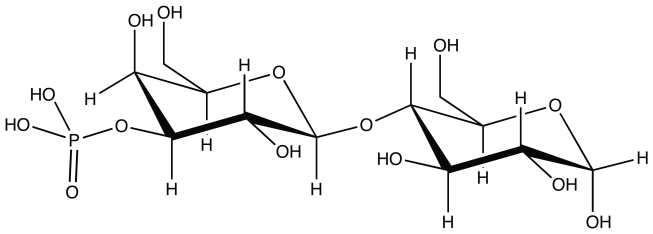

(d)

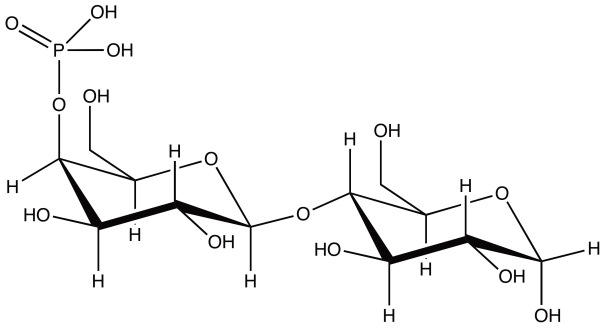

Figure 2-15 α-Lactose monophosphates (a) 6- (b) 6'- (c) 3'- (d) 4'-

2.1.4.3 Growth rate of purified α-lactose monohydrate

Studies were later performed to further substantiate the growth inhibiting behaviour of lactose phosphate (Visser, 1988). Growth rates were determined by mixing the 'non-ionic' lactose with increasing quantities of pharmaceutical grade lactose whilst maintaining the same overall lactose concentration (Figure

2-16). In essence the impact of increased lactose phosphate concentration can be inferred from these data. Pharmaceutical grade lactose is a purified form of lactose that is relatively free of other salts, minerals and proteins, however, the main contaminant of lactose phosphate remains.

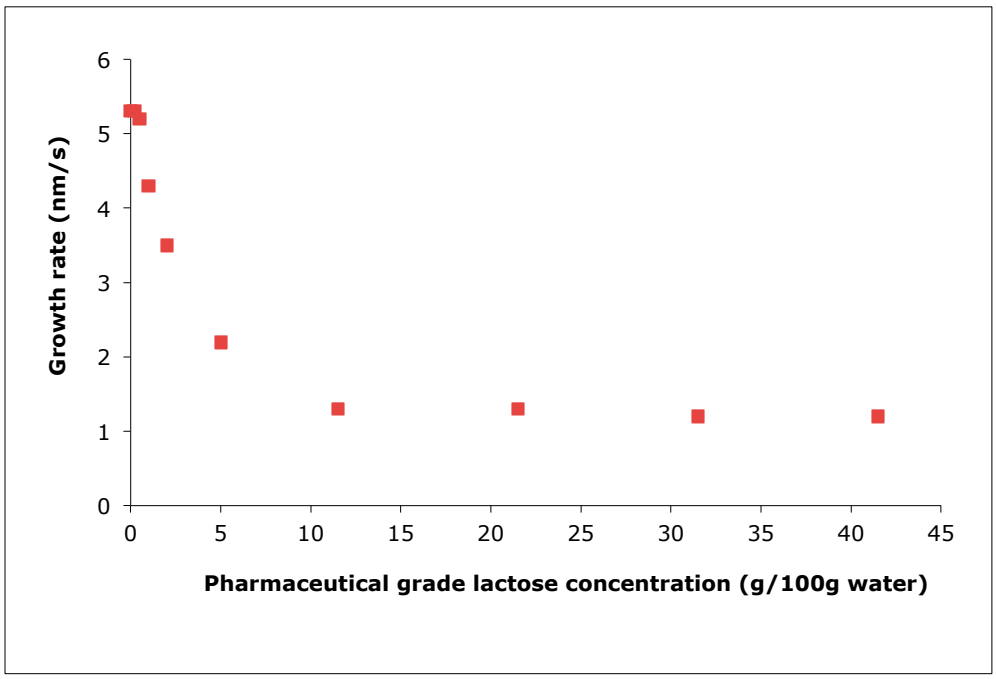

Figure 2-16 The results of growth rate experiments in mixed solutions of 'non-ionic' lactose and pharmaceutical grade lactose (lactose concentration maintained at 41.5 g/100 g water) (data taken from Visser 1988)

Lifran et al (2006) used a patented process, which will be discussed in a later section, to produce purified lactose. They were able to establish the impact that lactose phosphate has on the growth rate of α-lactose monohydrate. The lactose phosphate used in the investigation was recovered by recrystallization and anion exchange of a pharmaceutical grade lactose product.

As indicated in Table 2-2, the impact of the lactose phosphate is a reduction in crystal size, crystal content and final yield. Figure 2-17 highlights the reduction in the median crystal size with increasing concentrations of lactose phosphate. The authors demonstrate strong growth rate inhibition with increasing concentrations of lactose phosphate up until 60 ppm lactose phosphate where the inhibitory action plateaus.

Table 2-2 Effect of lactose phosphate concentration on the final values of different parameters of the isothermal crystallization of pure lactose in water at 30 ˚C (Lifran et al, 2006)

Lactose Phosphate concentration (ppm)	0	15	30	45	60	75	90	120	150
Length (μm)	72.8	71.60	69.09	69.20	67.87	68.01	67.00	66.45	66.52
cc (g/100g)	6.24	5.45	5.18	5.10	5.09	4.80	4.80	4.69	4.63
° Brix	22.23	22.20	22.26	22.27	22.29	22.37	22.48	22.52	22.72
Final yield (% w/w)	24.70	21.30	20.70	20.40	19.90	19.20	18.70	18.60	18.34

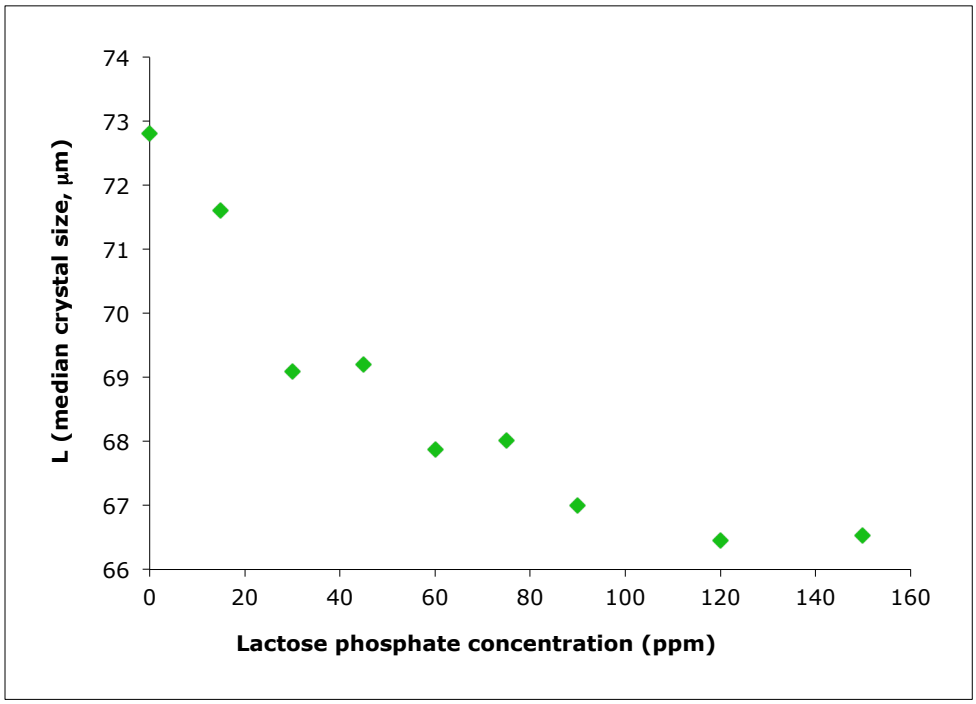

Figure 2-17 Observed impact of lactose phosphate on median crystal size of α–lactose monohydrate (values taken from Lifran et al, 2006)

2.1.4.4 Whey Impurities

Many authors have studied the influence that individual salts present in whey have on the growth behaviour of α-lactose monohydrate.

Herrington (1934) was the first to study the results of lactose crystallization in the presence of impurities and observed that high salt concentrations had a

retarding effect on crystal growth. Bhargava and Jelen (1996) suggested that the effect salts have on the growth rate of α-lactose is directly dependent on the solubility of lactose in the salt solution.

Potassium salts have been shown to decrease the growth rate of α-lactose, according to studies by Smart (1988), Guu and Zull (1991) and Bhargarva and Jelen (1996). However Visser (1984) and Jelen and Coulter (1973) found potassium salts increase the growth rate by 10 %.

Jelen and Coulter (1973) and Smart (1988) identify sodium phosphate salts as growth rate enhancers. Smart (1988) also suggests that they decrease α-lactose solubility. Calcium phosphate seemed to have insignificant effects according to Guu and Zall (1991).

It would appear the effect of calcium chloride is more concentration dependent than observed with other impurities. Jelen and Coulter (1973), Visser (1984) and again Bhargava and Jelen (1996) found significant growth rate increase above 2 % total solids, below which Smart (1988) reports no significant effect. Jelen and Coulter (1973) observed that calcium chloride increased growth rate by up to three times the normal rate. Herrington (1934) observed an increased solubility of lactose when calcium chloride was added and hypothesized is due to the formation of lactose – calcium chloride complex, which he was able to isolate in crystalline form. This complex is more soluble than lactose itself (Jensen et al 1940 in Swartz et al 1978).

Smart (1988) noted that sodium chloride and magnesium chloride had insignificant effects on growth rate, whereas according to Visser (1984) they significantly increased the growth rate. Magnesium sulphate was shown to increase growth rate by Visser (1984) and Bhargava and Jelen (1996), the latter also found magnesium sulphate to enhance the growth rate.

Swartz et al (1978) studied the interaction of metal ions with lactose and found that when lactose combined with metal salts in a ratio of one to one, cations Ca^{2+}, Ba^{2+},Sr^{2+}, Fe^{2+}, Mg^{2+}, Mn^{2+}, Zn^{2+}, Na^{+} and Li^{+}, formed a complex. It was noted that complex formation decreased with increased ionic strength. This work supports the earlier work of Herrington (1934) where he separated a

lactose–calcium chloride complex. The structure of the calcium-lactose complex is shown in Figure 2-18 (Cook and Bugg, 1973). Two lactose molecules coordinate to each calcium atom to make a polymeric chain.

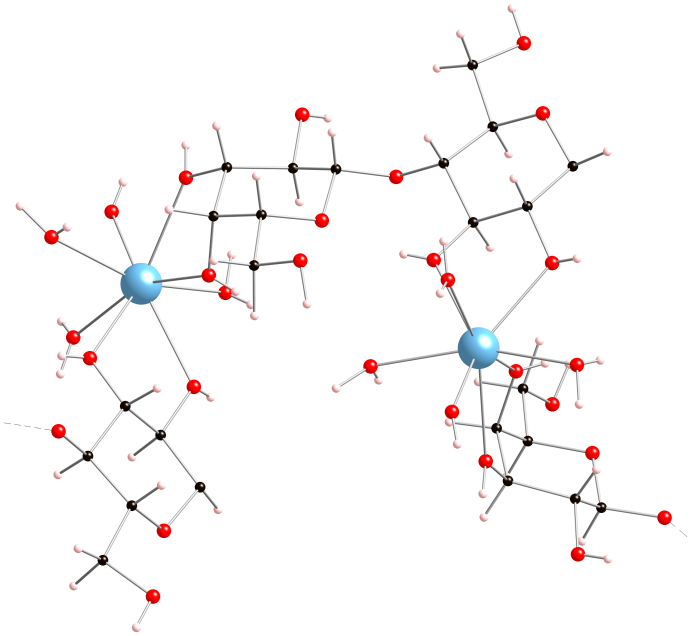

Figure 2-18 A partial structure of the polymeric coordination chain formed in the calcium-lactose complex, $CaCl_2$.(lactose).$7H_2O$ (Cook and Bugg, 1973)

The effect of the natural acid in whey, lactic acid, has been looked at quite extensively and the results appear inconclusive when considered as a whole. Smart (1988) and Bhargarva and Jelen (1996) suggest that lactic acid increases the growth rate, whereas earlier work by Jelen and Coulter (1973) and Nickerson and Moore (1973) shows a decrease in growth rate. Michaels and van Kreveld (1966) observed no effect with lactic acid. It has been conceded by Jelen and Coulter (1973) that the lactate concentration and pH of the solution may be important factors in this discussion.

According to Michaels and van Kreveld (1966), riboflavin decreases the growth rate of α-lactose when present at concentrations above 50 ppm, Smart (1988) however considered the decrease insignificant.

2.1.4.5 Non-Whey Additives

Numerous studies have been performed on the influence that various additives, which are not found in whey, have on the growth of α-lactose.

Michaels and van Kreveld (1966) studied the effects of acids, carbohydrates and surface-active substances. They found that acids such as hydrochloric, lactic and acetic decreased the pH sufficiently to accelerate the mutarotation between α- and β-lactose, such that growth rate was only slightly increased. Sorbic acid had significant growth promoting effects. It was observed that the forming α-lactose nuclei tended to adhere to the seed crystal. Glucose and maltose had no apparent effect.

The most effective additives were the surface active ones. Gelatin retards growth in all directions, trimethyloctadecylammonium chloride retards growth particularly in the –b direction, and sodium dodecylbenzenesulfonate has no detectable effect. Alcohols accelerate growth in all directions, which is thought to be due to a decrease in lactose solubility (Herrington 1934). The Michaels and van Kreveld (1966) theory is supported by Nickerson and Moore (1973), such that alcohols increase the growth rate due to the promotion of step generation, maybe as a result of increased supersaturation.

Michaels and van Kreveld's (1966) studies with glucose and maltose yielded no detectable effect, however Nickerson and Moore (1973) found them to have an inhibitory effect, similar to that seen with β-lactose. They also found that after addition of acids to achieve pH < 1, crystallization was greatly accelerated particularly with sulphuric acid where the growth rate increased to that of sucrose (sucrose grows much more rapidly than lactose). Michaels and van Kreveld (1966) support the work of Nickerson and Moore (1973) and also observed that addition of sucrose increases the growth rate of α-lactose.

Structurally similar carbohydrates (lactulose, cellobiose, galactose) to α-lactose were shown to significantly retard growth and alter morphology, according to van Kreveld (1969) and Visser (1984). It is also suggested that the addition of a structurally similar additive may influence the mutarotation equilibrium. Contradictory evidence published by Michaels and van Kreveld

(1966) and Smart (1988), suggested no significant effect was observed. More recent studies by Garnier et al (2002) reported several habit modifiers. Sucrose and β-glucuronamide were shown to have no effect on the morphology. However α-glucosamine hydrochloride, maltitol, α-galactose and β-cellobiose all proved to significantly alter the morphology. It was also shown that these habit modifiers are not incorporated into the α-lactose crystal.

2.1.4.6 Experimental Factors

Experimental conditions must also be considered when discussing the influences of additives/impurities. Supersaturation, pH, temperature and solubility all play a vital role in the influence that additives have on the growth rate of α-lactose, or any crystallizing system for that matter (Mullin, 1997).

Kubota et al (2000) explains that supersaturation dependence occurs in one of two ways; firstly where the growth rate is suppressed over a range of supersaturation and secondly where it is suppressed only in the low range of supersaturation while at the higher supersaturation range the impurity effect disappears completely. This is observed with the lactose system, as shown by Michael and van Kreveld (1966). It was noted that the impurity addition had a much greater effect on the growth rate at the lower supersaturations of the study. Garnier et al (2002) has shown that increasing the supersaturation during crystal growth of α-lactose induces an increase in the mean crystal size. They explain that this is largely due to β-lactose acting as a strong growth inhibitor at low supersaturations.

The pH of the crystallizing solution must also be considered and was studied at length by Visser (1980). For the lactose system it was observed that the growth rate increased with increasing pH. The maximum pH for accelerated growth was reached at 7, after which the lactose is thought to decompose and the decomposition products become inhibitors. This is supported by Nickerson and Moore (1974), although they proposed decomposition became significant at a higher pH of 10. Smart (1988) also observed increased growth velocity above pH 6.0. According to Visser, the lower the pH (with hydrochloric acid)

of the lactose system the slower the growth rate on all growing faces. However, as discussed previously, authors Nickerson and Moore (1973), found that very high acidity, pH < 1, growth is accelerated greatly with sulphuric acid. Michaels and van Kreveld (1966) found some effect from the addition of HCl to a pH of 2, slowing growth on all growing faces, and with acetic and sorbic acid only slowing growth on the (010) face and promoting growth on the other faces. The effect of lactic acid has already been discussed in a previous section and remains in dispute.

Smart (1988) evaluates the effect that temperature has on crystallizing lactose. It was found that increased temperature increases the growth rate and as a consequence increased yield. Thurlby (1976) had also found the α-lactose crystallization rate increases for a given supersaturation over an increasing temperature range of 15-50 ˚C.

The effect that impurities and additives have on the solubility of α-lactose has not been considered in many of the experiments. Smart (1998) reported observing showers of crystals upon addition of a salt. Increased lactose solubility resulting from additional impurities has been thought to retard the growth of α-lactose (Herrington, 1934). In contrast Bhargava et al. (1996) report a decrease in α-lactose solubility with the addition of individual salts LiCl, $MgSO_4$ and $CaCl_2$ hence an increased growth rate. They report a decreased growth rate due to the solubility enhancement upon the addition of KH_2PO_4.

It is clear from this literature review, that the impact of additives and impurities on lactose crystal growth is not thoroughly understood. Making a contribution to this area is one of the aims of this project. A key requirement for any such work is an understanding of lactose purification methods.

2.1.5 Purification of saccharides

Chromatographic separation is a widely used unit operation in sugar or sugar derivative production.

The typical separation media used for large scale chromatographic systems applied to aqueous saccharide purifications are sulfonated crosslinked styrenic divinylbenzene cation exchange resins in a salt form. There are some applications that use anionic resins in salt form. Typically, sugar separations are carried out with resins in the calcium form, though sugar/non-sugar separations are achieved with resin in the potassium form (Chaplan and Kennedy, 1994). Table 2-3 below shows typical commercial separation media for sugar solutions.

Table 2-3 Separation support type according to the type of separation (Chaplan and Kennedy, 1994)

Separation support	Type of separation
Cation exchange resin, Ca^{2+}	Fructose/dextrose Sorbitol/mannitol Mannose/dextrose Glucose/galactose
Cation exchange resin, Na^{+}	Dextrose/higher saccharides Maltose/higher saccharides
Cation exchange resin, K^{+} or Na^{+}	Sucrose/fructose and dextrose Sucrose from molasses

Resins in the calcium form invoke a two-fold simultaneous separation process. Firstly, the resin acts as a molecular sieve such that the larger molecules cannot enter resins beads and are excluded due to their size. Secondly, the stability of certain calcium-sugar interactions enables the separation of certain sugar mixtures. Fructose and glucose readily form calcium-sugar complexes, whereas sucrose and galactose do not. Resins in the potassium form separate sugar mixtures based on the principles of ion exclusion.

2.1.5.1 Ion Exclusion Chromatography

Ion exclusion chromatography (IEC) is a technique widely applied to separate ionic compounds from non-ionic compounds and mixtures of acids (or bases). The principle of operation is that negatively charged ions are separated on

cation exchange resins with anionic functional groups (usually sulfonic moieties). Positively charged species are separated on an anion exchange resin containing cationic functionality (usually tetralkylammonium groups). Typically the same columns used for ion exchange chromatography can be used for IEC.

When water is used as the mobile phase, water molecules build up hydration spheres around the dissociated functional groups of the styrene/divinylbenzene copolymer support. Water accesses the pores of the support and is immobilized in the hydration spheres thus forming the stationary phase. The retention mechanism is based on neutral molecules penetrating the resin, while similarly charged cations are repulsed, due to the presence of the dissociated functional groups immobilised in the stationary phase. The hydrated resin network behaves like a semi-permeable membrane between the stationary and mobile phases.

2.1.5.2 Acid – Sugar Separations

As discussed above, IEC can effectively separate ionic from non-ionic species. In recent decades more industrial applications of IEC are surfacing whereby sugars are being separated from acid solutions.

The use of a strongly acidic cation exchange resin for the separation and recycling of acid from synthetic solutions of glucose and sulfuric acid has been investigated. A successful separation of a synthetic solution of 7.7 % sulfuric acid and 1.0 % glucose was reported (Neuman, 1987).

The application of this approach, quite removed from sugar processing, is in the commercially viable process for the conversion of lignocellulosic materials to fuel grade ethanol (Springfield, 1999). The process utilizes sulfuric acid to hydrolyse cellulose into simple sugars. Undesirable compounds such as lignin are removed; the resulting sugar/acid mix is separated using IEC. The acid is re-used and the fermentation of the sugars produces fuel grade ethanol. After optimisation of this IEC process, 95 % of the feed sucrose and 98 % of the feed acid was recovered.

Modifications of such applications have found a use in the purification of nutrients from food process streams, including the purification and extraction of lactose from whey in the dairy industry.

2.1.5.3 Purification of α-lactose monohydrate

Commercially, α-lactose monohydrate is extracted from whey. Whey is comprised of lactose, minerals, proteins, and riboflavin and lactose phosphate. The growth of α-lactose monohydrate from whey leads to the incorporation of impurities, which have been shown to greatly affect the growth kinetics.

The work carried out by Visser has been covered in section 2.1.5 (1980, 1982, 1988). Visser was able to remove mineral and other impurities by recrystallization, but was unable to remove lactose monophosphate, which was proven to be a significant growth inhibitor. It was confirmed that lactose monophosphate preferentially incorporates into the α-lactose monohydrate crystal as it grows. Thereby the repeated recrystallizations performed by Visser were essentially concentrating the lactose monophosphate. Visser was able to isolate, remove and identify lactose monophosphate via ion exchange chromatography and produce a pure form of α-lactose monohydrate.

It may be of interest to the dairy industry to produce a purer form of α-lactose monohydrate compared with what has historically been available. The very simple approach taken by Visser of ion exchange chromatography has since been expanded upon to incorporate the use of ion exclusion chromatography (IEC) to produce a highly purified form of α-lactose monohydrate.

An Australian patent developed by researchers from the University of Western Sydney, Commonwealth Scientific and Industrial Research Organisation and the Dairy Research and Development Corporation, describes a process for the production of ultra pure α-lactose monohydrate. This Australian patented process applies the principle of IEC in a similar way to the methods discussed in section 2.1.6.2.

One of the applications of the patent is the production of purified whey components and more appropriate to this review is the production of pure lactose. A schematic of this patented process is shown in Figure 2-19.

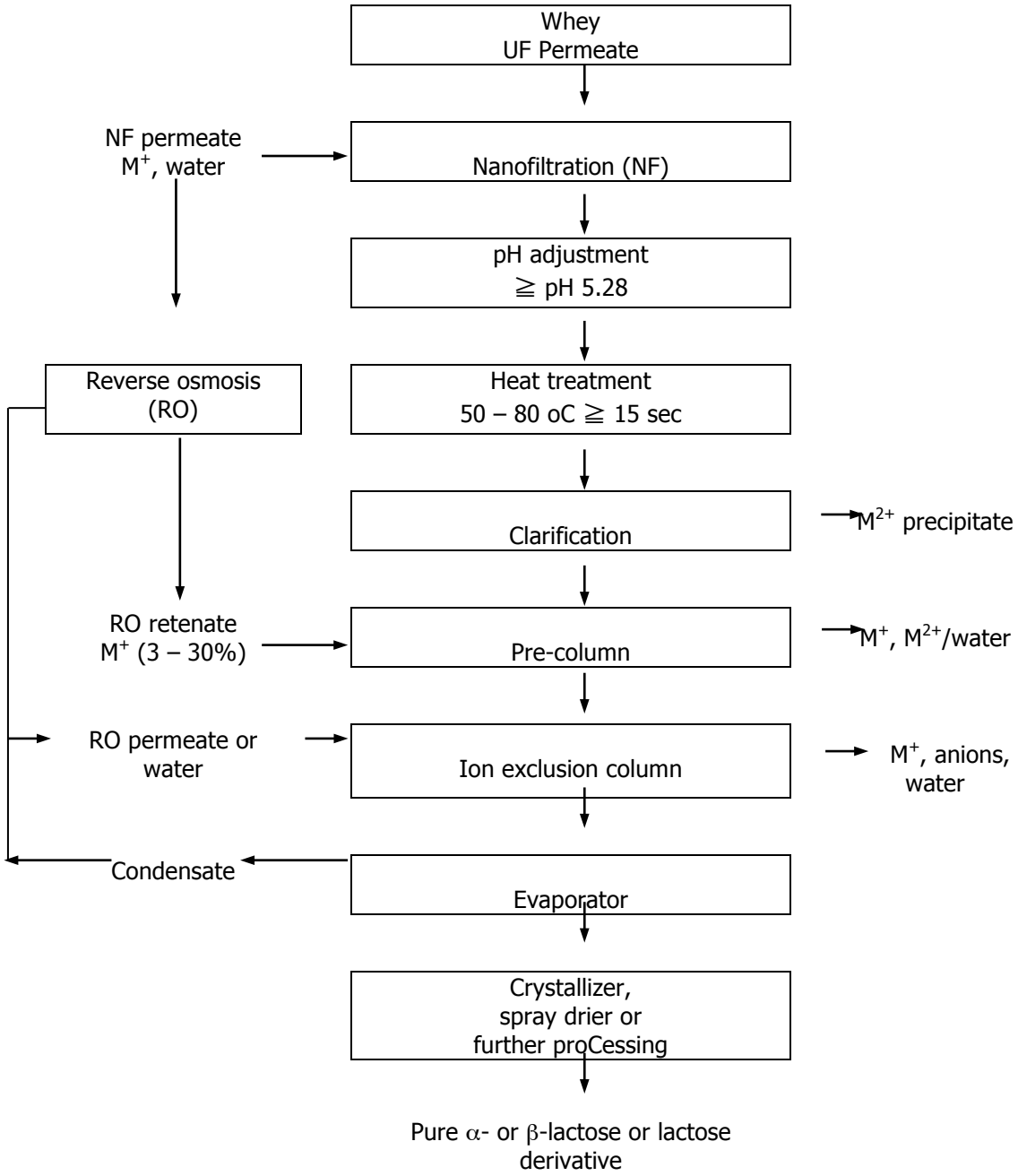

Figure 2-19 Purification scheme for cheese whey permeate (AU199884264 C)

The process outlined in Figure 2-19 is dependent upon the whey permeate to be processed and depending upon its composition the pre-treatment steps (precipitation, nano-filtration, ion exchange) can be rearranged to produce the

desired result. According to the process outline the whey permeate is processed by nano-filtration (NF) to a concentration between 15 – 25 ˚Brix *(˚Brix is the amount of sugar in a solution per weight of the total solution, ie. A solution that is 10 ˚Brix has 10 g sugar in 100 g of solution*). The NF permeate which contains monovalent cations is collected and can be recycled throughout the process. The pH of the retentate of the NF whey permeate is adjusted to 5.8 using a monovalent alkali or alkali salt and then heated to 50 – 80 ˚C for such a time that any precipitation is accelerated. The precipitate is then removed via a clarification step. The resulting clarified retentate is then fed into a pre-column packed with the appropriate cation exchange resin balanced with monovalent cations, to absorb any remaining divalent cations present. This pre-treated whey-permeate now contains monovalent cations, anions, peptides and vitamins and is concentrated up to 60 ˚Brix.

The pre-treated whey permeate is then fed into a column loaded with a cation exchange resin suitable for IEC. Elution is performed using water and the separation of the ionic compounds and the non-ionic compounds (or the minerals and peptides from the lactose) is performed.

The ionic compounds elute preferentially and are collected first. Typically such solutions would contain potassium and sodium, phosphates (lactose phosphates), citrates, lactates and small ionic peptides. Finally the purified lactose passes through the column. The pure lactose solution can be concentrated by evaporation or undergo alternative processing for specific products.

This patent process provides a convenient and efficient means to producing α-lactose monohydrate of a high purity, extending the work of Visser to an industrial scale. The process is successful in removing lactose phosphate, as it is a compound of acidic character.

2.1.6 Characterisation of lactose

A number of reviews have been published which deal with the determination of lactose and its derivatives. Quantitative determination of lactose and its

derivatives can be achieved with numerous techniques; polarimetry, colorimetry, enzymic procedures, gas liquid chromatography and high performance liquid chromatography.

2.1.6.1 Colourimetric methods

Colourimetric methods are typically employed when the gross determination of a carbohydrate is required. Specific enzymic assays of mixtures can also determine quantitatively individual saccharides. Total sugar assays generally rely on the hydrolysis of the glycosidic linkages with concentrated sulfuric acid and subsequent dehydration of the monosaccharides, which can react with specific compounds to give a coloured product. Reducing sugars can be determined by reacting them with alkaline cupric salts to form cuprous oxide, which can be titrimetrically evaluated with reference to standard tables (Chaplan and Kennedy 1994).

2.1.6.2 Ion-exchange chromatography

Ion-exchange chromatography has been exploited to purify saccharides as discussed in section 2.1.6, and also has application is quantifying and characterising saccharides.

Low pressure column chromatography

Anion-exchange resins fractionate oligosaccharides in order of decreasing molecular size. Anion-exchange can cause sugar inter-conversions which can be overcome by using some cation-exchange resins. Typically water is the applicable eluent. However it is possible to use a water/alcohol mixture as the eluent whereby a partition mechanism is responsible for the separation. Equilibria are established between the phase within the resin and the bulk solution. Anion-exchange resins typically retain more water within the resin compared to the bulk solution, which favours the retention of higher molecular weight saccharides and a reversed elution order can be achieved such that

disaccharides and oligosaccharides elute before the monosaccharides (see Figure 2-20, sucrose elutes first, M_w 342.3 and glucose elutes last, M_w 180.2).

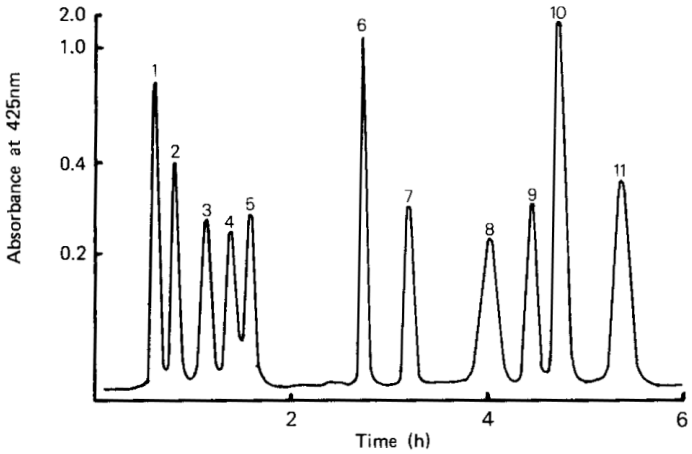

1. sucrose (M_w 342.3)
2. cellobiose (M_w 342.3)
3. maltose (M_w 342.3)
4. lactose (M_w 342.3)
5. rhamnose (M_w 164.2)
6. ribose (M_w 150.1)
7. mannose (M_w 180.2)
8. fructose (M_w 180.2)
9. galactose (M_w 180.2)
10. xylose (M_w 150.1)
11. glucose (M_w 180.2)

Figure 2-20 Ion-exchange chromatography of monosaccharides and disaccharides (Chaplan and Kennedy 1994)

Borate buffers can also be used to form complexes with carbohydrates. These exhibit different affinities for the ion-exchange resin. This can be exploited as an extension to the normal range. The extended analysis times and alkaline conditions can cause inter-conversion of the reducing sugars. This can be overcome by changing the eluting buffers. This effectively enables the structurally similar families of disaccharides and trisaccharides, to be separated and identified (see Figure 2-21).

1. pannose
2. maltotriose
3. maltose
4. isopanose
5. isomaltose
6. D-glucose

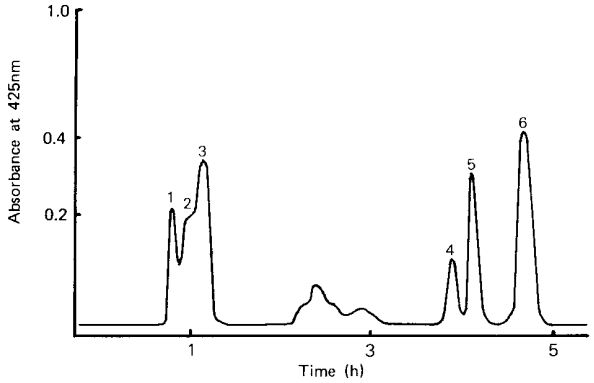

Figure 2-21 Ion-exchange chromatography of starch derived oligosaccharides showing structural features enhanced by borate ion complexation (Chaplan and Kennedy 1994)

High performance liquid chromatography

Many of the separation principles that are used in low-pressure column chromatography apply in high performance liquid chromatography (HPLC). The advantages are that the use of narrow bore columns, high inlet pressures, shorter analysis times and smaller analyte volumes, produce a highly resolved chromatogram.

The most frequently used HPLC systems for separation of saccharides is bonded-phase chromatography and high performance ion exchange chromatography. With bonded phase chromatography the saccharides elute in order of increasing molecular weight resulting from the relative affinities the sugar has for the mobile and bonded phase (Chaplan and Kennedy 1994).

As previously mentioned, separations are routinely performed on γ-aminopropyl group modified silica or with cation-exchange resin (Brons and Oliman, 1983). Retention and selectivity for certain sugars differs greatly between the column media types. Resins separate on the principles of exclusion, complexation and hydrophobic absorption, such that the larger saccharides elute before the smaller ones. The silica medium separates by partition of the sugars between a liquid phase and the surface of the stationary

phase. The elution order is the reverse, monosaccharides followed by the larger sugars.

Comparative studies of the two medium types revealed that reducing sugars are problematic on amino-bonded silica columns (Brons and Oliman, 1983), due to the formation of Schiff bases between the sugar and the stationary phase. Using a diol-modified silica column or a calcium dianion cation-exchange resin has been shown to overcome the issue. The application of a cation-exchange is deemed more suitable as it is shown to have a reduced signal-to-noise ratio (by 10 times). The limitation is, however, that this method does not resolve disaccharides whereas the diol-modified silica does (Figure 2-22).

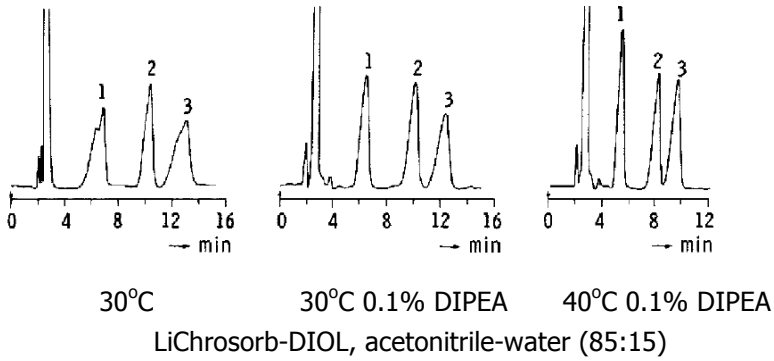

Figure 2-22 Separation of galactose (1), sucrose (2) and lactose (3) (Brons and Oliman 1983)

As shown in Figure 2-22 a successful separation is achievable using a diol-modified silica column (LiChrosorb-DIOL) which requires an acteonitrile and water eluent. The addition of tertiary amine diisopropylethylamine (DIPEA) to the eluent demonstrates that improved baseline resolution is achievable. It is the resultant increase in pH that enhances the mutarotation rate enabling greater chromatographic resolution.

2.1.6.3 Gas chromatography

Gas chromatography is a useful technique in saccharide analysis. It is used in structural studies, determination of monosaccharide residues, the positions of glycosidic bonds and for routine quantitation of saccharides (Chaplan and Kennedy 1994). Gas chromatography (GC) relies on the differential extractive distillation of components in a mixture, so volatile carbohydrate derivatives must be prepared for analysis. It is often necessary to isolate the analytes from the sample matrix before derivatization is performed, which is often deemed problematic (Jager, Tonin et al. 2007).

2.1.6.4 Capillary electrophoresis

In recent years, capillary electrophoresis (CE) has been considered for carbohydrate analysis in food samples. There are many approaches to presenting a sample to CE, however typical sample preparation steps include only dilution and filtration, thus insuring minimal handling and low cost analytical methodologies (Jager, Tonin et al. 2007).

CE is a technique that consumes a very small amount of sample, is capable of rapid and high resolution separation, characterisation and reproducible quantitation (Koketsu 2000). It is a technique that is widely used in the analysis of proteins, peptides, nucleic acids and oligosaccharides. Studies have been performed which have developed ways to overcome the issues of isomerism and α/β linkages that are commonly found in oligosaccharides. It is for these reasons that it has been investigated and method development performed as a part of this study.

Capillary electrophoresis methodology

Electrophoresis has evolved from the age of plate and gel techniques, into a compact and rapid process inside a very thin glass capillary. Fused silica capillaries employed in CE provide the ideal surface on which electrophoresis mechanisms can take place, the polyimide coating on the exterior imparts flexibility on to what would otherwise be a very fragile structure (Landers 1997).

CE can be run in a number of different modes of operation. The main modes are capillary zone electrophoresis (CZE), micellar electrokinetic capillary chromatography (MEKC), capillary isoelectric focussing (CIEF), capillary gel electrophoresis (CGE) and capillary isotachophoresis (CITP). Each method of operation has a target analyte group as summarised in Table 2-4 below.

Small ions	Small molecules	Peptides	Proteins	Oligo-nucleotides	DNA
CZE	MEKC	CZE	CZE	CGE	CGE
CITP	CZE	CITP	CGE	MEKC	
	CITP	MEKC	CIEF		
		CIEF	CITP		
		CGE			

Table 2-4 Modes of CE used for the analysis of different classes of analytes (Landers 1997)

Capillary zone electrophoresis

The most commonly used and robust of the modes is capillary zone electrophoresis (CZE) and is the method of particular interest in this review.

A fused glass capillary is filled with a buffer solution. At pH values above 2 the silanol groups on the capillary surface ionise to give a negatively charged surface. Cations from the buffer solution are attracted to the surface forming an electrical double layer (Figure 2-23a). When a dc voltage is applied the mobile positive charges in the outer double layer migrate toward the cathode. As the ions are solvated the buffer is dragged along by this migrating charge creating a flow of the bulk solvent. The flow that is generated is called electroosmotic flow (EOF). The analyte molecules are subject to migration dependent upon their charge; this is termed electrophoretic mobility. The smaller, more positively charged ions migrate most rapidly, conversely the larger more negatively charged ones move the most slowly, and the neutral molecules migrate at the EOF rate as they are not influenced directly by the electric field (Figure 2-23c).

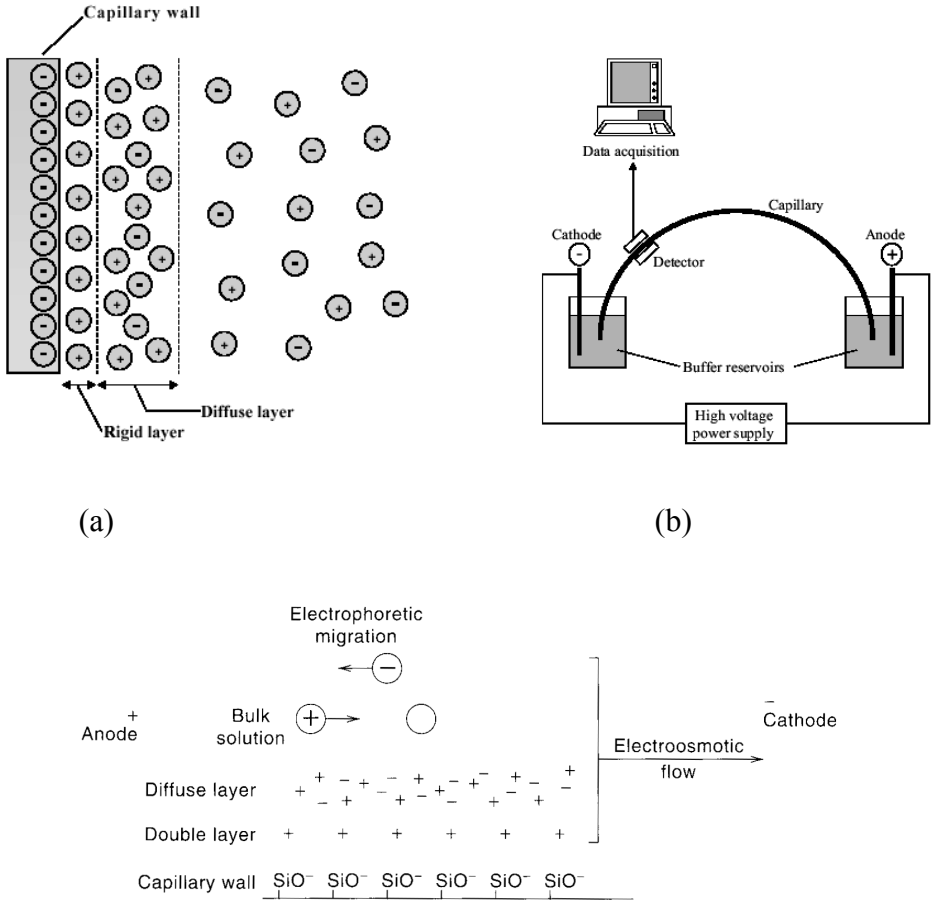

Figure 2-23 (a) Stern's model of charge distribution-electrical double layer, (b) schematic representation of typical CE instrument, (c) charge distribution and electroosmotic flow in fused silica (Christian 2004)

The exploitation of EOF is what enables the high resolution of CE techniques. In pressure driven techniques, such as GC and HPLC, the flow profile imparts peak broadening on the chromatogram. The pressure driven techniques operate under a laminar flow mechanism where the flow at the centre is moving twice as fast as the average velocity. The EOF mechanism in the CE technique provides constant flow along all dimensions of the entire capillary thus minimizing sample dispersion and generating very sharp peaks on the resultant chromatogram (see Figure 2-24).

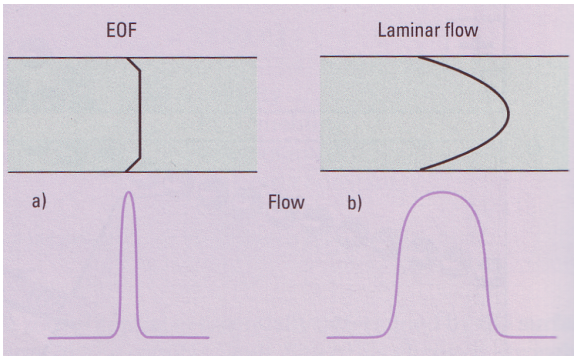

Figure 2-24 Flow profile and corresponding solute zone for (a) electroosmotic flow, and (b) laminar flow. (Heiger 2000)

There are a large number of separation parameters that need to be considered with CE method development. A change in one parameter often has an affect on others. A schematic found in Landers (1997) is a useful reference tool to evaluate the relationships between the influencing parameters (see Figure 2-25).

Sample injection can be done via either hydrostatic injection (gravity, pressure or vacuum) or by electromigration. The reproducibility of the hydrostatic injection is of the order of 1-2 %. The electromigration method allows more sample to be introduced thus improving detection limits but is less desirable as the plug that enters the capillary is influenced by different mobilities and not considered representative of the sample (Christian 2004).

Detection is done near to the cathode end of the capillary. The very small volumes enable very low detection limits with moderately sensitive detectors. The common method of detection is via UV absorbance. Some other methods are electrochemical, conductometry and mass spectrometry (Christian 2004).

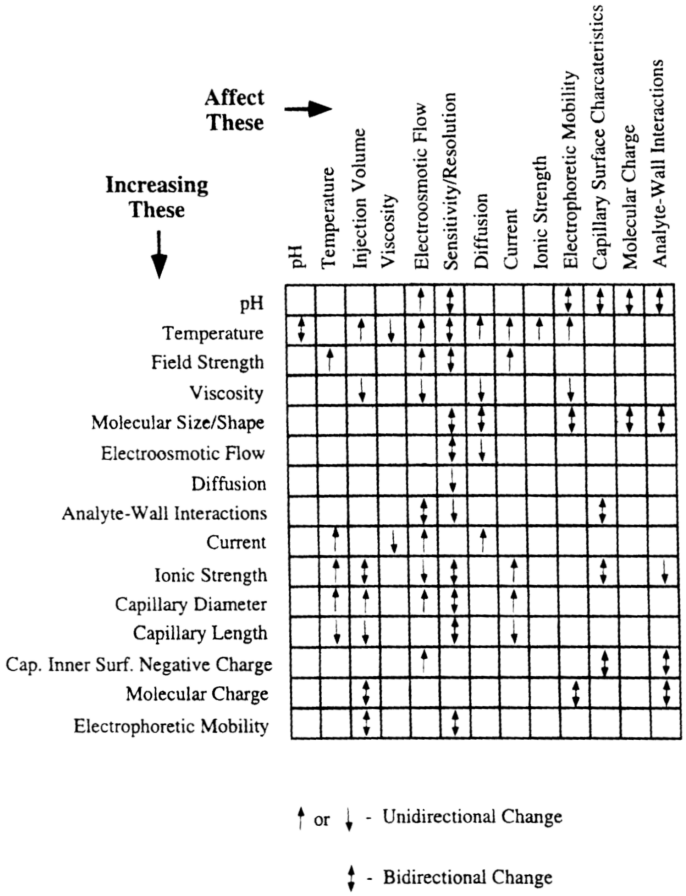

Figure 2-25 Reference chart for the evaluation of the relationships between variables influencing CE (Landers 1997)

3 Purification of Lactose

3.1 Introduction

As identified in Chapter 2, Visser (1980) observed that lactose from different sources exhibits different crystal growth rates. Visser gleaned information from a large number of crystallization experiments using pharmaceutical grade lactose. Pharmaceutical grade lactose requires very stringent quality control standards and it might be expected that between producers the growth rates would be very similar. This, however, was not the case. The objective was then to define the reason for such variations (Visser 1980). A compound was identified as being present in pharmaceutical grade lactose that was incorporated preferentially into the growing crystal; it was of acidic nature and had a pronounced growth retarding impact on faces (010) and (110).

Growth rate information on lactose was therefore incomplete, as the growth rate of the pure system was not accurately known. Later work by Visser (1984) identified the growth rate retarder as a disaccharide phosphate. The disaccharide phosphate was subsequently identified by Breg *et al* (1988) as a mixture of lactose monophosphates.

To fully understand the impact of the targeted growth retarders, a growth rate of pure lactose needs to be determined, and access to a consistent grade of purified lactose is required.

3.2 EXPERIMENTAL PLAN

To comprehensively understand the causes of growth rate inhibition in lactose, a pure source has to be obtained and studied. Growth rate studies (see Chapter 4), on a non-ionic lactose obtained through collaboration with the University of Western Sydney (UWS) showed that the average growth rate increases by a factor of ten, relative to the commercially supplied lactose. Due to limitations in the supply of non-ionic lactose, the work reported in this Chapter was undertaken to independently produce a highly purified form of lactose and then

to perform rigorous growth rate studies whilst varying the parameters of the crystallizing system.

Attempts were made to adapt the patent process used by our collaborators at the University of Western Sydney, UWS, to purify commercially available α-lactose monohydrate on a laboratory scale. This proved to be very difficult and expensive, and alternative methods were investigated.

Following the work of Visser (1980), initial attempts to purify lactose utilised ion exchange chromatography. The resultant product was analysed for elemental purity and phosphate content.

Alternative methods were also investigated; recrystallization under modified conditions, ion-exchange with different exchange materials and a novel surface interaction with zirconyl chloride functionalised surfaces.

3.3 METHODS AND MATERIALS

The purest form of commercially available α-lactose monohydrate was sought to conduct these studies. The lactose used in these preparations is from commercial chemical supplier Sigma-Aldrich, SigmaUltra α-lactose monohydrate, Lot 030K0189 and will be referred to as SUP.

3.3.1 Ion-exchange Chromatography

The purified form of lactose produced via ion-exchange chromatography is essentially 'ion-free' and for this study all Curtin preparations are termed *non-ionic lactose, NIL*.

Materials

The ion exchange resins were also from Sigma-Aldrich; DOWEX® 50WX4-50 ion-exchange resin and DOWEX® 550A OH anion exchange resin.

Solutions of hydrochloric acid and sodium hydroxide were prepared from analytical grade products. Purified water, milliQ, was used in all preparations.

Two glass columns were used, dimensions 250 mm length, 20 mm internal diameter with a straight flowing tap. The resin was held in place with a plug of glass wool.

Conductivity measurements were made with a calibrated Metler-Toledo conductivity meter.

Solutions were freeze-dried. Gelman vacuum filtration units were used with Supor membranes for filtration tasks.

Method

With heating and stirring 50 g of SUP lactose was dissolved in 200 g of milliQ water. The solution was filtered through a 0.45 μm membrane to remove insoluble impurities.

The cation exchange column was prepared by making a slurry of about 40 g of the DOWEX® 50WX4-50 ion-exchange resin in a 10 % HCl solution and pouring into a supported glass column. The tap was opened to allow the elution of the acid to settle the resin. The eluent was topped up as required. Resin was added to a height of 15 cm. The remaining resin was stored in the 10 % HCl solution. The resin was then washed with milliQ water. The resin swells and occupies the column to a height of 19 cm. The conductance of the output water was typically 2-8 μS. A quantity of this water was stored to use as eluent in the anion exchange resin.

The anion exchange column was prepared by making a slurry of about 30 g of the DOWEX® 550A OH anion exchange resin in a 5 % sodium hydroxide solution. The tap was open to allow the elution of the base to settle the resin uniformly. The eluent was topped up as required. Resin was added to a height of 22 cm. The resin was washed with milliQ water. The conductance of the output water was 1-5 μS.

The prepared SUP lactose solution had a starting conductivity of 78 μS. The SUP solution was introduced *via* a dropping funnel to the top of the cation exchange column. Care was taken not to disturb the surface of the resin and

the solution was run down the wall of the column. Elution was maintained at about 2 $mLmin^{-1}$. The conductivity of the output was measured and was typically 5-15 μS. The lactose solution was then washed through with an additional 50 mL milliQ water.

The now more dilute SUP lactose solution was similarly passed through the anion exchange column via a dropping funnel. Again the output conductivity was monitored and was typically 1-8 μS. The lactose solution was then washed through with previously treated milliQ water from the cation exchange column.

A significant quantity of the water was evaporated off the dilute SUP lactose solution via rotary evaporation and the lactose allowed to crystallize out, obtaining a ~50 % yield of NIL. It was determined that freeze-drying was a more efficient method for extracting the lactose, yielding ~74 % of NIL.

The ion-exchange resins were used until the conductivity of the output of the lactose solutions had increased significantly (ie.4 μS to 50 μS). The resins were then regenerated. The cation exchange resin was removed from the column and washed in an excess of 10 % HCl solution, which was sufficient to regenerate the H^+ loading. Problems were encountered with the anion exchange resin, as it appeared to discolour after it had been washed with water after treating the lactose solution. The resin could not be satisfactorily regenerated and a fresh quantity of resin was used for each batch.

3.3.2 Alternative Methods

At this stage the removal of phosphate analogues is the primary goal and these are expected to be anionic in solution. Lithium chloride/gibbsite compound ($[LiAl_2(OH)_6]Cl$) is a double-layered hydroxide that can be used as an anion-exchange material (Wang, 2007). The anion present is chloride in the material as synthesised, but often anions can be incorporated to fine-tune the anion-exchange properties.

25 g of SUP was dissolved in 100 g milliQ water with heat and stirring. Once dissolved the solution was allowed to cool to room temperature and filter with a 0.45 μm membrane.

SUP lactose contains approximately 130 ppm sugar-bound phosphate (0.325 g in 25 g SUP). The $[LiAl_2(OH)_6]Cl$ was added in excess to ensure sufficient anion-exchange capacity.

1 g of $[LiAl_2(OH)_6]Cl.H_2O$ was introduced to the cooled lactose solution and left to stir at room temperature for two hours. The solid was then filtered off. Ethanol (300 mL) was added to the solution, which was left overnight to crystallize. The lactose was then removed and dried, yielding 10.4 g lactose (41.6 %).

Activated carbon is a commonly used material for the removal of impurities from aqueous solutions. 25 g of SUP was dissolved in 100 g milliQ water with heat and stirring. Once dissolved the solution was allowed to cool to room temperature and filter with a 0.45 μm membrane. Approximately 5 g of analytical grade activated carbon was added to the solution and was stirred at room temperature for two hours. The solid was the filtered off. Ethanol (300 mL) was added to the solution, which was left overnight to crystallize. The lactose was then removed and dried.

3.3.3 Recrystallization

The aim of this approach was to reproduce Visser's earlier studies (Visser, 1980, 1982,1984), and use the affinity of lactose monophosphate for the growing lactose crystals to produce purified lactose through a fractional crystallization process.

Materials

Sodium hydroxide solutions were prepared from analytical grade products. Purified water, milliQ, was used in all preparations. Merck HPLC analytical grade methanol and analytical grade ethanol was also used.

A Metler Toledo pH meter and standard probe calibrated with Merck pH buffers was used.

Methods

The intention of these variations of procedure is to recover a lactose product that is phosphate rich. The remaining liquor will then be depleted of phosphate species and a purer form of lactose can be recovered. These procedures are termed 'enrichment'.

Following on from enrichment, a set of procedures was trialled to inhibit the incorporation of phosphate. The procedures are termed 'depletion.

Enrichment – 1 and 2

With stirring and heating to 70 ˚C, 30 g of SUP lactose and a quantity of sodium hydroxide was dissolved in a mixture of 175 mL milliQ water and 300 mL methanol. A small amount of SUP didn't dissolve and was removed whilst hot by vacuum filtration. The pH of the resultant solution was 11.7. This solution was left to cool at room temperature. An additional 100 mL of methanol was added and then placed in an ice bath for 45 minutes to encourage crystallization. The cold solution was then filtered by vacuum filtration through 542 Whatman filter paper. The solution was still cloudy and filtered again through a 0.45 μm Supor membrane, solution pH 11.8. The mother liquor was returned to the ice bath and a second crop of crystals was collected with the addition of 100 mL methanol. The final mother liquor pH was 11.9.

Depletion - 1

15 g of SUP lactose was dissolved in 80 mL water. Ethanol was then added (150 mL), the solution pH was 7.8. The pH of the solution was raised to 8 with a 5 % solution of sodium hydroxide. Complete dissolution was ensured with stirring and heat (max 70 ˚C). A quantity of ethanol was added to the warm solution, which in turn went cloudy. The solution was then warmed to 70 ˚C, the solution remained turbid. The solution was cooled and filtered (4 g, recovery 1). The pH of the solution was then increased to 11.9 with the

addition of 5 % sodium hydroxide. The solution was then allowed to cool and crystallize at room temperature. After 105 minutes there was little solid, which was filtered off (recovery 2). 70 mL of ethanol was added to the mother liquor, and the resulting solids were removed. An additional 50 mL was added to the mother liquor and an additional crop removed. These were combined (recovery 3).

Depletion - 2

An attempt was made to dissolve 15 g SUP lactose in 120 mL milliQ water and 150 mL ethanol, with heat and stirring. The lactose didn't appear to dissolve; an additional 50 mL of milliQ water was added. With heating and stirring, dissolution was complete after 90 minutes. The solution was cooled and had a pH of 5.3. The solution was filtered though a 0.45 μm membrane. An additional 200 mL of ethanol was added, the solution was placed in an ice bath and crystallization induced. The solids were removed (recovery 1) and the pH of the resulting solution was 5.6. An additional 100 mL of ethanol was added, no crystallization was apparent so a further 100 mL was added. A crop of solids were removed (recovery 2), the pH of the solution was now 6.3. Additional solids were recovered with the addition of a further 250 mL of ethanol (recovery 3). The resultant pH was 6.6.

The resultant purity is discussed in section 3.4.3.

3.3.4 Zirconium-phosphonate modified surfaces

In addition to these investigations a more novel approach to remove the lactose phosphate has been attempted. The hypothesis was that lactose phosphate might be successfully removed from a lactose- saturated solution by exploiting the strong affinity between zirconium and phosphate moieties. (Dong, J. *et al*, 2007).

Essentially, this procedure builds zirconium-based functional groups onto a silica surface, which then can react with the lactose phosphate in solution, binding it to the surface.

Materials and Methods

Zirconium phosphonate modified silica preparation

5 g of silica (Sigma-Aldrich, ~99 % purity, 0.5-10 μm) was dispersed in 50 mL of dry toluene to which 3-aminopropyl-triethoxysilane (APTES) (5.53 g, 25 mM) was added. The suspension was then refluxed for two hours. After cooling the solids were filtered off and washed with toluene and then dried under vacuum for 24 hours. The solids were then cured in an oven at 120 ˚C for 16 hours.

The treated silica was then slurried in a solution of 1:1 2,4,6-collidine (3.63 g. 30- mM) and phosphoryl chloride (4.60 g, 30 mM) in anhydrous acetonitrile (50 mL), to phosphorylate the surface. The solids were then separated by filtration, washed and dried.

The phosphorylated surface was zirconated by slurrying the silica in an aqueous solution of $ZrOCl_2$ (100 mL, 0.155 M) for 12 hours. The zirconium loading was not quantified, however, a qualitative investigation of the silica using energy dispersive X-ray spectroscopy confirmed the presence of Zr.

Lactose phosphate removal

A saturated solution of lactose was prepared at room temperature, 50 g SUP in 200 mL milliQ water. 200 mL of lactose solution was treated with 1.5 g of the zirconium-phosphonate functionalised silica. This was stirred for 36 hours at room temperature. The solid was then filtered off and the α-lactose monohydrate was crystallized out using ethanol.

3.3.5 Analysis

The recovered lactose samples from the methods outlined above were analysed for inorganic phosphate and total phosphate. From these quantities organic phosphate (referred to as sugar-bound) can be deduced. The method is described in the following sections.

Elemental analysis was also conducted on all samples using ICP-OES and AAS.

3.3.5.1 Total Phosphate

5 g of the lactose sample was accurately weighed into a 40 mL porcelain crucible with a lid. After the addition of 3.5 mL of a solution of 26.5 g $Mg(CH_3COO)_2$. $4H_2O$ in 1L ethanol the mixture was warmed on a hot plate to evaporate off the ethanol and then placed in a cold furnace and heated to 600 ˚C for 12 hours. The resulting ash was dissolved with 2 mL of 3 M HNO_3, rinsed with milliQ water, and filtered through a Whatman 541 filter, to give a solution that was analysed for total phosphate as described below.

3.3.5.2 UV/Visible Spectrophotometry

The phosphate concentration was determined by an optimised phosphomolybdic acid complexation using UV/Visible Spectrophotometry detection (Murphy and Riley, 1962). The method involves the formation of molybdophosphoric acid from ammonium paramolybdate and phosphate acid in solution, followed by reduction with ascorbic acid to form an intense blue coloured complex. Standards were prepared with potassium dihydrogen phosphate.

Reagent Preparation

The molybdate colour reagent was prepared by dissolving 1.61 g ammonium paramolybdate in 100 mL milliQ water, followed by 0.04 g potassium antimony tatrate and 14 mL 7 M H_2SO_4 then made to 250 mL with milliQ water.

Solution Preparation

Solutions of standards and samples were prepared to a total volume of 50 mL. 20 mL of each standard from the desired range and the samples (with adequate dilution) were added along with 500 μL of 7 M H_2SO_4, 5 mL of the molybdate colour reagent and 1 mL of freshly prepared 3 % ascorbic acid. The pH was

adjusted to between 3.5 and 4 with dilute sulphuric acid and made to volume with milliQ water. After agitation the solutions were left to develop the blue complex for 35 minutes at 30 ˚C in a water bath. Upon completion the samples were analyzed on a Shimadzu Mini UV/Visible Sprectrophotometer at 882 nm.

3.3.5.3 Inorganic Phosphate

Inorganic phosphate is determined spectrophotometrically in the same manner as the total phosphate, but instead of the ashing procedure the lactose is simply dissolved in water and the pH of the resulting solution is adjusted as outlined above. It is assumed that the inorganic phosphates are readily water soluble, and it is known that organic phosphates do not hydrolyse in this pH range and consequently do not interfere.

3.3.5.4 Elemental Analysis

Elemental analysis was performed on the ashed sample by ICP-OES and/or AAS.

3.4 RESULTS AND DISCUSSION

A number of purification techniques have been investigated. The criterion of success was specified as the degree to which the sugar-bound phosphate content was reduced. In practice, the efficiency of the techniques is also a consideration for any practical application, whether this is laboratory studies, or industrial processing.

The principles applied by Visser (1980, 1984) have been used in investigating ion-exchange chromatography and recrystallization. In addition to this, the more novel approach of exploiting zirconium-phosphonate chemistry has been studied.

To assess the purification procedures, it was necessary to select and test an appropriate method for phosphate analysis in lactose solutions.

3.4.1 Phosphate determination

As has already been discussed, to analyse lactose solutions for phosphate, organic and inorganic phosphate must be elucidated. This was done by determining the total phosphate content and subtracting the inorganic phosphate content. Despite this being an indirect method for determining organic phosphate it is suitable as an approximate means of calculating the organic phosphate.

To determine the total phosphate concentration the lactose product first must be digested to break the organic complex down and release the phosphorus to be available for complexation.

Care must be taken when preparing lactose samples for analysis of inorganic phosphate. If the solution is too acidic or too alkaline the sugar bound phosphate can be hydrolysed and lead to high phosphate results.

For the purpose of these initial investigations, a method of determining phosphate concentrations was sourced and trialled. The well-known colourimetric method utilising molybdenum blue has been optimized for the determination of total phosphate concentrations in the lactose products. This method involves the formation of molybdo-phosphoric acid from ammonium paramolybdate and phosphate acid in solution, followed by reduction with ascorbic acid to form an intense blue coloured complex, which absorbs at 882 nm.

Consistent colour development is the crucial component in an accurate determination. This relies on several factors; pH, reaction time and temperature and other ions present in solution.

The pH of the solution plays a crucial role in the analyte concentration. It must be controlled, to prevent hydrolysis of the organic phosphates, which would otherwise interfere with the inorganic phosphate determination. Lowry (1945), Visser (1984) and Bernabe et al. (1995) modified the molybdenum blue to maintain the lactose solution at pH 4.

A trial experiment was performed using lactose-1-phosphate and KH_2PO_4 to determine what is the most appropriate pH for measuring organic phosphate. Because lactose-1-phosphate is expensive and difficult to source the analysis was not exhaustive, but gave a reasonable indication of pH ranges for analysis.

A standard solution of 5 ppm inorganic phosphate from KH_2PO_4 and 5 ppm organic phosphate from lactose-1-phosphate barium salt was prepared with a resultant pH of 3.8. The solution was acidified with the addition of 7 M H_2SO_4 or made more alkaline with 5 M NaOH and stirred for 30 minutes in a 30 ^oC water bath. The slight concentration variations that occurred as a result of these additions was not considered significant. The results are shown in Table 3-1.

The results demonstrate that the pH of the lactose solutions should be maintained between 3.5 and 4 to avoid any hydrolysis of the sugar bound phosphate, which would lead to false high results (Figure 3-1).

Table 3-1 Inorganic phosphate measurement with varying pH

pH	Inorganic [PO_4] (ppm)
2	5.82
3	6.05
3.5	5.05
3.8	5.11
4	4.98
5.5	5.70

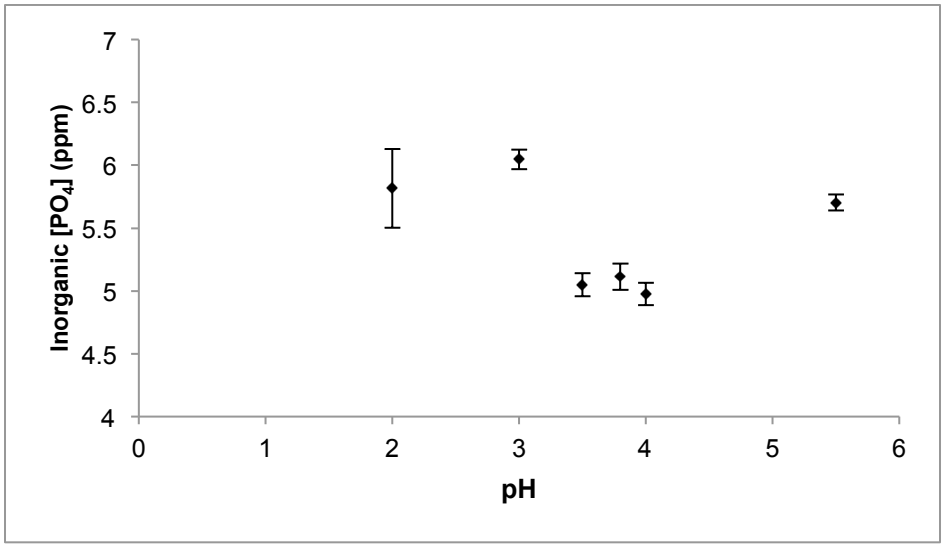

Figure 3-1 Impact of pH on Inorganic Phosphate Determination

In the initial stages of method validation it was observed that the colour development was inconsistent when the solutions were mixed and left at room temperature. Similarly the time taken to develop the blue colour and the maximum intensity also varied. To determine the optimum time for colour development, two standards (2 and 5 ppm) were made and absorbance measurements were taken at intervals. The solutions were maintained at 30 ˚C in a water bath. It was observed that colour development is relatively slow, taking 20 - 30 minutes to reach optimum absorption and then the colour rapidly depletes (Table 3-2). The colour of the solution does not completely fade but the shade changes from a royal blue to a grey/purple shade.

Table 3-2 Change in absorbance with time of molybdenum blue complex using PO_4 standards at 30 ˚C

	Absorbance	
Time (mins)	5ppm	2ppm
5	0.343	0.013
10	0.349	0.013
20	0.417	0.186
30	0.417	0.174
40	0.407	0.091
60	0.218	0.096

The molybdenum blue complex exhibits absorption maxima across a range of wavelengths and depending upon the path length in the measurement cell certain sensitivities can be achieved. For this study it was determined that for concentrations greater than 1 ppm phosphate, a 1 cm path length using an 882 nm wavelength provided good linearity. For less than 1 ppm, a 4 cm path length using a 700 nm wavelength provided good sensitivity and reasonable linearity (see Figure 3.2).

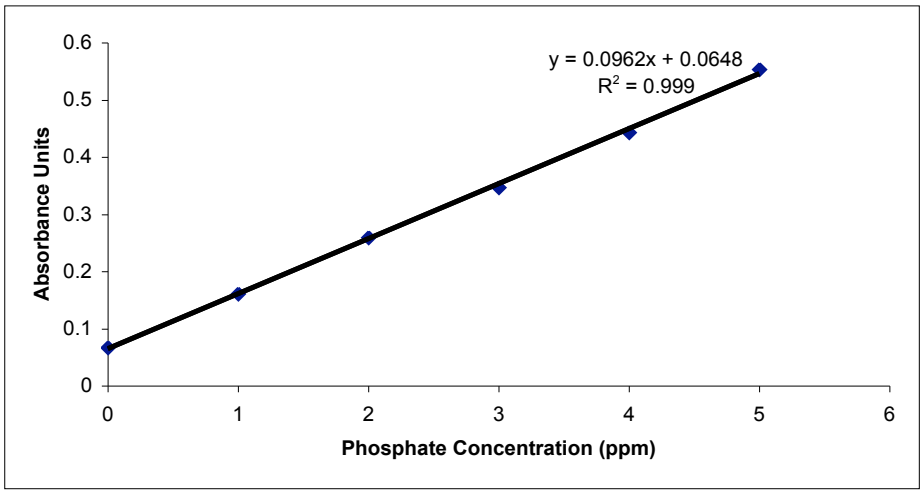

(a)

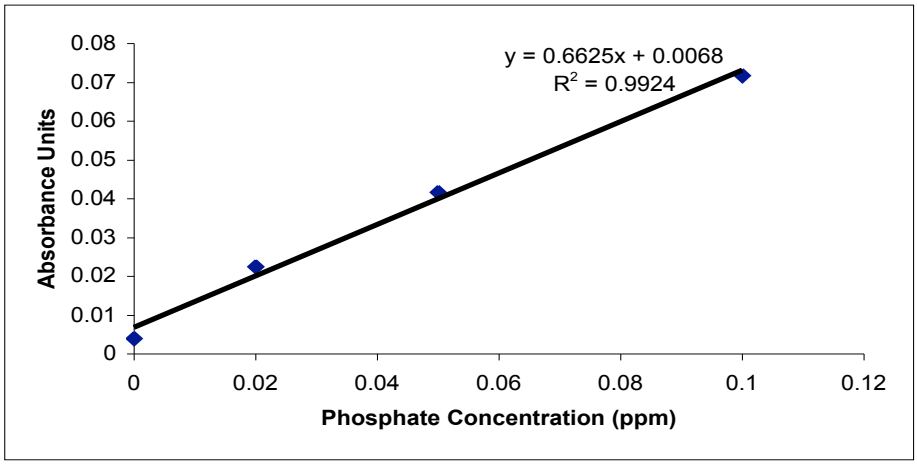

(b)

Figure 3-2 Molybdenum blue absorbance vs phosphate concentration for (a) 1 cm path length @ 882 nm and (b) 4 cm path length @ 700 nm

The intention is to determine low levels of phosphate after the lactose has been purified and it is therefore important to determine the detection limit. The method detection limit (MDL) is the constituent concentration that, when

processed through the complete method, can be detected at a chosen probability level.

The method detection limit was calculated for the blanks of the total phosphate with ashing and the inorganic phosphate method. Applying a *Student's t test* with a 99% confidence level, it was calculated that the total phosphate method detection limit is 0.003ppm. The inorganic phosphate method detection limit was calculated to be 0.062ppm

From these investigations it was concluded that the phosphomolybic acid complex was suitable for the intended application. It was determined that the pH of the reaction mixture should be maintained between 3.5 and 4, it should be held at 30 ˚C for at least 25 minutes and not longer than 35 minutes for complete colour development. Depending upon sensitivity required, a 4 cm or a 1 cm path length could be used reliably.

3.4.2 Ion-exchange chromatography

SUP lactose solutions were eluted successively through a cation exchange column and anion exchange column. The lactose was then recovered as so-called 'non-ionic lactose'.

Ion-exchange was successful in removing phosphate contaminants from the SUP lactose solution. Typically the conductivity of the initial lactose solution was about 90 μS and after ion exchange the output was less than 10 μS. This would suggest that some de-ionisation mechanism is taking place. This procedure was repeated a number of times and elemental and phosphate analysis were performed on the recovered lactose (NIL 1, 2 and 3). The total phosphate content of the SUP lactose has been reduced significantly. The results of a number of purifications are outlined in Table 3-3.

Alternative ion-exchange mediums were also trialled. Lithium intercalated gibbsite has been demonstrated to be effective at removing phosphate from water (Wang et al, 2006). $[LiAl_2(OH)_6]Cl$ was added in excess to a SUP lactose solution (25 g in 100 mL of water). This was unsuccessful at removing

phosphate species from the lactose solution. The analysis suggests that the intercalate may have promoted hydrolysis of the lactose phosphate, giving an increase in inorganic phosphate, with no change in the total phosphate level.

Activated carbon is a well-known filter agent, commonly used as a water purification medium. As a result of its porous nature it is known to remove a variety of cations and anions from aqueous solutions. An excess of activated carbon was added to a SUP lactose solution (25 g in 100 mL). This was successful at removing all detectable quantities of inorganic phosphate species. However, as shown by the results given in Table 3-3, it was not able to remove sugar bound phosphate to the required extent.

Table 3-3 Phosphate content of lactose samples produced by ion exchange

	Total $[PO_4]$ (ppm)	Inorganic $[PO_4]$ (ppm)
SUP	170.6	44.0
NIL 1	1.4	<dl
NIL 2	6.5	<dl
NIL 3	1.6	<dl
$[LiAl_2(OH)_6]Cl$	177.6	95.5
Activated C	64.8	<dl

Ion-exchange chromatography has been demonstrated to successfully remove inorganic and organic phosphate species, along with other metal impurities (Figure 3-3), successfully producing a significantly purified α-lactose monohydrate (NIL). There is some variability with the metal cation removal, but consistent reduction of phosphate species.

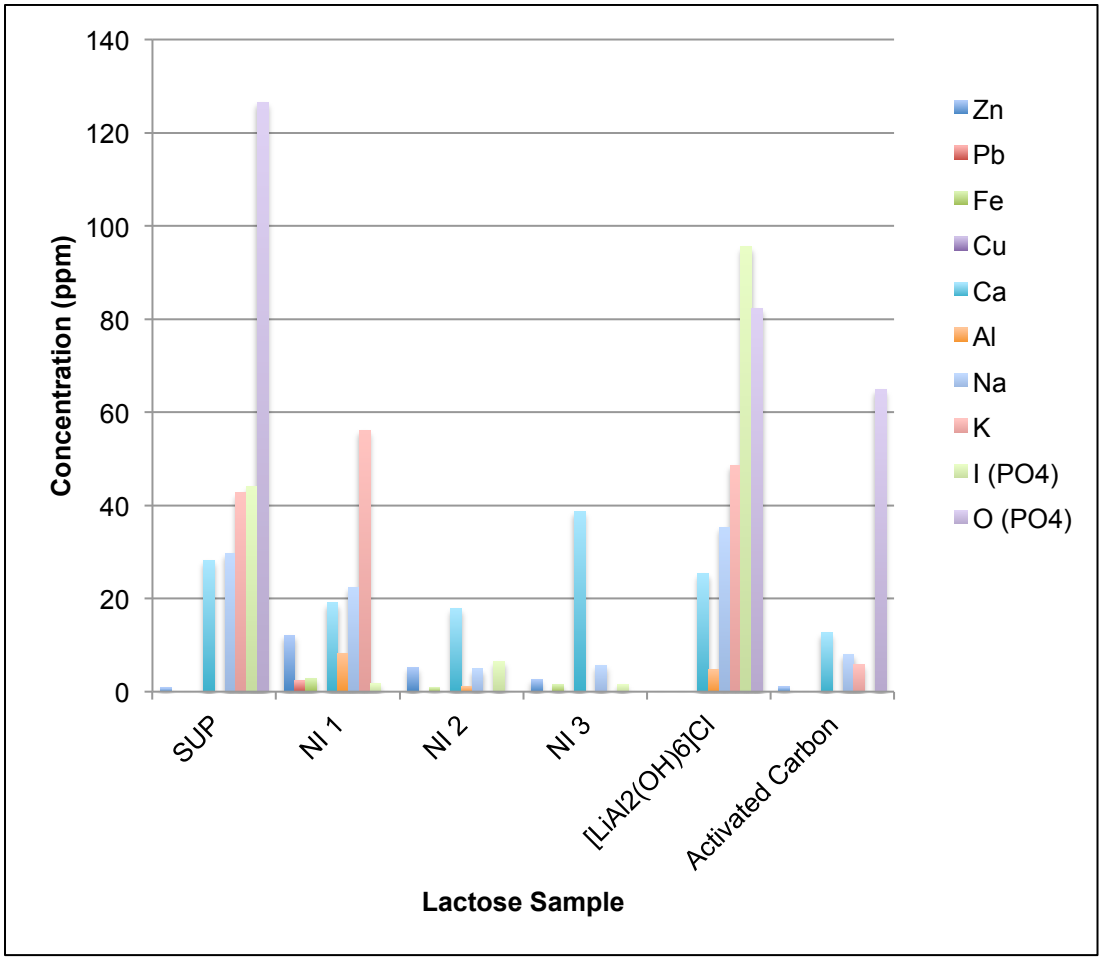

Figure 3-3 Analysis of lactose samples produced by various ion-exchange

3.4.3 Recrystallization

Applying a similar approach to Visser (1980, 1984) exploiting the recrystallization of lactose, the pH and lactose solubility has been altered in an attempt to either enrich the lactose with sugar phosphates or to remove it via recrystallization.

The key variables in the series of recrystallizations are pH and solvent. Recrystallizations were carried out over a range of conditions to determine the impact of these variables and the extent of phosphorous incorporation. The aim is to either prevent lactose phosphate incorporation or to enrich incorporation, allowing a small amount of highly impure material to be discarded with the bulk remaining in the purified form.

With the first attempt at recrystallization it was hoped that by raising the pH the sugar phosphates could be more efficiently concentrated into the first crop of crystals. Sugar phosphate species typically have pKa values of ~1 and ~6, (Jencks et al, 2010) which results in the speciation curve shown in Figure 3-4. Hence at a pH of 10, the dominant species will be the dianionic phosphate anion, which may be strongly absorbed onto the lactose nuclei.

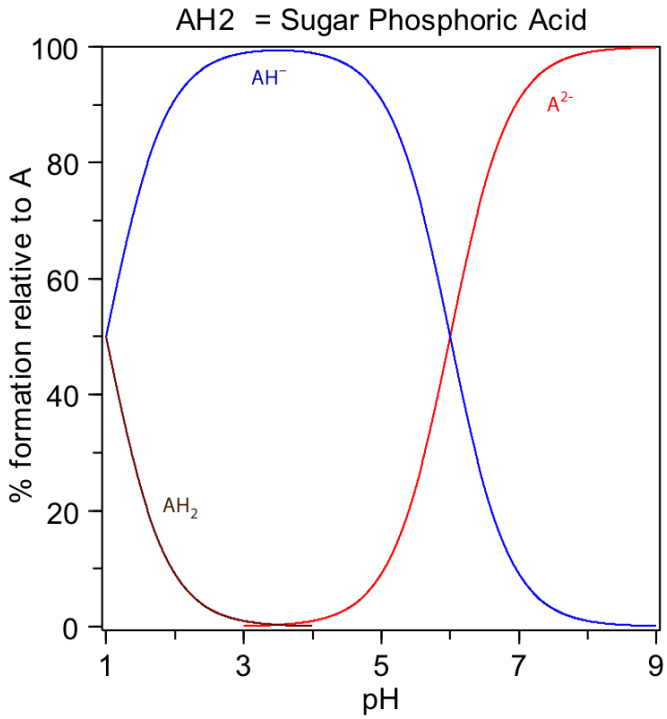

Figure 3-4 The relative concentrations of typical sugar phosphate species at different values of pH (generated using *HySS* L. Alderighi et al, 1999)

As shown in the recrystallization trials, the sugar phosphates were retained to the first crystallization and enriched with phosphate relative to the second fraction recovered (Table 3-4).

Table 3-4 Recrystallization – enrichment of lactose phosphates

	pH	Organic $[PO_4]$ (ppm)
Enrichment 1		
Initial recovery	11.8	99.6
Secondary recovery	11.9	11.1
Enrichment 2		
Initial recovery	11.8	91.1
Secondary recovery	11.9	10.8

Enrichment attempts 1 and 2 (Table 3-4) demonstrate that the initial recovery of lactose at the high pH can be consistently enriched with sugar bound phosphates. Subsequent lactose recovery from the remaining liquor has a reduced sugar bound phosphate content. The initial phosphate rich fraction yielded 7-8 g of lactose with the subsequent fraction only 2-3 g. The recovery of reduced sugar bound phosphate product is inefficient as a purification technique, with only a 13 to 20 % recovery of α-lactose monohydrate. It should be noted that at pH values greater than 8, lactose is likely to convert into lactulose and other unwanted products, (Playne, 1997) and this could have had an impact on these recrystallization processes. Given the poor recoveries, this aspect was not investigated.

An alternative approach was trialled using added ethanol to "drown out" the lactose, with the aim being to leave the lactose phosphate in solution. Solution pH values ranging from 5.6 to 11.9 were tested. Regardless of the pH used, and variations in the introduction of the ethanol before or after dissolution, the results were quite consistent in terms of lactose phosphate incorporation. (Table 3-5). The method does not eliminate or remove the sugar bound phosphate efficiently enough for it to be a suitable purification method.

Table 3-5 Recrystallization – depletion of lactose phosphate incorporation

	pH	Organic [PO_4] (ppm)
Depletion 1		
Recovery 1	7.8	29.1
Recovery 2	11.9	38.7
Recovery 3	11.8	31.9
Depletion 2		
Recovery 1	5.6	30.5
Recovery 2	6.3	30.4
Recovery 3	6.6	33.6

The enrichment recrystallizations performed at higher pH clearly gave a better result in terms of removing organic phosphates with the first crop of lactose recovered. There appeared to be little preferential absorption at lower pH values. This could be due to a number of factors which are difficult to resolve. Mutarotation of lactose is affected by changes in pH and temperature. Holsinger (1988) reports that mutarotation is minimal at pH 5 but rapidly increases at pH values < 2 and > 9. Mutarotation is directly affected by temperature, with the rate increasing rapidly with increasing temperature. The mutarotation equilibrium is not affected by pH (37.3 % α and 62.7 % β) and the amount of α-lactose present at equilibrium is slightly increased with temperature. The more rapid rate of mutarotation at higher pH may have resulted in more rapid crystal growth, thus capturing any adsorbed lactose phosphate more efficiently. It is also possible that the speciation of the lactose phosphate, particularly at the crystal surface, is substantially different at the different pH values studied. The surface charge of the lactose crystal surface could also change and influence adsorption of the lactose phosphate species. Given the poor recovery of only partly purified lactose, this approach was not deemed worthy of more detailed investigation.

3.4.4 Zirconium-phosphonate modified surfaces

Zirconium-phosphonate modified surfaces are reported to immobilize phosphate functionalised molecules (Lane, 2007). There are a number of

methods of preparing a surface, typically starting with a silica substrate. For this study the silicon oxide surface was functionalised by aminating with 3-aminopropyl-triethoxysilane (APTES) and then phosphorylating with phosphoryl chloride ($POCl_3$) in the presence of the tertiary amine 2,4,6-collidine. The prepared surface is then exposed to aqueous zirconyl chloride to form a surface terminated with reactive zirconyl chloride groups. A simplified diagram of this chemistry is shown in Figure 3-5. While much of the reported work involved phosphonates, Nonglaton (2003) reports that the coordination properties of free phosphate (OPO_3H_2) are very close to those of the phosphonic acid function and can graft similarly to the zircomium-phosphonate surface. Hence, a surface terminated with the reactive zirconyl chloride moieties as shown in Fig 3-5 may be a useful means of removing phosphate-containing species from a lactose solution.

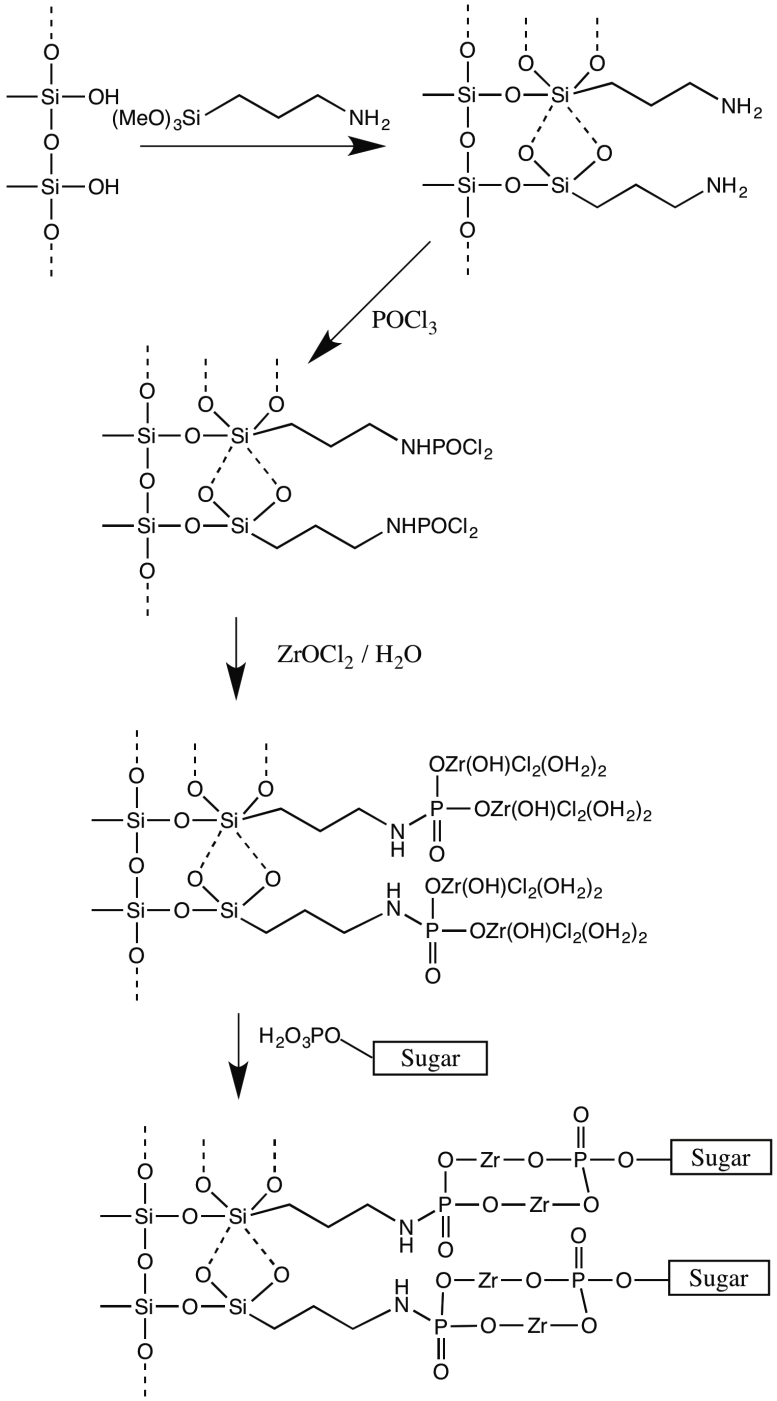

Figure 3-5 Zirconium-phosphonate modified surface.

The majority of the work reported exploiting this interaction is focused on building layers on silica wafers or glass slides (Massari et al, 2003). One property of the chemistry not reflected in Figure 3-5, is that the zirconyl moieties can react with multiple phosphonate groups and similarly the

phosphonates can bind to more than one Zr^{4+} ion. This cross-linkage can be used to provide a very stable mono- or multi-layer of zirconium-phosphonate sites (Nonglaton, 2003). In this work, monolayer formation is not critical, as it is the selective binding of phosphate-containing species that is of interest. Hence, instead of a silica wafer or slide, silica gel was used. Silica gel allows an increased surface area providing more reactive sites for phosphate capture and is easier to handle with the required volumes of lactose solution. Indeed, similar chemistry has been used to modify a monolithic capillary column, to selectively capture phosphopeptides. (Dong et al, 2007).

A solution of SUP α-lactose monohydrate (50 g in 200 mL milliQ water) was prepared. A quantity (1.5 g) of zirconium-phosphonate silica was added to the lactose solution and left to stir at room temperature for 36 hours. A blank run using silica gel only and a lactose solution was prepared simultaneously. All solutions were filtered and the α-lactose monohydrate was crystallized.

All accumulated lactose samples were then tested for total and inorganic phosphate. The results are summarised below in Table 3-6.

Table 3-6 Impact of Zirconium-phosphonate product on phosphate content in SUP lactose.

	Total $[PO_4]$ (ppm)	Inorganic $[PO_4]$ (ppm)	Organic $[PO_4]$ (ppm)
SUP	174.5	46.0	128.5
Silica Gel	179.8	45.6	134.2
Zr-phosphonate	13	8.4	4.6

The total phosphate content was reduced ten fold. Total phosphate for the SUP lactose was determined as 0.017 % and after treatment was 0.001 %, which is largely the inorganic phosphate component. Treatment was also performed using untreated silica gel to confirm that the action was due to the zirconium-phosphonate functionalisation. The phosphate analysis indicated that the silica gel alone had no impact on the phosphate content. While time constraints prevented a more detailed assessment of this method, it appears this could be a

useful means of preparing phosphate-reduced lactose samples, particularly on a laboratory-scale.

3.5 CONCLUSIONS

Ion exchange chromatography has proven to be the most effective means of purifying the SUP α-lactose monohydrate. It is, however, a cumbersome and time-consuming technique. The technique requires constant monitoring of conductivity and fraction collection. The purified α-lactose needs to be recovered from solution, and being so dilute any method employed is again, slow. There was always difficulty in regenerating the resins. Often the resin would decompose and would have to be discarded, making the method quite costly. Overall, this method is best suited to a large-scale continuous industrial process where the column conditions can be controlled more tightly.

Recrystallization methods and activated carbon were able to reduce the inorganic phosphate content, but were unable to reduce the organic phosphate content significantly enough to produce a pure α-lactose monohydrate. While Visser's work shows that multiple recrystallizations can achieve the desired outcome, it is a time-consuming process that is difficult to scale-up in the laboratory.

The zirconium phosphonate modified surface preparation was surprisingly effective at reducing the overall phosphate content of the SUP α-lactose monohydrate. This technique is simple to execute on a laboratory scale in comparison to the other techniques. Very little materials, intervention and handling are required for the method, and this may make it particularly useful for future lab-scale crystal growth studies.

4 Growth Rate of α-lactose monohydrate

4.1 INTRODUCTION

The crystallization of α-lactose monohydrate is complicated by several factors. Principally, the α-lactose exists in equilibrium with its isomeric β- form. At room temperature an equilibrium solution of lactose will contain 38 % α-lactose and 62 % β-lactose. The two isomers exhibit significantly different properties. The constant presence of β-lactose means that α-lactose is very difficult to grow from a pure environment, and this certainly can't be achieved under industrially relevant conditions. These studies focus on the growth of α-lactose only, as the properties of the system are such that β-lactose does not crystallize under the conditions of interest here.

The growth mechanism is additionally influenced by the typical crystal growth factors; temperature, solubility, supersaturation, nucleation, impurities and growth rate dispersion.

It is the presence of impurities that has been the main focus of these investigations. As discussed in the preceding chapter, obtaining a pure source of lactose is not without complications, and hence crystallization in the presence of impurities is of relevance in any practical situation.

As observed by Visser (1980), lactose from different sources exhibit varied single crystal growth rates. Crudely speaking, lactose is a by-product of cheese manufacturing and is recovered from whey. The means of purifying is generally recrystallization. It has been identified by Visser (1980) that lactose contains a 'natural growth retarder'. The details have been summarized in chapter 3, section 3.1.

In these studies the growth rates of purified lactose and analytical grade lactose (SUP) have been investigated.

The objective is to quantify the true growth rate of α-lactose monohydrate under defined conditions. Initial investigations will involve measuring the

growth rate of the un-purified lactose, SUP. Additional analyses will then be performed on the product obtained after further purifying the SUP lactose by ion exchange chromatography (refer to 3.2.1).

The growth rate of the (010) face will be measured as a surrogate for overall growth rate, as it is reported to be the fastest growing face (Dincer, 2000).

4.2 METHODS AND MATERIALS

4.2.1 *In situ* optical microscopy

In situ optical microscopy has been utilized to monitor the growth of individual α-lactose monohydrate crystals. This technique allows for the growing crystal to be observed at constant temperature and supersaturation. The experimental set-up comprises an optical microscope, camera and software and an *in situ* growth cell. A schematic of the *in situ* cell is shown in Figure 4-1.

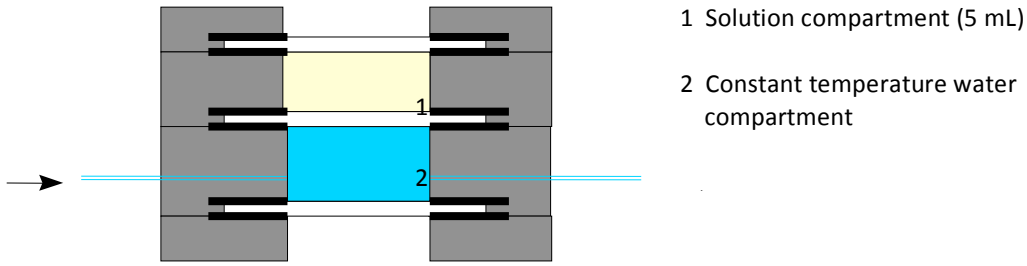

Figure 4-1 Schematic of *in situ* cell used for crystal growth experiments.

The *in situ* cell consists of two compartments, the upper one houses the supersaturated and seeded solution and the lower is the re-circulated water compartment, which maintains the desired cell temperature. Images of the crystal are captured at nominated time intervals using a video camera and software (Figure 4-2).

The cell is made from stainless steel and the compartments are separated by thin glass slides and sealed with rubber o-rings.

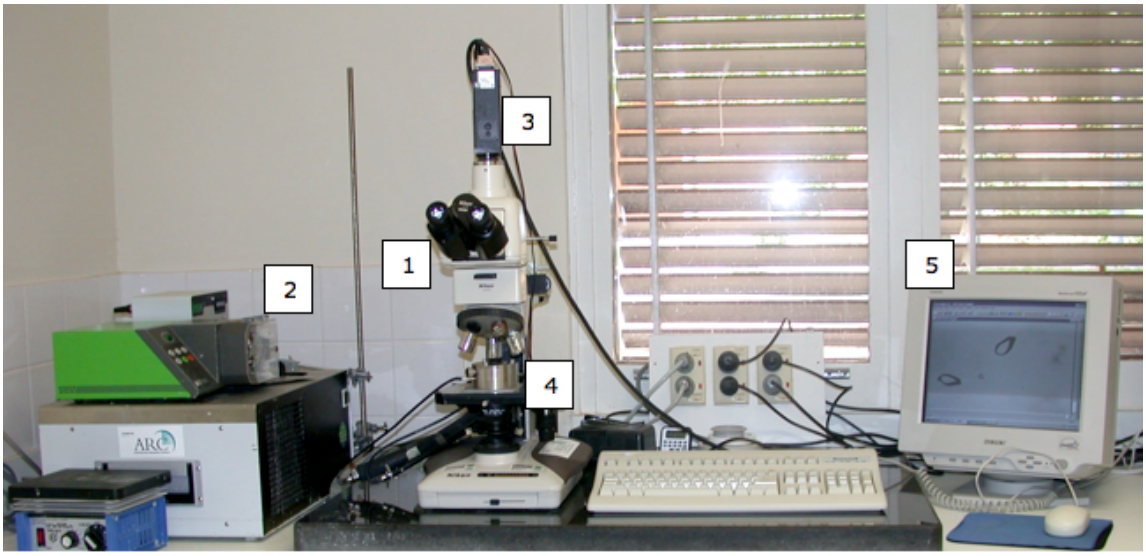

Figure 4-2 *In situ* growth rate experimental set-up (1) Transmission type Optical Microscope, (2) Grant Instruments W14 re-circulating water bath, (3) Pulnix TM-9701 Progressive Scanning full-frame-shutter camera, (4) *In situ* cell, (5) Optimas Version 6.2, Optimas Corporation,Bothell, Wa., U.S.A.

The α-lactose monohydrate crystals were grown using the 'common history seed' (CHS) method devised by Bronwen Butler (1998), as described below.

A suitable quantity of α-lactose monohydrate is dissolved with heat and stirring to prepare an adequate volume of lactose solution with 0.55 supersaturation (equivalent to 10 g lactose in 25 g milliQ water). Upon cooling to room temperature the solution is vacuum filtered with 0.45 μm Millipore membrane. The solution is then transferred to a 50 mL glass conical flask covered with parafilm, to initiate nucleation, it was placed into an ultrasound bath (0.73 A, 35 KHz) for 3 minutes and then into a 30 ˚C water bath for 20 hours. After at least 20 hours the seed crystals have formed. The solution was gently agitated and an aliquot of the seed containing solution is transferred into the *in situ* growth cell containing a supersaturated solution of lactose, equilibrated at 30 ˚C. Images of the growing crystals were then captured at recorded time intervals. Measurements of the crystal were taken of the length of the $(0\bar{1}1)$ face, the b direction (see Figure 4-3). Measurements were performed using the Optimas software and ImageJ software (freeware download http://rsb.info.nih.gov/ij).

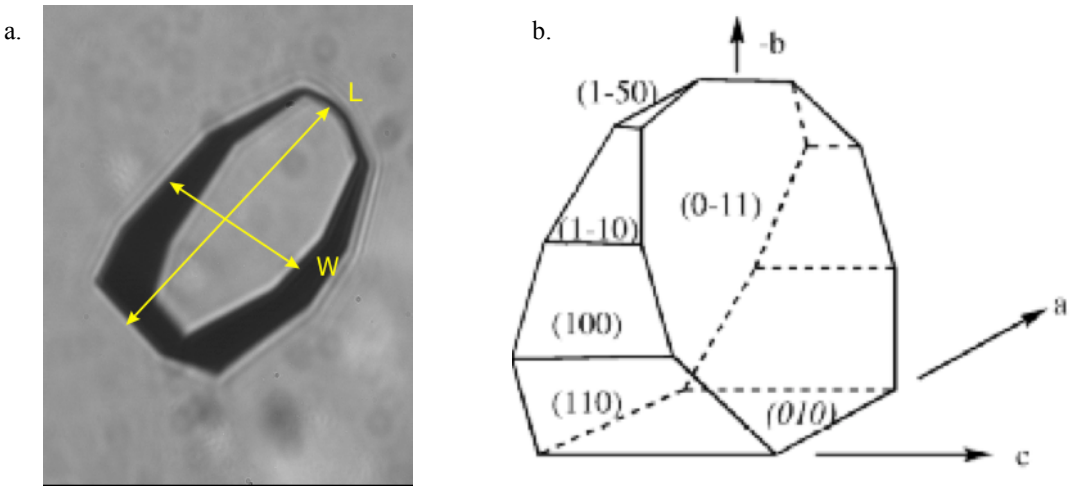

Figure 4-3 (a) Tomahawk morphology indicating length and width measurement
(b) Schematic of lactose crystal, tomahawk morphology (Visser and Benema, 1983)

After analysis the solutions were filtered with a 0.45 μm membrane. The mother liquor was frozen and stored for further analysis. The crystals were washed in succession with a series of solutions with varying water and ethanol (ratios 75:25, 50:50, 10:90 and pure ethanol), all saturated with SUP α-lactose monohydrate. The crystals were then placed in an oven at 50 ˚C, overnight and then stored for further surface observations.

The single crystal measurements were compiled and rates were calculated in Microsoft Excel. The rate for individual crystals was determined; standard error and relative standard deviation was also calculated based on a linear trend. Figure 4-4 illustrates a single crystal growth rate determination. Figure 4-5 is the compiled growth rate data. Growth rates for individual crystals have been calculated for the one experiment. All measurements of each data set have been acquired under identical conditions.

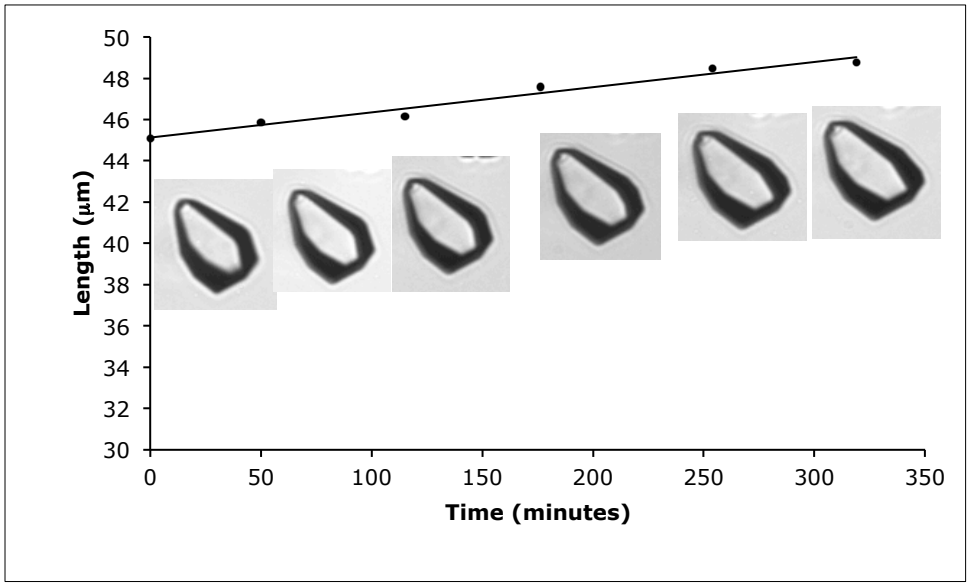

Figure 4-4 Growth rate determination of single crystal, growth rate 0.0122 µm/min, SE 0.0011, RSD 0.965

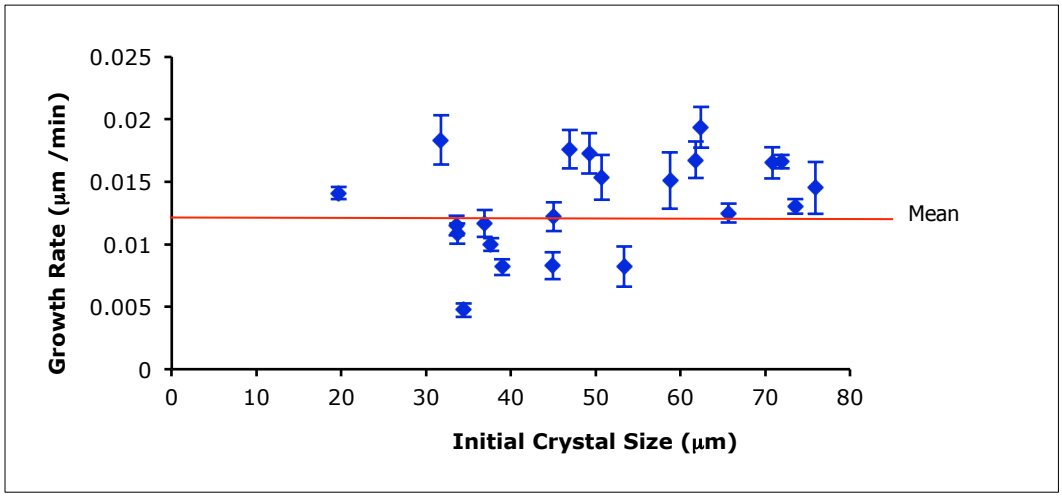

Figure 4-5 Growth rate dispersion plot of multiple single crystal measurements of the (010) face (SUP pH 3.59)

In Figure 4-5 error bars have been applied. These are based on the standard error that has been calculated for each growth rate calculation.

4.2.2 Lactose Solution Concentration

High Performance Liquid Chromatography (HPLC) was used to determine lactose concentrations. A Waters Resolve 5 µ C_{18} column, 3.9 mm x 300 mm,

Waters 510 HPLC pump and a Waters 410 Differential Refractometer detector were used. The column was conditioned prior to use by running de-gassed milliQ water for 45 minutes. The temperature was maintained at 35 ^{o}C and the flow rate was set at 0.5 mLmin^{-1}. Standard solutions were prepared from the SUP α-lactose monohydrate dissolved in milliQ water, then filtered through a 0.45 μm Millipore membrane and diluted in series to make 200, 400, 600, 800 and 1000 ppm solutions.

Typically the solutions were frozen after growth rate measurements were performed, and accumulated to allow for efficient use of time and equipment. The solutions were defrosted in a water bath and homogenized. They were all filtered with a 0.45 μm Millipore prior to injection into the HPLC.

The Waters Resolve column used was able to separate α-lactose and β-lactose, however baseline resolution was not achievable. An example of a typical chromatogram is below (Figure 4-6). The first peak to elute is α-lactose with a retention time typically about 5.20 minutes, followed by the elution of the β-lactose with a retention time of 5.50 minutes.

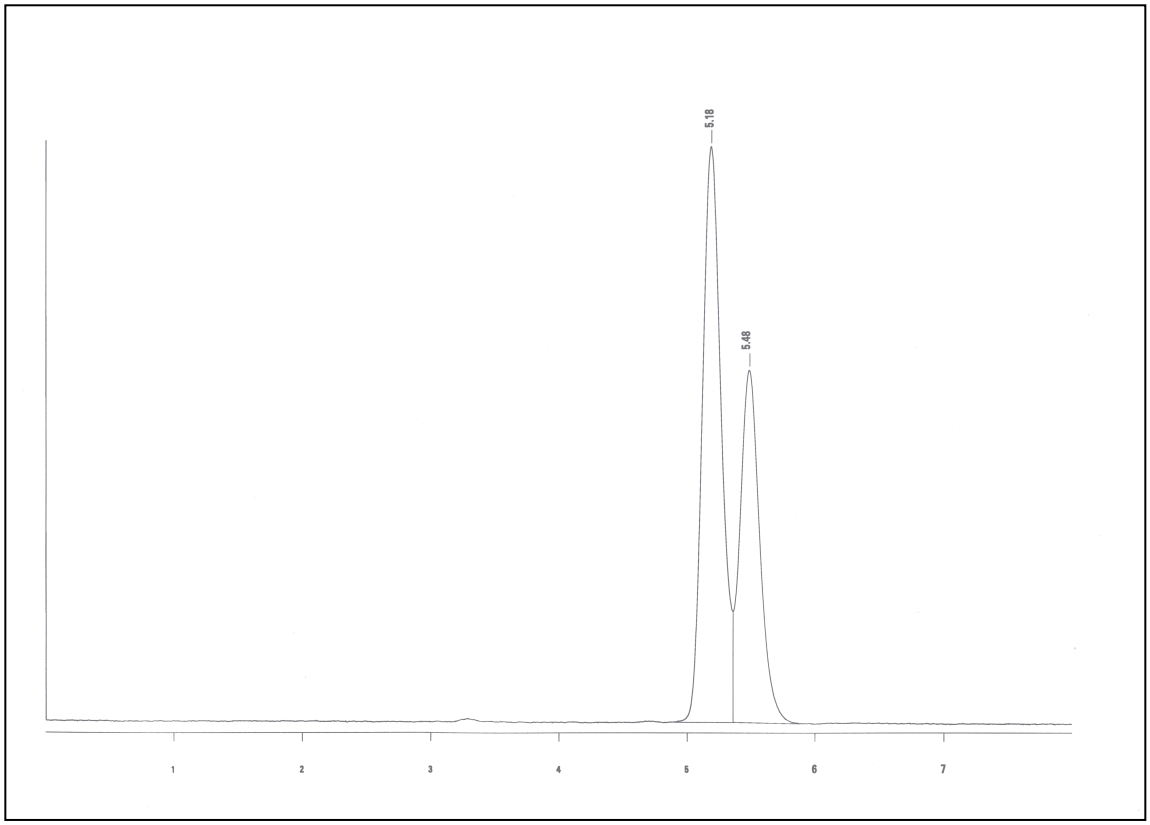

Figure 4-6 Typical HPLC chromatogram of α-lactose and β-lactose

Calibration curves were constructed from the output of the standard solutions. This is determined by measuring the integrated area of the peaks to a suitable baseline using the software on the HPLC unit. These results are then compiled and calculations are made in Microsoft Excel (Figure 4-7).

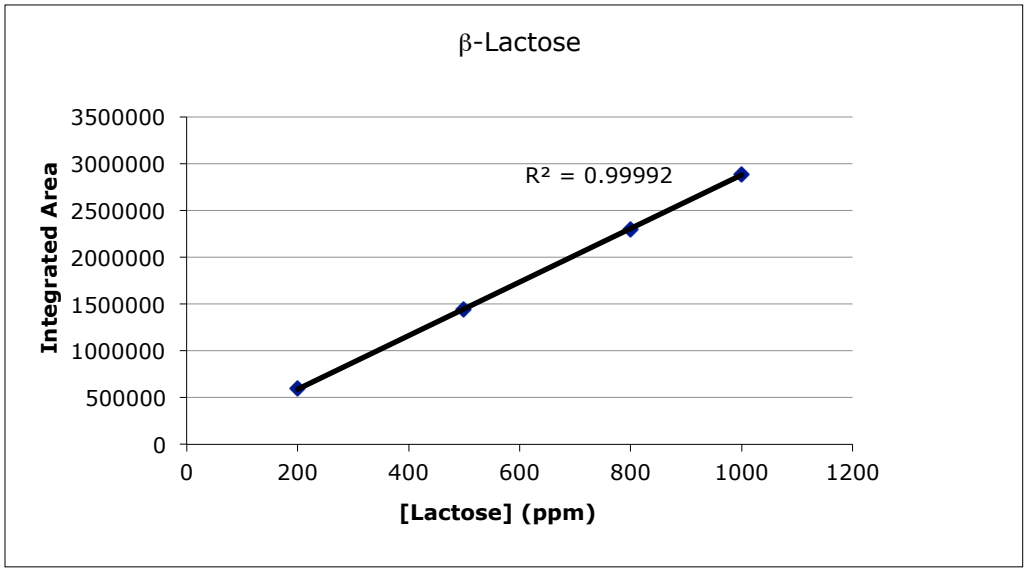

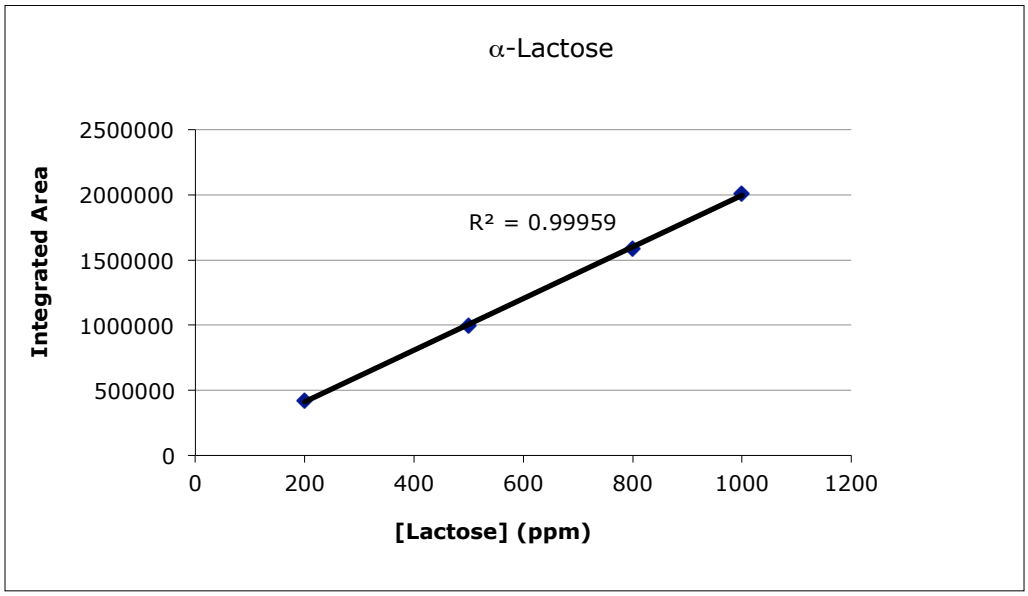

Figure 4-7 Typical calibration curves for determining α- and β-lactose concentrations in solution using HPLC.

4.3 RESULTS AND DISCUSSION

Growth rate experiments have been conducted on a number of different lactose samples of varying levels of purity, and the growth behaviour has been examined under a range of pH conditions.

Samples of α-lactose from our collaborators at the University of Western Sydney have been studied. These lactose samples are a product of the patented ion exclusion process (IEL) that has been engineered to purify lactose (Process

for the purification of nutrients from food process streams, Australian Patent Office, Patent No. 726559). Sigma-Aldrich, Sigma Ultra α-lactose monohydrate (SUP) and the purified product from ion exchange, NIL (refer to section 3.2.1) have also been examined.

4.3.1 Ion Exclusion Lactose (IEL) from the University of Western Sydney

Samples of α-lactose monohydrate were obtained from the University of Western Sydney (UWS). These samples were obtained throughout the development of the ion exclusion pilot-plant. Upon receipt, these samples were analysed for phosphates and elemental content using the methods detailed in section 3.2.5. Growth rate studies were performed following the procedures outlined in section 4.1.1. The samples named IEL-1 and IEL-2 are samples acquired by purifying The UWS Blank via the 'Ion Exclusion' process. The elemental analysis of the UWS-provided samples and the SUP α-lactose monohydrate used throughout these investigations is outlined below in Table 4-1. The IEL-1 sample was the first to be supplied and the elemental results show some improvement in purity after the process with respect to sodium and potassium, but with some increase in trace amounts of other contaminants. The IEL-2 sample was acquired some time later, after refinements had been made to the process at UWS and the results indicate dramatic improvement in the purification.

Table 4-1 Elemental Analysis of UWS lactose samples

Element	Concentration (ppm)			
	UWS Blank	IEL-1	IEL-2	SUP
Zn	<dl	1.31	<dl	0.87
Pb	<dl	1.93	<dl	<dl
Fe	<dl	0.69	<dl	0.02
Ca	3	8.63	3	28.14
Na	33	27.03	5	29.61
K	79	16.37	15	42.66

dl = detection limit

Table 4-2 Phosphate analyses and growth rates of UWS lactose samples

	UWS Blank	IEL-1	IEL-2	SUP
Total [PO_4]	217.6 ppm	131.8 ppm	10.77 ppm	170.6 ppm
Inorganic [PO_4]	73.18 ppm	8.65 ppm	1.63 ppm	43.98 ppm
Organic [PO_4]	144.4 ppm	123.2 ppm	9.14 ppm	126.6 ppm
Growth Rate (μm/min)	0.004 (1)	0.025 (7)	0.049 (7)	0.013 (1)

The effectiveness of the process is highlighted by the phosphate results. As the results given in Table 4-2 show, the total phosphate levels are significantly reduced.

Growth rate experiments were then performed to confirm the impact of purification; a summary of the results is displayed in Table 4-2. There is a clear inverse correlation between phosphate levels and growth rate, consistent with the expected impact of lactose phosphate as a growth rate inhibitor.

4.3.2 Non-ionic Lactose (NIL)

To attempt to determine the optimal growth rate of α-lactose monohydrate, Visser's (1980) ion exchange method was initially applied to purify lactose to higher levels. This purer form of lactose was successfully produced and is

termed here ‘non-ionic lactose’ or ‘NIL’. The product has been thoroughly analysed and the growth rate of the α-lactose monohydrate has been determined.

Table 4-3 Elemental analyses of NIL products

Element	Concentration (ppm)			
	SUP	NIL 1	NIL 2	NIL 3
Zn	0.87	3.07	5.29	2.71
Pb	<dl	1.91	<dl	<dl
Fe	0.02	0.92	0.98	1.6
Ca	28.14	14.97	17.78	10.59
Na	29.61	27.54	4.88	5.65
K	42.66	<dl	<dl	<dl
Total [PO_4]	170.6	1.4	6.5	1.6
Inorganic [PO_4]	43.98	<dl	<dl	<dl
Organic [PO_4]	126.62	<dl	<dl	<dl

dl = detection limit

Elemental analysis shows that the ion chromatography does contaminate the lactose with trace levels of zinc, lead and iron. The significant contaminators, calcium, sodium and potassium are however substantially reduced (Table 4-3).

The most significant component is the levels of phosphate. Phosphate levels are reduced by a factor of 25 and are present in trace levels only in the NIL (Table 4-3). As expected this has a substantial impact on the growth rate of α-lactose monohydrate. The growth rate of the non-ionic lactose is 0.12 ± 0.023 μm/min. This can be compared with that of the SUP α-lactose monohydrate, average growth rate of 0.013 ± 0.001 μm/min (organic phosphate, 126.6 ppm), and the IEL-2, with a growth rate of 0.049 ± 0.007 μm/min (organic phosphate, 9.14 ppm). There is a ten-fold increase in the growth rate after removing the organic phosphate from the typical pharmaceutical grade SUP sample.

When comparing the growth rates it is important to make note of growth rate dispersion (GRD). GRD is the phenomenon where it is observed that individual crystals, grown under identical conditions, can grow at different rates. This is generally a result of different interferences with the surface integration on different crystals. Poisoning by impurities is thought to be the common cause, but can also be the result of varying degrees of strain, deformation and dislocation in the individual crystal structures (Mullin, 1997). The origin of GRD in specific systems is an active area of research.

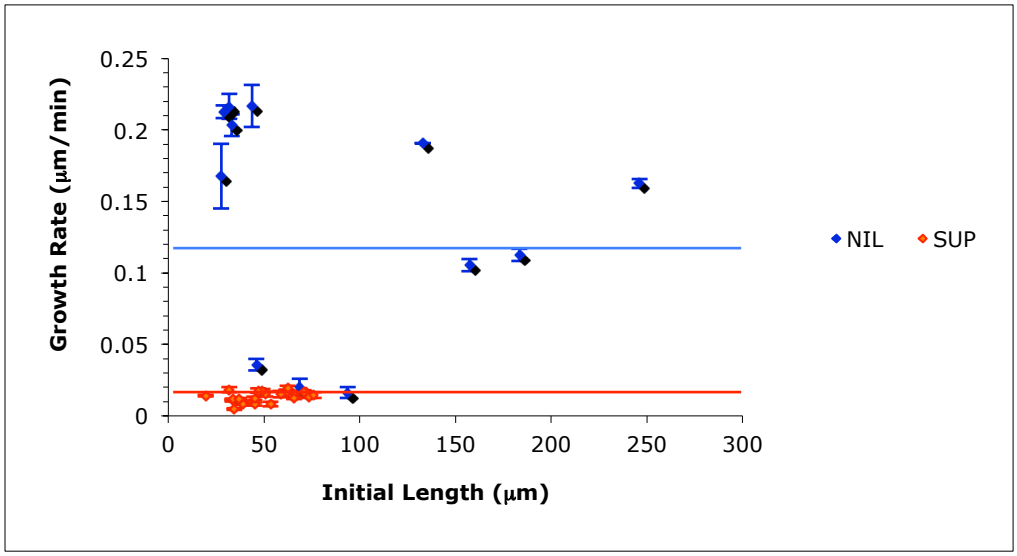

Figure 4-8 Growth Rates of NIL product and SUP starting material

GRD is observed in Figure 4-8. The SUP growth rate data shows minimal variance in GRD, with very little spread about the average growth rate. In contrast, the NIL growth rates exhibit significant variance from the average. Higher growth rates are reported to exhibit greater GRD variance (Liang *et al*, 1991). Shi et al (1989) studies revealed that each lactose crystal grows at a constant rate, but different crystals have different growth rates. Growth rate dispersion was shown to increase on the (010) face as the mean growth rate of that face increased.

There is a distinct difference in the crystal morphology of the SUP α-lactose monohydrate and the NIL α-lactose monohydrate. As shown in Figure 4.9 the

NIL crystal is larger in the b-direction producing an elongated tomahawk morphology.

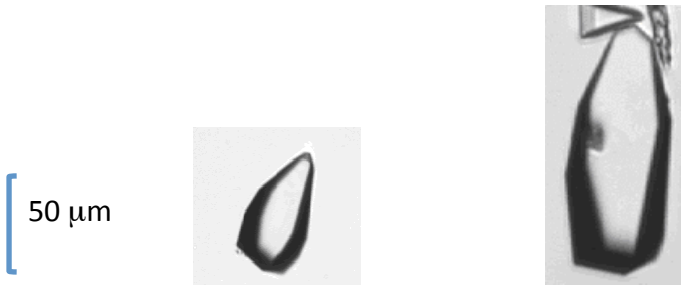

(a) (b)

Figure 4-9 Micrographs of a) SUP α-lactose monohydrate, b) NIL α-lactose monohydrate grown for 48 hours, ss 0.55 @ 30 ^{o}C.

Table 4-4 Morphology factors of SUP and NIL α-lactose monohydrate

	SUP α-lactose monohydrate	NIL α-lactose monohydrate
Mean crystal size	85.7 μm	150.5 μm
Starting pH	3.6	6.9

Overall, the NIL crystals have a much higher average length, 150.5 μm compared to the SUP α-lactose monohydrate of 85.7 μm. The NIL preparation has a significantly broader crystal size dispersion compared to that of SUP, Figure 4-10. The pH of the two solutions are different, as expected given the removal of the acidic lactose phosphate from the NIL sample. In these preliminary experiments, the natural pH values of the lactose samples were used for the crystallisation experiments.

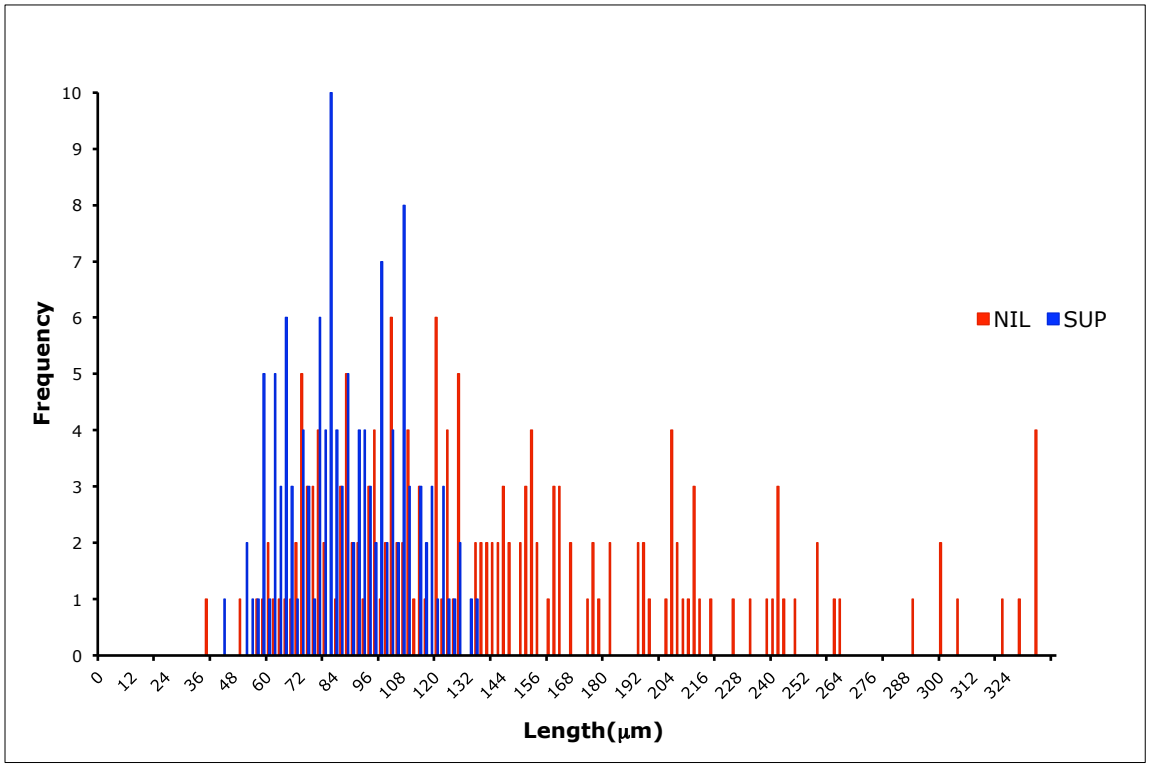

Figure 4-10 Crystal size distribution after 48 hours, ss 0.55 @ 30 ^{o}C

When the length versus the length on width ratio is plotted (Figure 4-11) there is a positive correlation for the NIL data. The ultimate impact of this trend on the morphology would be to grow out the (010) face, a possible consequence of a faster growing system. The SUP doesn't appear to exhibit this trend, but this may be due to the slower growth rate limiting the observations. It is possible that a comparable trend may be observed if the growth period for the SUP crystals is extended. The differences in pH and average growth rate may also account for this difference, and these aspects were targeted for further investigation.

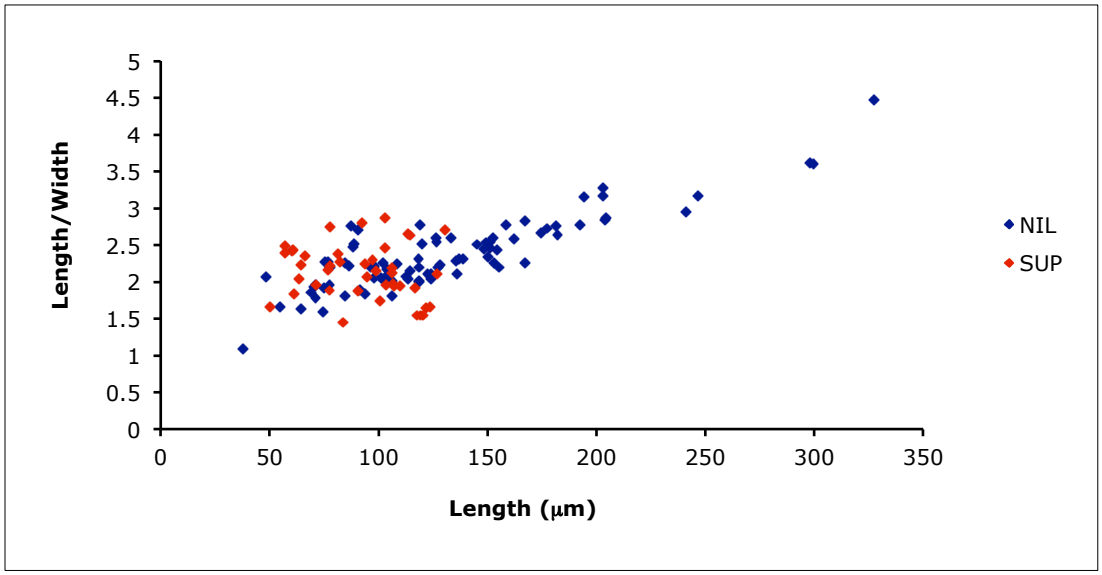

Figure 4-11 Difference in morphology between SUP and NIL α-lactose monohydrate

After this preliminary work, it became evident that producing NIL α-lactose monohydrate was inefficient, in terms of time and cost versus output. We were fortunate to acquire a suitable quantity of purified IEL α-lactose monohydrate from our UWS collaborators. As has already been discussed, this α-lactose product is highly purified and exhibits very similar growth rates to the NIL α-lactose monohydrate and it was deemed suitable for use as a source of pure α-lactose for the rest of this study.

4.3.3 Impact of pH

It is clear from the results discussed in the previous section that the pH of the crystallizing system may also have an impact upon the growth rate of the α-lactose monohydrate. To examine an impure system, growth rate experiments were conducted on the SUP α-lactose monohydrate at three different pH values; a pH close to neutral (6.96), the natural pH for a solution of 0.55 supersaturated SUP α-lactose monohydrate (3.59) and a low pH (1.68).

As observed in the plot below (Figure 4-12) growth rates and growth rate dispersion differ greatly between pH values. It is apparent that at a lower pH

the growth rate of the SUP is considerably faster than the higher pH systems. However the higher pH systems are producing in general a longer crystal and a greater spread of sizes.

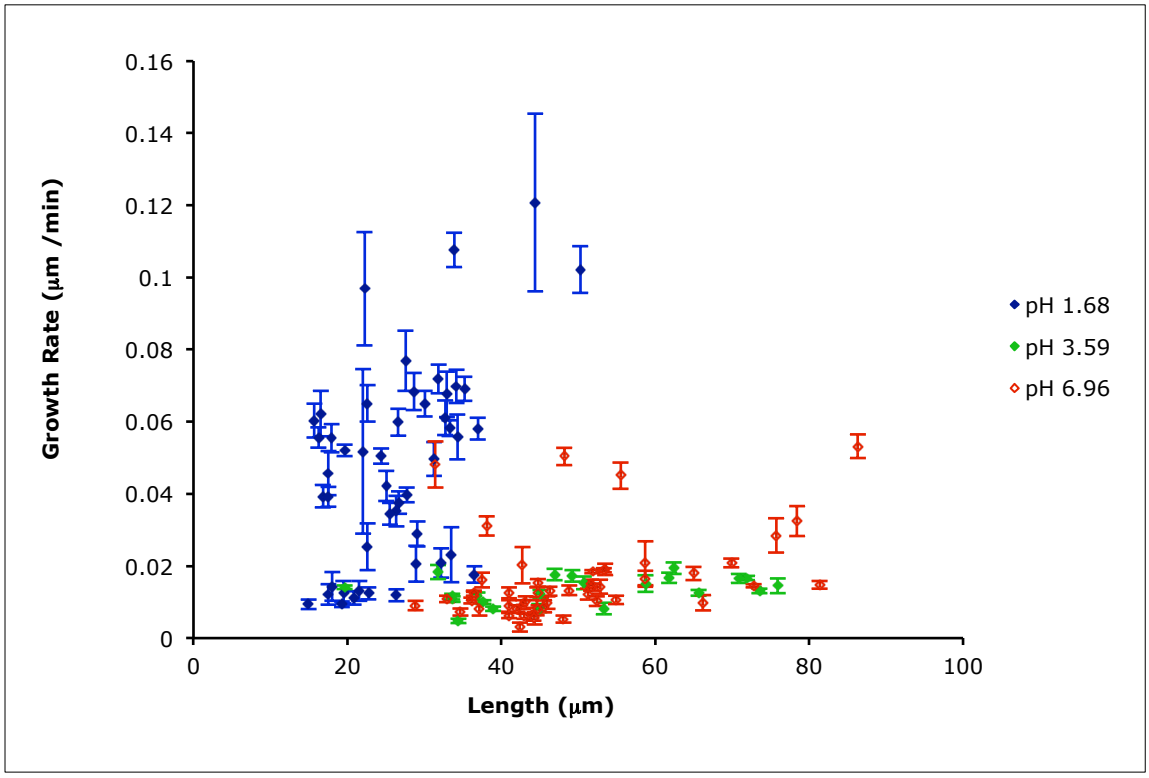

Figure 4-12 Growth rate dispersion of SUP α-lactose monohydrate with varying pH, ss 0.55 @ 30 °C

These results are consistent with the work of Visser, where it was shown that the growth rate of lactose crystals increased at lower pH. It is not clear, however, why the faster growing crystals are not also the largest crystals observed (Figure 4-12). This may be due to secondary nucleation occurring more readily at lower pH, or relate to the size range of the initial sample used to seed the supersaturated solution. Indeed, a plot of the starting size distributions (Fig 4.13) shows that the average seed size decreases with decreasing pH. This is presumably a result of the different nucleation behaviour that occurs as the pH varies, a phenomenon that is examined in more detail in Chapter 5. Regardless of these issues, it is clear from the results

obtained that the growth rate of the SUP lactose does increase as the pH decreases (Table 4.5).

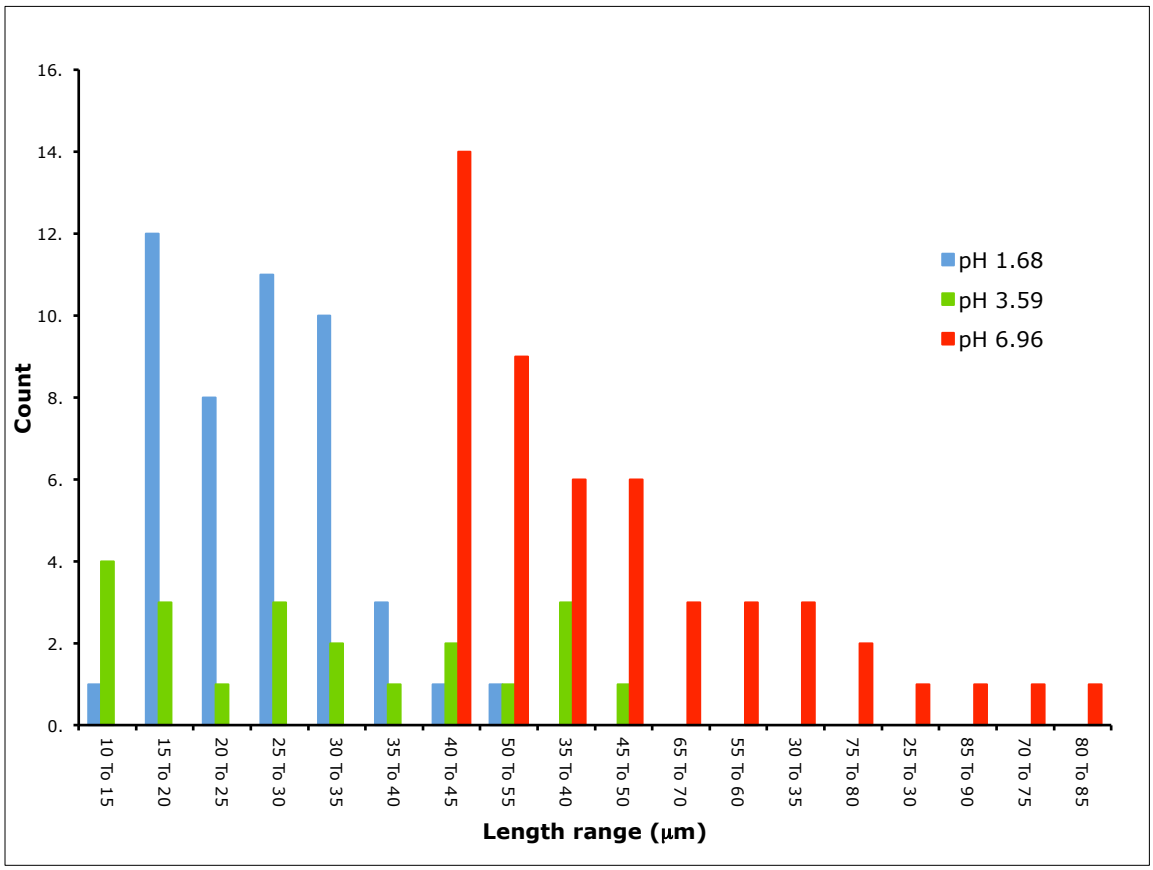

Figure 4-13 Initial seed size of SUP α-lactose monohydrate at different pH 1.68, 3.59, 6.96, ss 0.55 @ 30 ^{o}C

Table 4-5 Observed average growth rates and standard errors for SUP α-lactose monohydrate as a function of pH, ss 0.55 @ 30 ˚C

pH	Growth Rate (µm/min)
1.68	0.047 (4)
3.59	0.013 (1)
6.96	0.016 (2)

These results are consistent with protonation of the organic phosphate inhibitor at the lowest pH, decreasing its impact as a growth inhibitor. The comparable crystal growth rates at pH 3.59 and 6.96 suggest that the singly and doubly

deprotonated lactose phosphate have similar impacts on crystal growth, assuming the speciation behaviour is as shown in Figure 3-4.

It is notable that under the fast growth conditions at pH 1.68, the seed crystals undergo a significant change in morphology, with the (010) face reducing in size quite significantly in some cases, as expected for a fast growing face (Figures 4-14, 4-15).

(a)

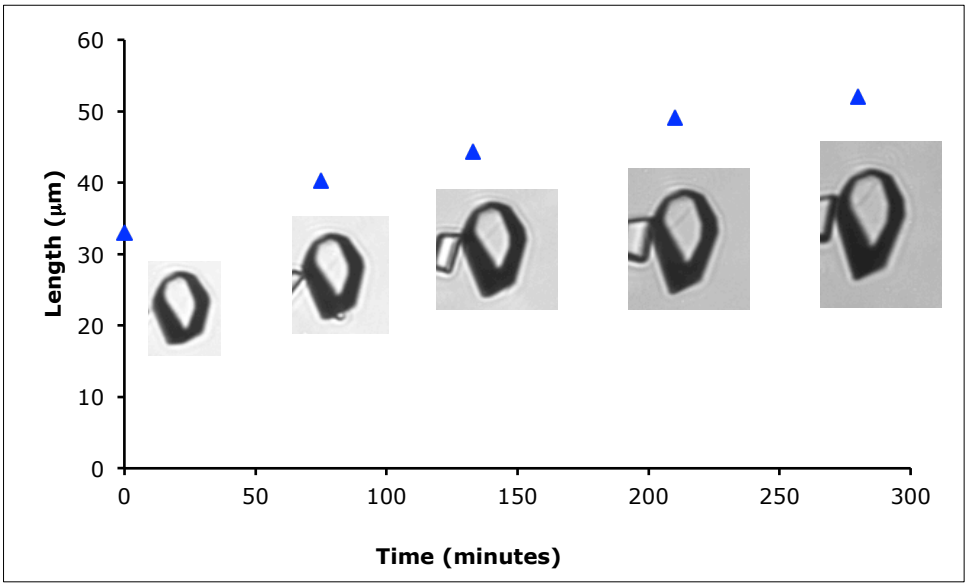

(b)

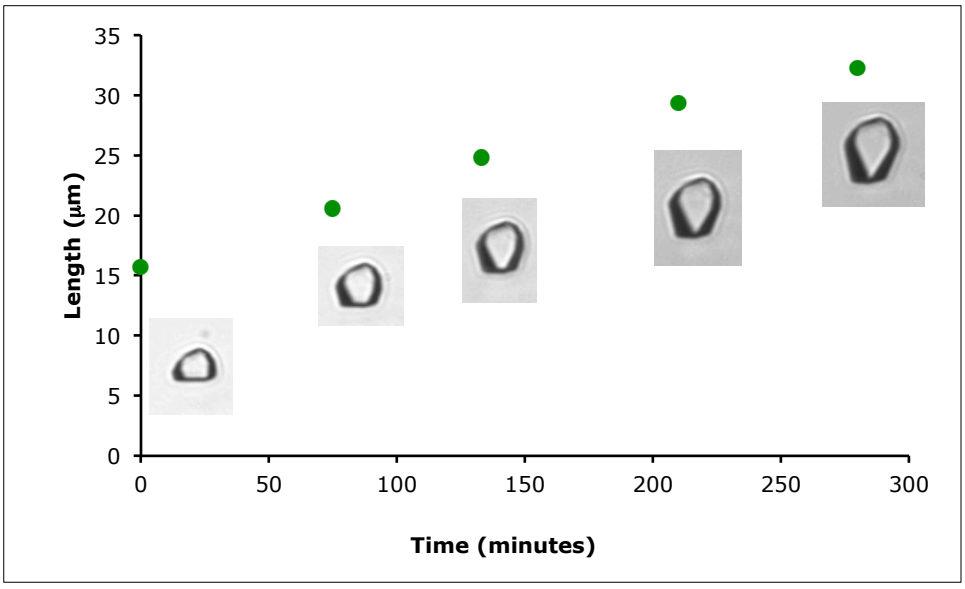

Figure 4-14 SUP @ pH 1.68 crystals resting on (0-11) face, (a) growth rate 0.0675 µm/min, (b), growth rate 0.0603 µm/min

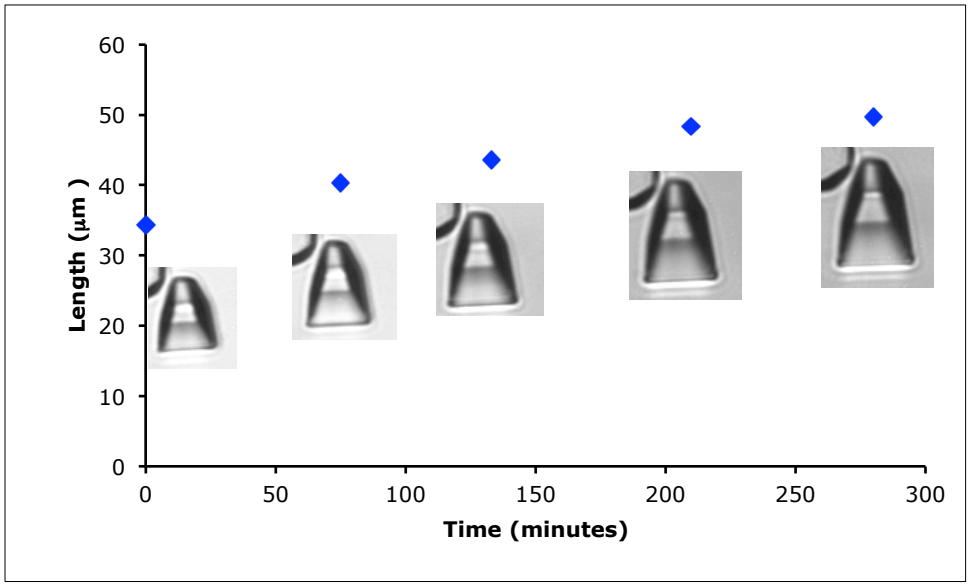

Figure 4-15 SUP @ pH 1.68 crystals resting on (110) face, growth rate 0.0557 µm/min

A similar experimental procedure was then carried out using IEL lactose. The results are shown in Figure 4-16. Surprisingly, the opposite trend is observed with the purified IEL α-lactose monohydrate, in that the lowest pH (1.95) results in the slowest growth rates and maintains low size dispersion. The higher pH systems have a greater growth rate and broader size dispersion.

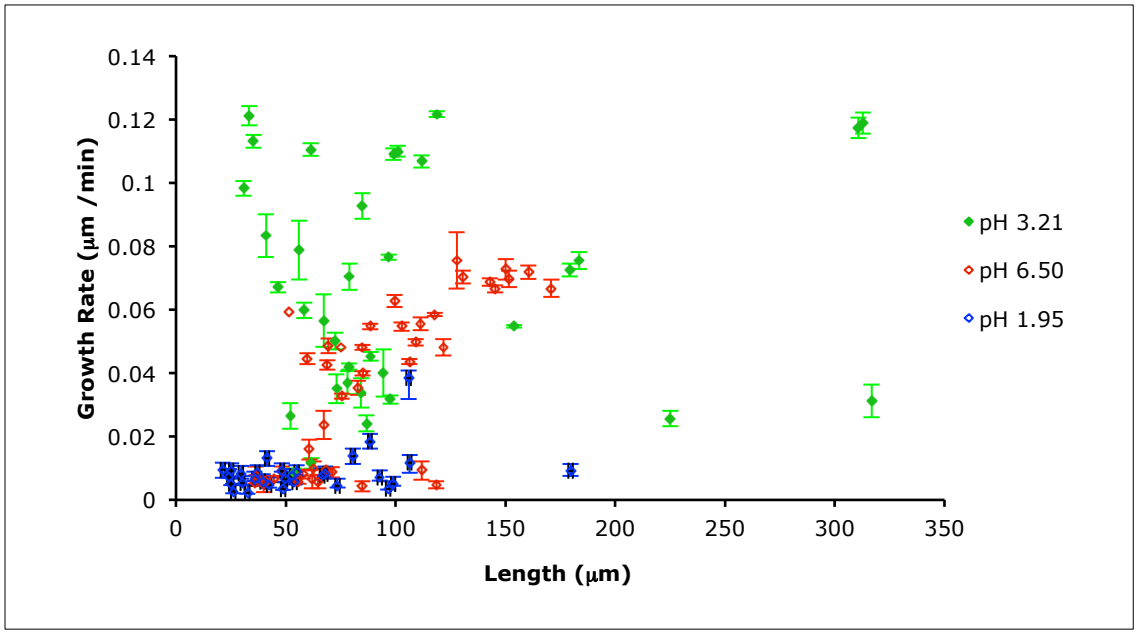

Figure 4-16 Growth rate dispersion of IEL α-lactose monohydrate with varying pH, ss 0.55 @ 30 °C.

Putting the IEL pH 1.95 results to one side for the moment, the remaining results are consistent with the expectation that the purified IEL lactose will exhibit a faster growth rate than the SUP lactose, which is contaminated with lactose phosphate (Figure 4-17).

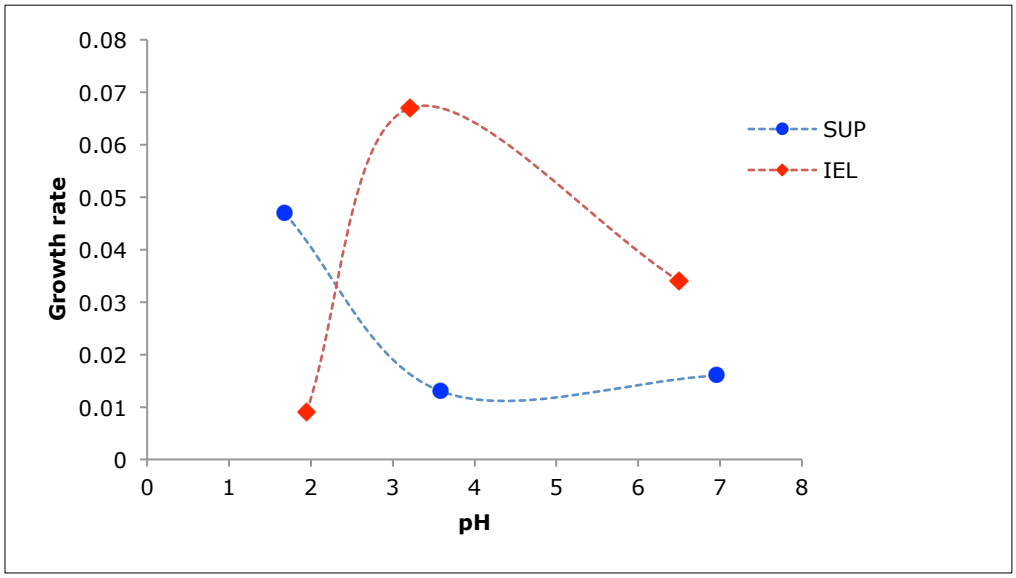

Figure 4-17 Observed average growth rates for SUP and IEL α-lactose monohydrate as a function of pH, ss 0.55 @ 30 °C. Dashed lines are added as a guide for the eye.

It was observed that there are changes to the tomahawk morphology of the IEL α-lactose monohydrate crystal with changing pH. Figure 4-18 shows some of the variations.

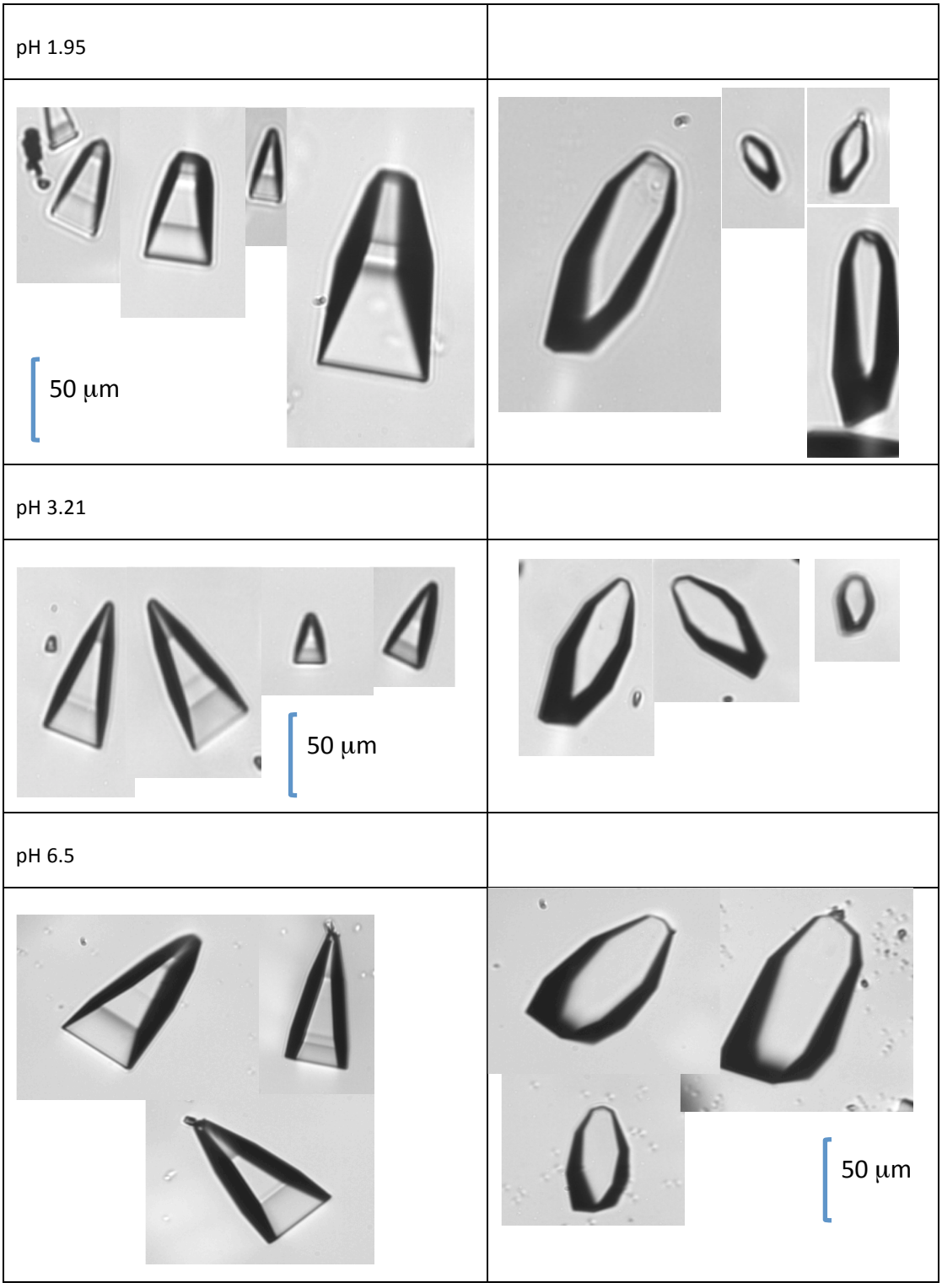

Figure 4-18 Morphology observations with changing pH of IEL α-lactose monohydrate in solution, ss 0.55 @ 30 °C. In the left column the crystal is resting on the (100) face and in the right column the crystal is resting on $(0\bar{1}1)$ face.

At the lowest pH value the (010) face seems to be getting smaller, therefore it seems that the crystal is becoming elongated in the b-direction. By comparing the two perspectives of the crystals at pH 1.95, it appears the crystal is narrowing on the a-axis, but broadening on the c-axis. The (110) face appears to be longer in the b-direction relative to the $(1\bar{1}0)$ face. A similar observation is made at pH 3.21. At pH 6.5, the (110) face is shorter than the $(1\bar{1}0)$ face. The resultant crystal does not appear to have the severe elongation or the narrowing of the (010) face on the a-axis. This property is observed across the size range of crystals in the samples observed, representative examples of small and larger crystals are shown in Figure 4-18.

Figures 4-19, 4-20 and 4-21, below demonstrate the progress of the changes in morphology as the IEL crystals grow in the b- direction.

The major discrepancy in the data reported here is that at pH 1.95, the IEL α-lactose monohydrate has the slowest growth rate across the pH range investigated, and in fact grows more slowly on average than the impure SUP sample at any of the pH values studied. It is proposed that this is due to the loss of the (010) face during the growth of the seed crystals, or early during the crystal growth experiments. Figure 4-19, for example, shows that the (010) face has essentially disappeared for the crystals shown. Once the face has grown out, it is unsurprising that the growth rate drops substantially, particularly as growth is being estimated in these experiments by measuring the growth in length in the *b*-direction. Significantly faster growth rates are observed at pH 3.21 and 6.5 for the IEL system. Figure 4-20 and 4-21 demonstrate that at the higher growth rates the typical tomahawk morphology is retained and the (010) face is still present, although very small in some cases. It is possible that if the growth experiments had been carried out over a longer time period, a drop in growth rate would have been observed when the (010) face grows out of a particular crystal.

(a)

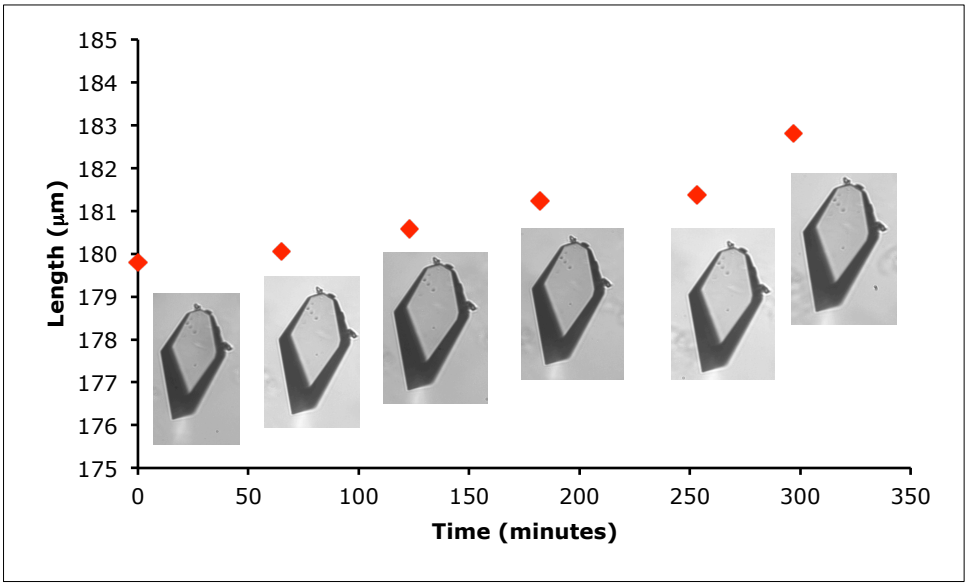

(b)

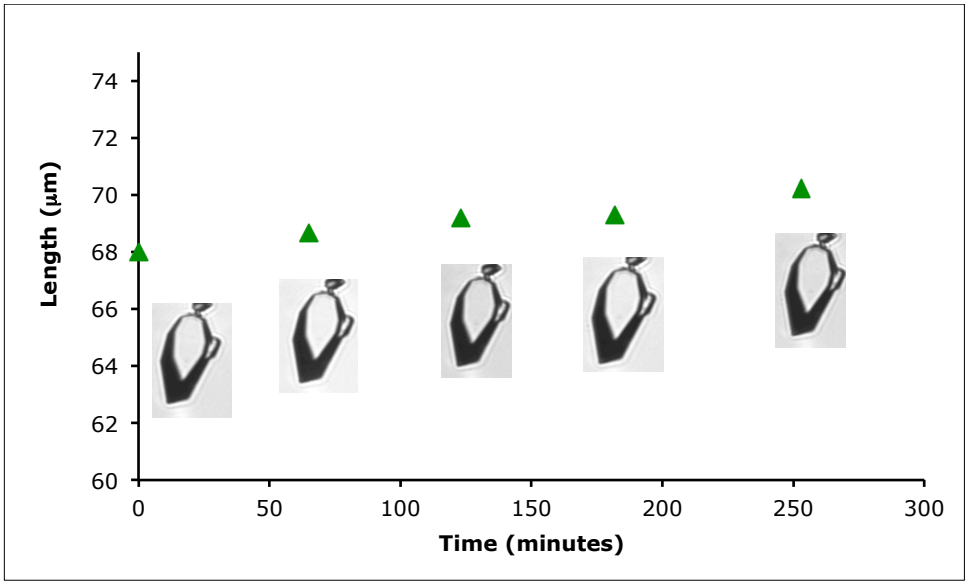

Figure 4-19 IEL @ pH 1.95 crystals resting on $(0\bar{1}1)$ face, (a) growth rate 0.0091 µm/min, (b) growth rate 0.0082 µm/min

(a)

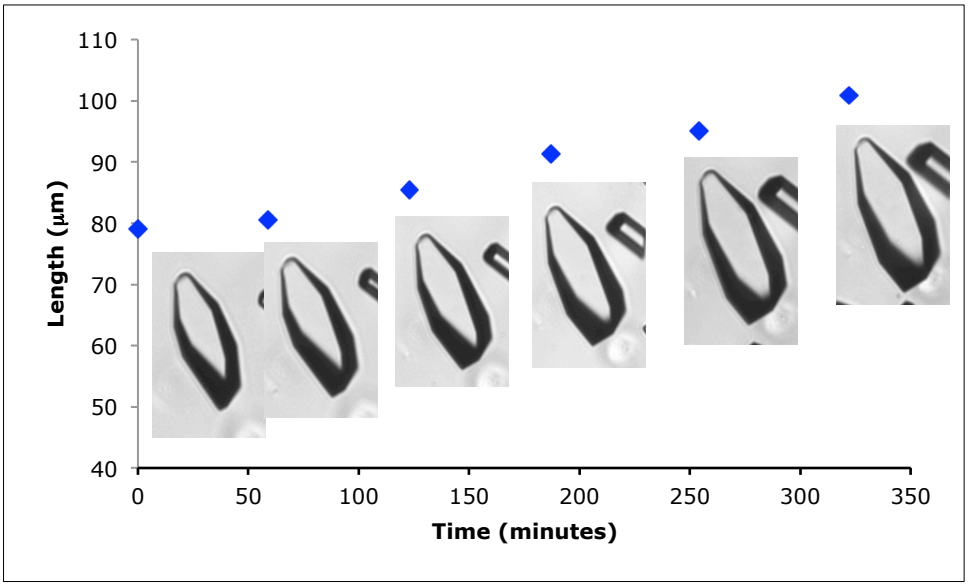

(b)

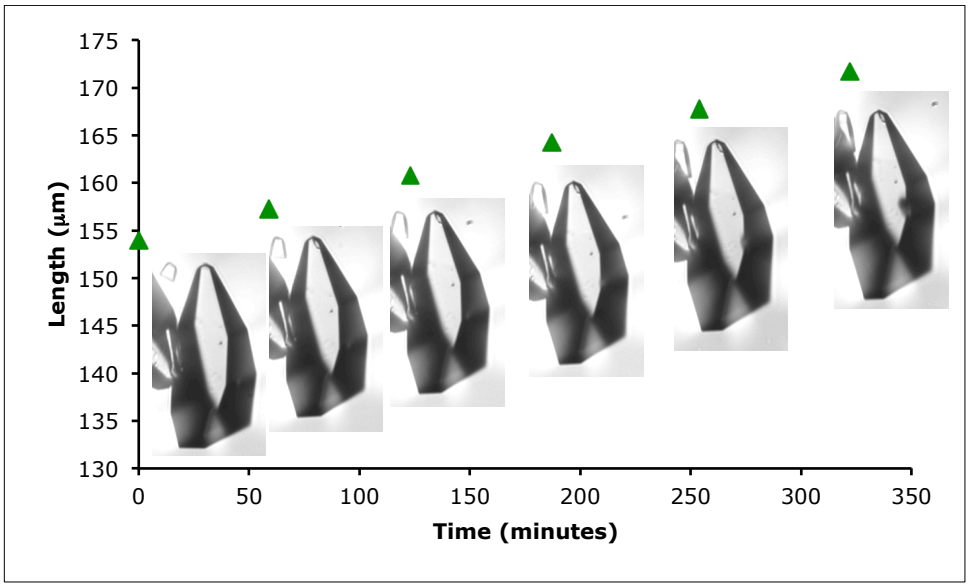

Figure 4-20 IEL @ pH 3.21 crystals resting on $(0\bar{1}1)$ face, (a) growth rate 0.0704 µm/min, (b) growth rate 0.0547 µm/min

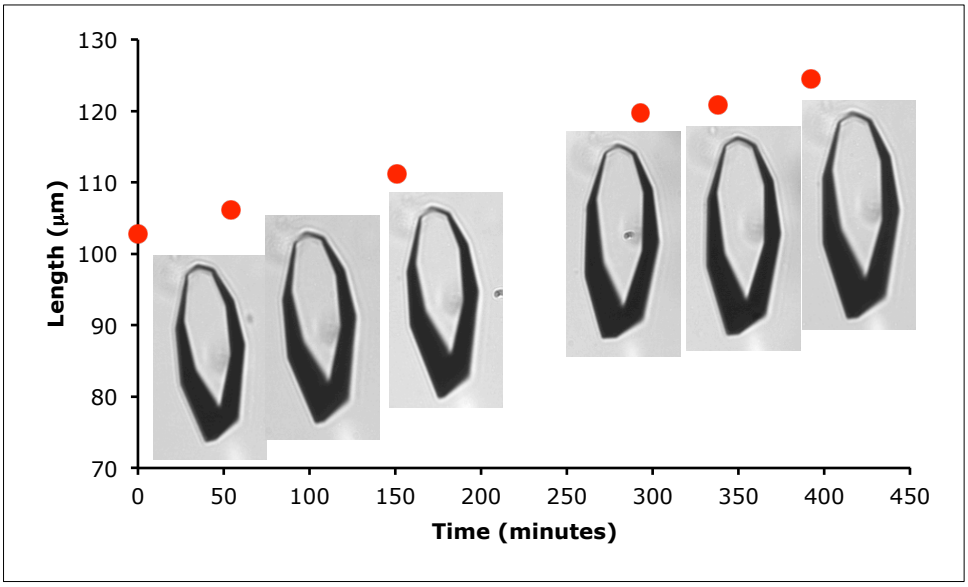

(a)

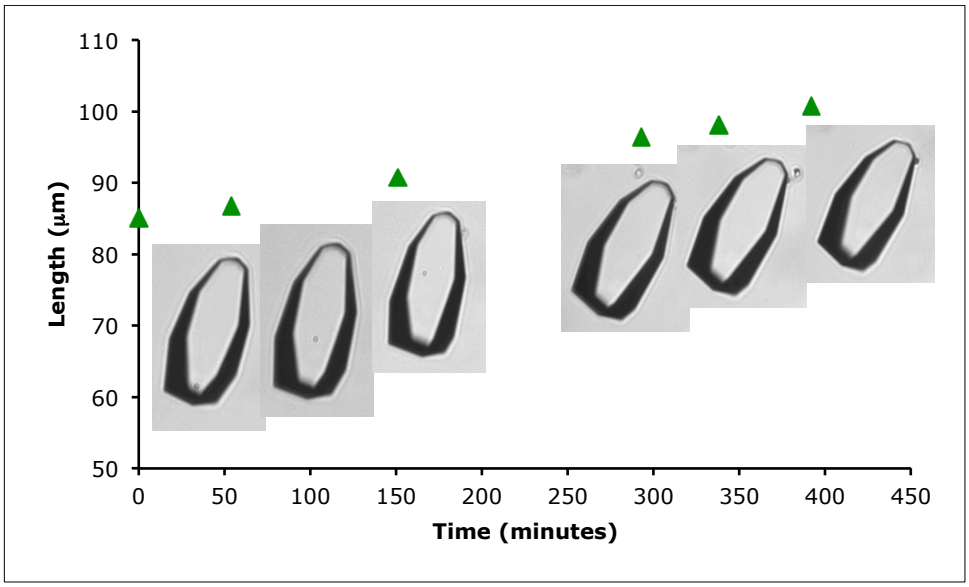

(b)

Figure 4-21 IEL @ pH 6.5 crystals resting on $(0\bar{1}1)$ face, (a) growth rate 0.0547 µm/min, (b) growth rate 0.0399 µm/min

It would seem that the faster growth rates have an impact on the crystal morphology of α-lactose monohydrate in a manner which has not been reported previously. As has already been mentioned, there is a paucity of literature available which studies pure α-lactose monohydrate. From the observations reported here, the growth rate is clearly affected by pH even in a purified lactose system, but the growth rate is likely to be strongly influenced by the morphology of the seed crystals used, and the period of growth.

4.4 CONCLUSIONS

It has been clearly identified that by removing impurities, with the emphasis on the removal of organic phosphates, that the growth rate of α-lactose monohydrate can be enhanced. Ion-exchange chromatography has been shown to effectively produce a highly purified form of α-lactose monohydrate with average growth rates ranging from 0.12 μm/min to 0.14 μm/min. It is, however, an inefficient means of production as it requires exhaustive use of resins that cannot be readily regenerated and the lactose recovery is only 40 %. Given the relatively high solubility of lactose, crystal growth studies consume a substantial amount of material, and hence the ion-exchange method is not an effective means of obtaining sufficient quantities of highly purified lactose.

Given these difficulties with the ion exchange process, a sample of lactose purified by ion exclusion was obtained from the University of Western Sydney. This had purity comparable to that achieved by ion exchange. The purified samples (IEL) were found to have faster growth rates than the SUP (at their natural pH), growing at an average of 0.034 μm/min compared to 0.013 μm/min.

The natural pH of the SUP product is 3.59 compared with pH 6.5 for the purified lactose products. The acidic nature of SUP is due to the presence of lactose phosphates (Visser, 1980). At the natural pH the growth rate is suppressed. Increasing or decreasing the pH enhances the growth rates of the SUP product. This may be because the concentration of the growth retarding phosphate species, possibly lactose-PO_4H^- is reduced. According to the relative concentration of phosphate species at different values of pH generated by the Hyperquad Simulation and Speciation program (HySS) (Alderighi, 1999) shown in Figure 3-4, at pH values 2 and 7 the phosphate species is most likely present as the lactose-PO_4H_2 and dianionic phosphate anion, lactose-PO_4^{2-} respectively.

Lactose phosphates are known to absorb to crystal surfaces during the early stages of crystallization of α-lactose monohydrate. Visser (1988) identified that lactose phosphate could dock on all α-lactose monohydrate crystal faces

but has a preference for the fastest growing faces, (010) and (110). This suggests that the lactose phosphate monoanions significantly cover all growth sites, which would then inhibit further incorporation of said anions. This is more significant when the lactose-PO_4H^- is present at higher concentrations because the monoanion can dock with greater stability by being an H-bond donor and acceptor. At the lower pH, the more prevalent phosphate species is neutral and unable to coordinate with the surface. At the higher pH, the more prevalent lactose-PO_4^{2-} dianion is less surface active, perhaps, as it is a H-bond acceptor only.

These growth rate studies have also identified the impact pH has on purified α-lactose monohydrate. At the natural, close to neutral, pH, growth rate was determined to be 0.034 μm/min for the (010) face. At the lower pH 3.21 the growth rate is doubled to 0.067 μm/min. The growth rate dramatically diminishes at pH 1.95 to 0.009 μm/min, which is proposed to be due to a change in morphology caused by the rapid growth of the (010) face when nucleated at the lower pH, such that the face grows out completely, leaving a crystal that grows at a much reduced rate.

Most studies identified in the literature are for impure systems of α-lactose monohydrate. There is very little information available regarding the impact of pH on the growth of pure α-lactose monohydrate growth. The work reported here shows that pH has a significant impact on the growth rate of α-lactose. In typical impure systems, this behaviour is convoluted with the impact of the pH on the speciation of the key lactose phosphate impurities. It is possible, therefore, that some of the conflicting literature results discussed in Chapter 2 arise from complex interplay of these factors. The following chapter reports the impact of pH and impurities on the crystal growth of lactose, underpinned by our improved understanding of the pure system.

5 Influence of inhibitors on the growth rate of α-lactose monohydrate

5.1 INTRODUCTION

The crystallization of α-lactose monohydrate of typical pharmaceutical-grade purity is inhibited by the presence of a sugar phosphate. The impact on growth rate was identified, and means of overcoming it with purification, were discussed in Chapter 3.

It was determined by Visser (1988) that the inhibiting compounds are a mixture of lactose monophosphates, substituted at the -3'. -4', -6' or -6 positions (Figure 5-1). The inhibition activity of the lactose phosphates on the lactose crystal growth is only apparent in relatively pure mother liquors. In more complex systems the inhibitory effect is suppressed or absent due to the presence of impurities such as inorganic salts (Visser 1988).

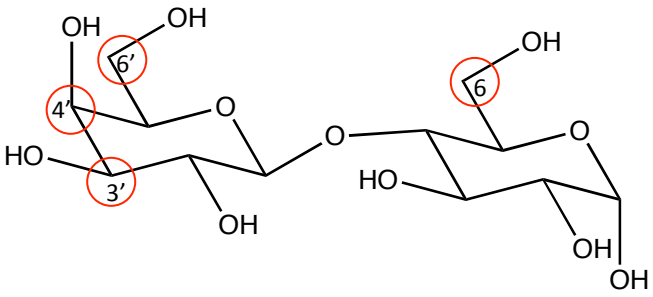

Figure 5-1 The mixture of lactose monophosphates found in pharmaceutical lactose as determined by Visser (1998) are substituted at the 6-, 6'-, 4'- or 3'- positions (where HO_3P-O- substitutes for an OH group marked by a red circle)

To add to the complexity in these systems, studies undertaken by several groups indicate that salts and components of whey can have an impact upon the crystallization of α-lactose monohydrate by either inhibiting growth rate or alternatively increasing growth rate (section 2.1.5.4).

The intention of these investigations is to study the impact of a selection of inorganic salts and structurally similar additives have upon the crystal habit of

α-lactose monohydrate. Experiments were initially conducted using SUP α-lactose monohydrate and then a select number of experiments were performed with IEL α-lactose monohydrate. The highly purified IEL product was employed to determine the true impact additives have on the α-lactose monohydrate habit in the absence of the potent lactose phosphate. It has also been identified that the pH of the system has a significant impact upon the growth of α-lactose monohydrate (see section 4.2.3), and thus this parameter has also been considered along with the additive studies.

5.2 METHODS AND MATERIALS

5.2.1 Morphology studies

Initial morphology studies were performed on α-lactose monohydrate by introducing inorganic salts; calcium chloride, sodium chloride, potassium chloride, disodium hydrogen phosphate and potassium dihydrogen phosphate, prior to nucleation as outlined in the 'common history seed' method (Section 4.1.1).

A suite of 1 M additive solutions of the aforementioned salts was prepared in milliQ water. A suitable quantity of α-lactose monohydrate was dissolved with heat and stirring to prepare an adequate volume of lactose solution with 0.55 supersaturation (equivalent to 10 g lactose in 25 g milliQ water). Upon cooling to room temperature the solution was filtered with 0.45 μm membrane vacuum filtration. 25 mL aliquots were then pipetted into 50 mL plastic vials, 25 μL of the additive solution was introduced and the vials sealed. The solution was then placed into an ultrasound bath (0.73 A, 35 KHz) for 3 minutes and then into a water bath at 30 ˚C for 48 hours. After 48 hours the solution was gently agitated and transferred into an *in situ* growth cell equilibrated at 30 ˚C (see Figure 4-1). Images of the growing crystals were then captured via a digital video camera mounted on an optical microscope.

Measurements of the crystals were taken of the length of the $(0\bar{1}1)$ face (the *b*-direction), and of the width between the parallel (100) faces (the *a*-direction).

5.2.2 Growth rate studies

Using the additive solutions prepared as described in section 5.1.1, a similar study was performed, this time measuring the growth rates. Identical dilutions and methods were used. The seed solution was introduced to the *in situ* cell after at least 40 hours growth, the cell area was mapped and single crystals were monitored, by capturing images at hourly intervals for several hours. Length measurements were taken. The solutions were stored and later analysed for their respective trace elements and supersaturation.

Structurally similar additives, glucose-6-phosphate, lactose-1-phosphate, and a mixture of lactose phosphates, were studied for their impact on morphology and growth rate. A mineral fraction supplied by collaborators from UWS was also examined.

5.2.3 Bulk Crystallization Studies

Bulk crystallization studies were performed to observe the impact the selected additives have on the nucleation and subsequent growth of α-lactose monohydrate. Turbidity, de-supersaturation and crystal size distribution were measured.

The required volumes of supersaturated (0.55) SUP α-lactose monohydrate solution were prepared by dissolving the lactose in MQ water with heat and stirring. The solution was cooled to 30 ^{o}C in a water bath and then filtered with a 0.45 μm membrane via vacuum filtration. The solution was then placed in an ultrasound bath for three minutes and then introduced to a 200 mL jacketed crystallizer equilibrated at 30 ^{o}C via a thermostated water bath. The solution was agitated with an overhead stirrer set to the slowest speed, 60 rotations per minute. A turbidity probe and conductivity electrode were calibrated and zeroed and then placed into the solution. The crystallizer was covered with a lid to reduce evaporation. Turbidity data was logged to

computer for subsequent processing. Samples were taken intermittently for CSD (1 mL) and supersaturation measurements (4 mL) via micropipette. Samples for analysis of supersaturation were filtered immediately with a 0.45 μm syringe filter, diluted 500 fold with MQ water and frozen until required for analysis. Samples taken for CSD were immediately placed in a petri dish and observed using an optical microscope. Images were taken and subsequent measurements of the crystal length (b direction) were taken. Upon completion of the experiment the turbidity data was extracted and analysed using Microsoft Excel. The pH of the solution was also recorded at the beginning and end of each experiment.

For experiments with additives, a final analyte concentration of 0.001 M was prepared and introduced to the crystallizer. Sample treatment was the same as described above.

Equipment used;

Agitation – IKA Labortechnik RW 20.n Overhead Stirrer
Turbidity – Analite High Sensitivity Model 156 Nephelometer
Toledo Inlab 730 Conductivity Probe, NTC, 0…1000mS, 0…1000 ˚C
pH – Metrohm 744 pH Meter, pH 0…14, 0…80 ˚C
Microscopy – Nikon Optiphot-2, Optimas 6.2 Software

5.2.4 De-supersaturation and Saturation Studies

The impact that selected additives have on the de-supersaturation and saturation of α-lactose monohydrate was studied.

5.2.4.1 De-supersaturation

A bulk solution of 0.55 supersaturated SUP α-lactose monohydrate in MQ water was prepared. The solution was filtered with a 0.45 μm membrane. Aliquots of 25 mL were then taken into 100 mL polyethylene Nalgene bottles. Eight bottles were put aside and used as the blank run to determine the de-supersaturation of SUP. Another eight bottles were spiked with 1 M Na_2HPO_4 to make a final analyte concentration of 0.001M. All bottles were then seeded with 0.100 g of SUP α-lactose monohydrate. The solutions were

then placed into the bottle roller, and kept at 30 ˚C. Samples of the SUP and the Na_2HPO_4 spiked solutions were taken across a nine day period. Upon sampling the solutions were filtered through a 0.45 μm membrane. The solid was retained for gravimetric analysis and dried in a 55 ˚C oven overnight and the solution was diluted 500 fold and frozen until analysed by HPLC for lactose concentration.

Lactose concentration was determined by HPLC using a Waters Resolve 5μ C_{18} column, 3.9mm x 300 and an RI detector. Standards were prepared from SUP α-lactose monohydrate (0.1091g) dissolved in milliQ water and filtered through 0.45 μm Millipore membrane and then diluted in series to make 200, 400, 600, 800 and 1000 ppm.

5.2.4.2 Saturation

The equivalent solutions prepared for the de-supersaturation experiments were prepared for the saturation experiments. To each bottle 10g of SUP α-lactose monohydrate was added, along with the required quantity of additive and MQ water. These were then placed into a bottle roller, thermostated to 30 ˚C. Samples of the SUP and the Na_2HPO_4 spiked solutions were taken across a nine day period. All other samples were removed after nine days. All samples were treated as for the de-supersaturation samples.

5.3 RESULTS AND DISCUSSION

5.3.1 Structurally similar additives

The growth rate of faces (010) and (110) on the α-lactose monohydrate crystal is inhibited by the lactose phosphate commonly found in pharmaceutical grade lactose, as was discussed in detail in Chapter 3. In an effort to more readily study the impact of this potent impurity, attempts were made to extract the lactose phosphate from impure lactose to use in this study. This was found to be very challenging and the lactose phosphate

components could not be resolved. Based on this initial work it was decided that the cost and time required to isolate substantial quantities of the lactose phosphates was beyond the scope of this project. Instead, the option of accessing and studying some structurally similar additives was pursued.

A wide variety of sugar phosphates are not readily available, however, lactose-1-phosphate (Figure 5-2) and glucose-6-phosphate (Figure 5-3) are commercially available and hence were used in this study.

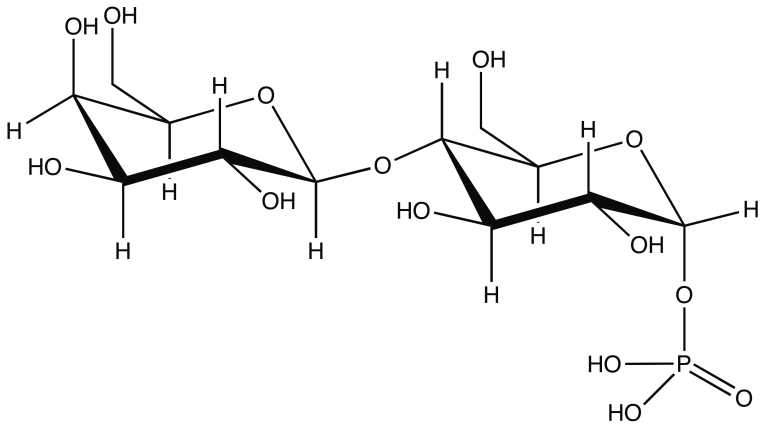

Figure 5-2 Structural formula of Lactose-1-phosphate

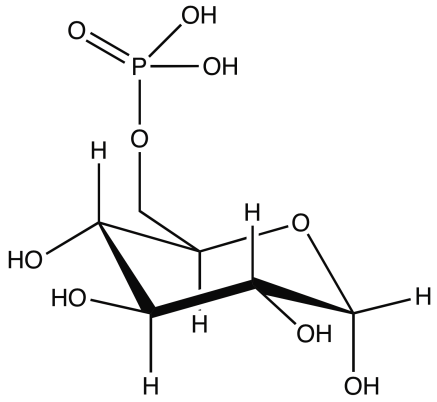

Figure 5-3 Structural formula of Glucose-6-phosphate

5.3.1.1 Glucose 6-phosphate

The impact of glucose 6-phosphate on the growth rate of both SUP and IEL lactose was investigated. Considering SUP lactose first, the glucose 6-

phosphate may slightly inhibit the growth of the lactose crystals. At a concentration of 0.001M, the pH is increased slightly from 3.57 to 3.90 with the additive. The average growth rate is modestly lowered to 0.012 μm/min from the blank growth rate of SUP 0.013 μm/min. Considering the growth rate dispersion data (Figure 5-4), it would be more appropriate to say that no experimentally significant change was observed.

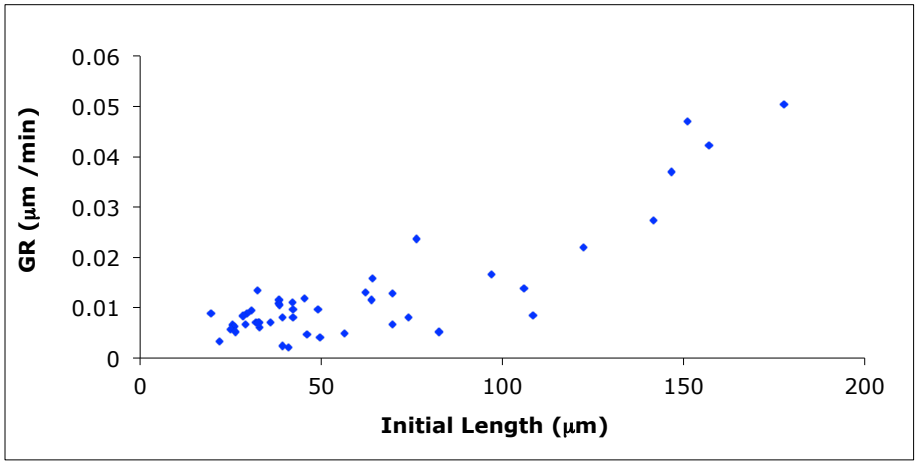

Figure 5-4 GRD of 0.55 ss SUP α-lactose monohydrate in the presence of 0.001M Glucose-6-Phosphate, pH 3.90

Glucose 6-phosphate does however strongly inhibit the growth of the IEL α-lactose monohydrate relative to the blank. The average growth rate is reduced from 0.067 μm/min to 0.017 μm/min. The GRD data is shown below (Figure 5-5), and it can be seen that some large fast growing crystals remain in the system, but the majority of crystals grow at a much slower rate.

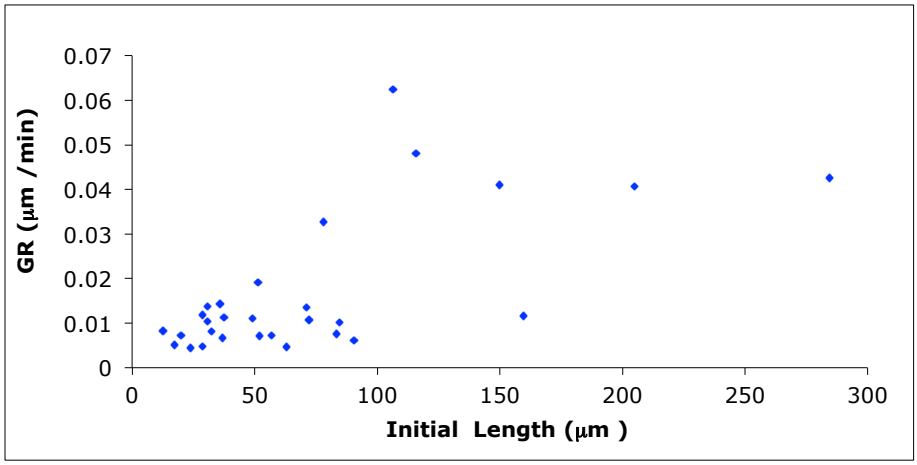

Figure 5-5 GRD of 0.55 ss IEL α-lactose monohydrate in the presence of 0.001M Glucose-6-Phosphate, pH 3.61

The additive appears to modify the morphology of the IEL α-lactose monohydrate crystal. The crystal is still elongated relative to the (010) face and the (110) face is more dominant at the expense of the (100) face. The crystal is then broader across the top of the $(0\bar{1}1)$ face (Figure 5-6). It is interesting to note that despite the negligible influence on growth rate, this morphology difference is also observed in the SUP crystals, although the (110) face does not dominate as much and the (100) face is still visible.

	Blank	+ 0.001M Glucose 6-PO_4
IEL	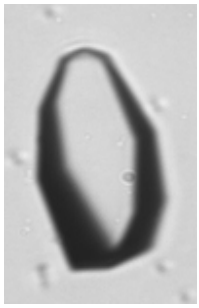	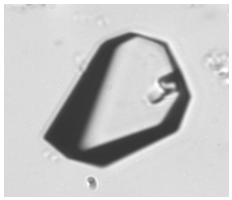
SUP	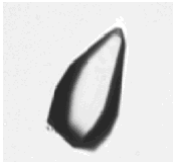	

Figure 5-6 Impact of Glucose 6-phosphate on the morphology of IEL and SUP α-lactose monohydrate.

5.3.1.2 Lactose 1-phosphate

The impact of lactose 1-phosphate on the growth rate of SUP α-lactose monohydrate is different again. The growth rate of the SUP is enhanced in the presence of lactose-1-phosphate, increasing from 0.013 μm/min of the SUP blank to 0.022 μm/min. The IEL growth is however, inhibited in the presence of lactose-1-phosphate with a growth rate of 0.028 μm/min compared to the IEL of 0.067 μm/min. The GRD plots are shown below (Figure 5-7 and 5-8), and it can be seen that both systems have substantial scatter in the crystal growth rates.

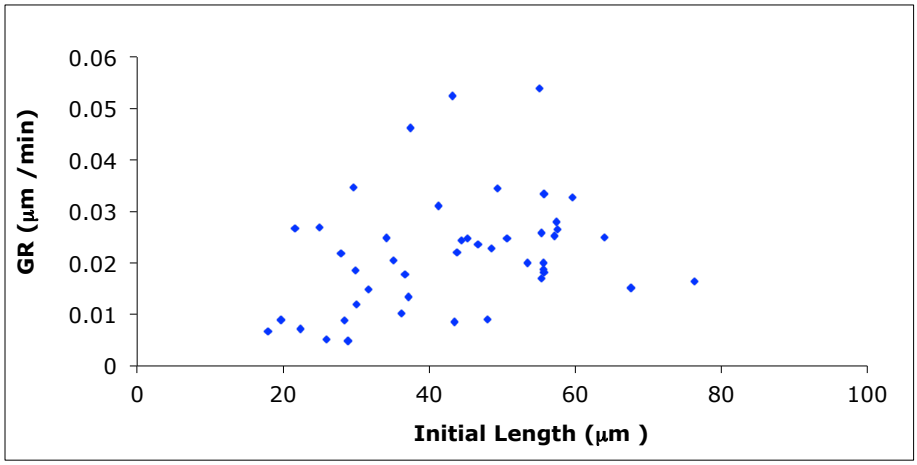

Figure 5-7 GRD of 0.001M Lactose-1-Phosphate in 0.55 ss SUP α-lactose monohydrate, pH 3.88

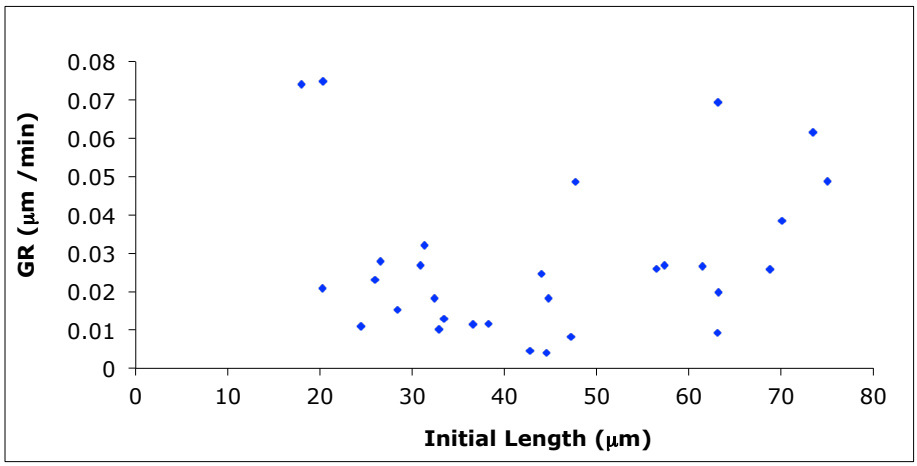

Figure 5-8 GRD of 0.001M Lactose-1-Phosphate in 0.55 ss IEL α-lactose monohydrate, pH 3.7

The morphology of the IEL α-lactose monohydrate crystal has changed notably (Figure 5-9), and such changes are also observed in the SUP crystals. As was observed in the glucose 6-phosphate in IEL study, the crystal is still elongated with respect to the (010) face and has broadened across the $(0\bar{1}1)$ face, suggesting that the $(1\bar{1}0)$ faces are growing faster. This broadness is not observed in all crystals, it is more apparent in some. It is also apparent the crystals have lost their symmetry; the size of the (100) faces varies on either side of the crystal.

	Blank	+ 0.001 M Lactose 1-Phosphate
IEL	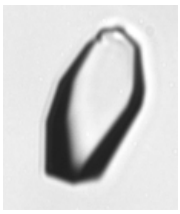	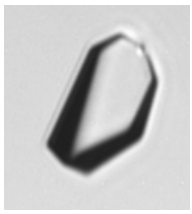
SUP	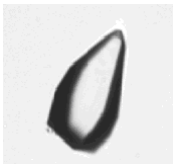	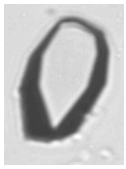

Figure 5-9 Typical morphologies observed in IEL and SUP lactose, in the blank, and in the presence of 0.001M lactose 1-phosphate

5.3.1.3 Discussion – structurally similar additives

Morphology change is commonly used as a simple method to determine if an additive or impurity is having an impact on crystal growth. By this measure, it is clear that both the additives used here, glucose 6-phosphate and lactose 1-phosphate, are having some influence on the crystal growth of α-lactose monohydrate. Both inhibitors also have a substantial impact on the growth rate of the pure IEL lactose, where sugar phosphates competing with the additives are absent or at very low concentration. Hence it is reasonable to conclude that both lactose 1-phosphate and glucose 6-phosphate inhibit lactose crystal growth, with the glucose 6-phosphate having the greater impact.

The situation is more difficult to analyse for SUP lactose. Here the glucose 6-phosphate had no significant impact, and the lactose 1-phosphate additive actually resulted in an increase in the average growth rate. A tentative explanation for this could be that the added sugar phosphates are competing with the lactose phosphate already present in the SUP lactose. If this is the case, then the less effective lactose 1-phosphate displaces some of the intrinsic lactose phosphate, resulting in an increase in the average growth rate. The more effective glucose 6-phosphate does not cause an increase, but nor does it

decrease the average growth rate, as might have been expected. This suggests that neither of the additives studied here are as effective as the lactose phosphate inhibitors already present in pharmaceutical grade lactose. A wider range of additives would be required to further test this hypothesis.

It should also be noted, given the clear changes in morphology induced by the additives, that the relative growth rates of some of the crystal faces must be changed by these additives, even in the presence of the intrinsic lactose phosphate present in SUP. The morphology does, however, remain elongated, consistent with the 010 face remaining as the fastest growing face. Hence the measurement of the length of the crystal is an appropriate technique to determine the crystal growth rate, despite the subtle changes in crystal morphology.

5.3.2 Inorganic additives

Another key class of additives relevant to lactose crystal growth is inorganic salts, which are commonly found in the industrial liquors. As discussed in Chapter 2, the literature is contradictory as to specific salts being inhibitors, accelerators, or having no impact. Hence it was decided to study some relevant inorganic salts under consistent conditions, commencing with an investigation of changes in morphology.

5.3.2.1 Morphology observations

Morphology studies highlighted the impact of inorganic salts on the habit of the α-lactose monohydrate crystal. Below in Table 5-1, are some of the captured images that are typical of the crystals found in the growth solutions.

The average crystal size differs slightly between the additives, the most significant change being observed in the presence of Na_2HPO_4. The observed crystal size is generally less than the blank run of the Sigma Ultrapure α-lactose monohydrate (SUP), suggesting some inhibition. The crystal shape does not appear to differ significantly, with the exception of the Na_2HPO_4 additive, where the crystals have a significantly different shape. The $(0\bar{1}1)$

face is broader and the (110) and (100) faces are longer, forming a substantially broadened tomahawk morphology. The length would appear to be increasing at a similar rate to the blank (SUP), the width however appears to be growing at an enhanced rate.

Table 5-1 Morphology studies using SUP

	Additive 1mM	pH	Average Length (μm)	Average ratio Width:Length
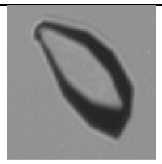	$CaCl_2$	4.9	73	0.4622
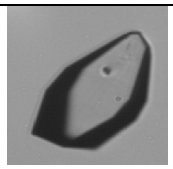	KCl	4.65	78.5	0.4484
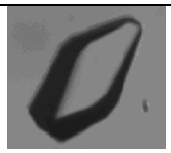	NaCl	6.36	76.6	0.4391
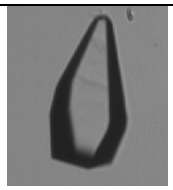	KH_2PO_4	5.67	71.9	0.4811
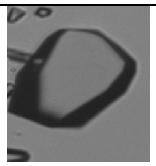	Na_2HPO_4	6.39	84.6	0.6020
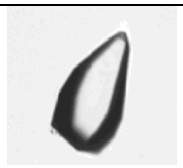	SUP	4.5	85.7	0.4842
	Non-ionic SUP	6.9	150.5	0.4361

80 μm

Upon taking the ratio of the width to length measurements (Table 5-1) the most notable difference is again found with the Na_2HPO_4, as expected from the optical images. While the variations in measured pH complicate direct comparisons of these results, some immediate observations can be made that provide preliminary information about the source of the unusual result obtained

in the presence of Na_2HPO_4. The NaCl and Na_2HPO_4 systems have similar pH values, but the morphology observed in the presence of NaCl is relatively unperturbed, suggesting that the sodium cation is not the cause of the change in morphology. The pH of the Na_2HPO_4 system (6.39) and that of the KH_2PO_4 system (5.67) are a little more divergent, suggesting that perhaps the specific species present based on the phosphate anion has a substantial effect on morphology. Using the Hyperquad Simulation and Speciation program, HySS (Alderighi, 1999) the relative concentrations of phosphate species at different pH values are shown in Figure 5-10, calculated using the HySS supplied pKa values (the assumption is made that under the dilute conditions used, the change from sodium to potassium will not significantly impact on the speciation). In fact, at both pH values $H_2PO_4^-$ is the dominant species in solution, although HPO_4^{2-} is significantly increased at pH 6.39, relative to 5.67.

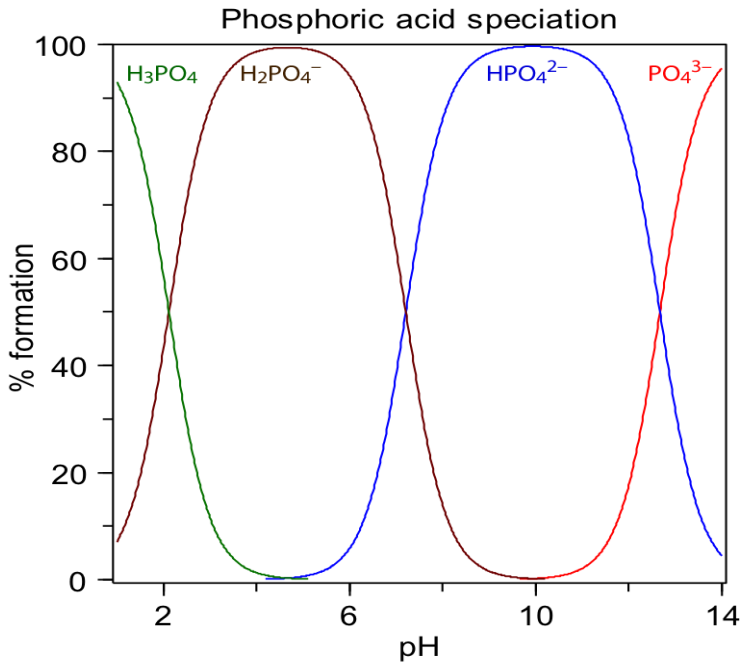

Figure 5-10 The relative concentrations of phosphate species at different values of pH (generated using HySS –Alderighi et al,1999)

Based on these results, it seemed likely that either the speciation of the phosphate anion has a very strong influence on lactose crystal growth, or that there is a synergistic effect when sodium and phosphate are combined. These

possibilities were investigated further by carrying out some growth rate studies in the presence of a selection of these additives at varying pH values.

5.3.3 Growth Rate Observations

In Chapter 4 the impact of pH on α-lactose monohydrate crystal was discussed and it became evident that by lowering the pH of the crystallizing system the impact of the lactose phosphates could be overcome to a degree, as an enhanced growth rate was observed.

The impact of pH is not so apparent upon the addition of the inorganic salts. Table 5-2 outlines the growth rate of SUP α-lactose monohydrate in the presence of calcium chloride, sodium chloride, potassium chloride, sodium phosphate and potassium phosphate at three different pH values.

Table 5-2 Growth rate of SUP α-lactose monohydrate with 1mM of additive

SUP α-lactose monohydrate + 1mM additive	pH	Average Growth Rate (μm/min)	Standard Deviation
$CaCl_2$	1.89	0.0092	0.0018
	3.32	0.0101	0.0025
	6.94	0.0126	0.0074
KCl	1.76	0.0110	0.0048
	3.2	0.0111	0.0037
	6.63	0.0157	0.0096
KH_2PO_4	1.98	0.0127	0.0008
	3.63	0.0132	0.0031
	6.89	0.0163	0.0050
NaCl	1.78	0.0074	0.0031
	3.27	0.0088	0.0029
	6.88	0.0183	0.0063
Na_2HPO_4	1.76	0.0071	0.0029
	5.55	0.0183	0.0073
	6.84	0.0129	0.0039
SUP only	1.68	0.0472	0.0274
	3.59	0.0133	0.0039
	6.86	0.0159	0.0116

Decreasing the pH of the systems results in growth rates that are only modestly decreased or unchanged. The decrease in the NaCl system is more marked, but overall the trend is opposite to that observed for the SUP blank.

If these data are studied graphically (Figure 5-11), including the standard deviation, it can be seen that the average growth rate is essentially unchanged across all additive experiments. The standard deviation is quite large for the fastest growing system, the blank SUP at pH 1.68, further complicating any comparisons.

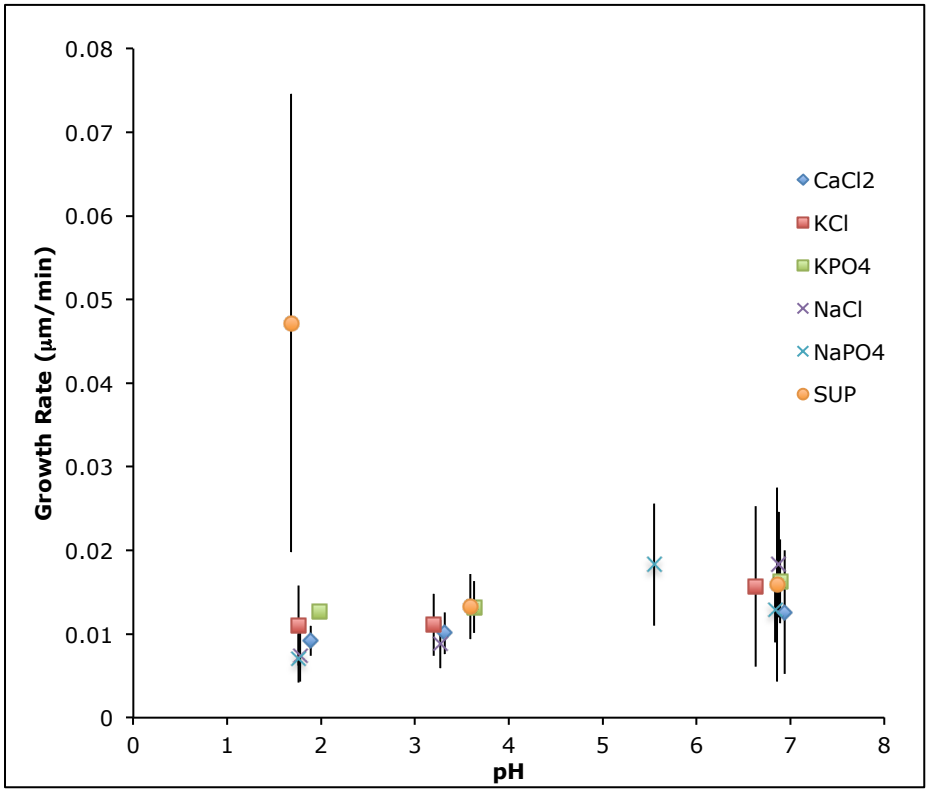

Figure 5-11 Growth rate of 0.55 ss α-lactose monohydrate in the presence of inorganic salts at various pH values. (Error bars are used to demonstrate the average standard deviation across all growth rate data sets)

The large standard deviation is consistent with growth rate dispersion (GRD). Shi *et al* concluded that each crystal grows at its inherent constant rate, but different crystals have different growth rates. It was observed that the variance

of the GRD of the (010) face increased as the mean growth rate of that face increased. This is consistent with the results reported here. The SUP α-lactose monohydrate at pH 1.68 has an average growth rate more than double of any of the other systems studied, and also has a variance several factors greater than the other systems.

Below is a plot of the growth rate distribution of SUP α-lactose monohydrate at pH 1.68 (Figure 5-12). The spread of growth rates at pH 1.68 is three times the breadth of the experiment conducted at pH 3.59 (Figure 5-13).

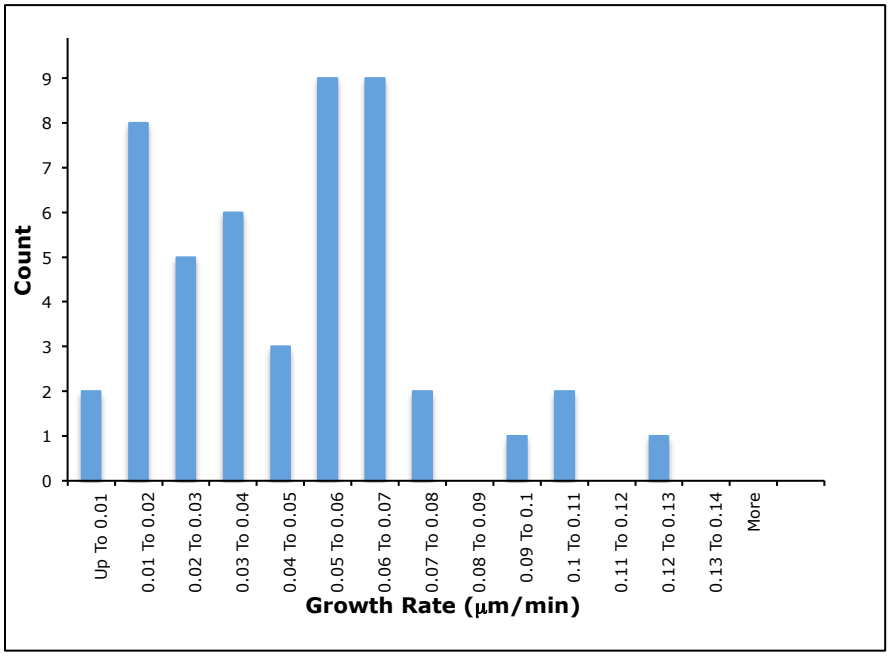

Figure 5-12 Growth rate dispersion of SUP α-lactose monohydrate at pH 1.68

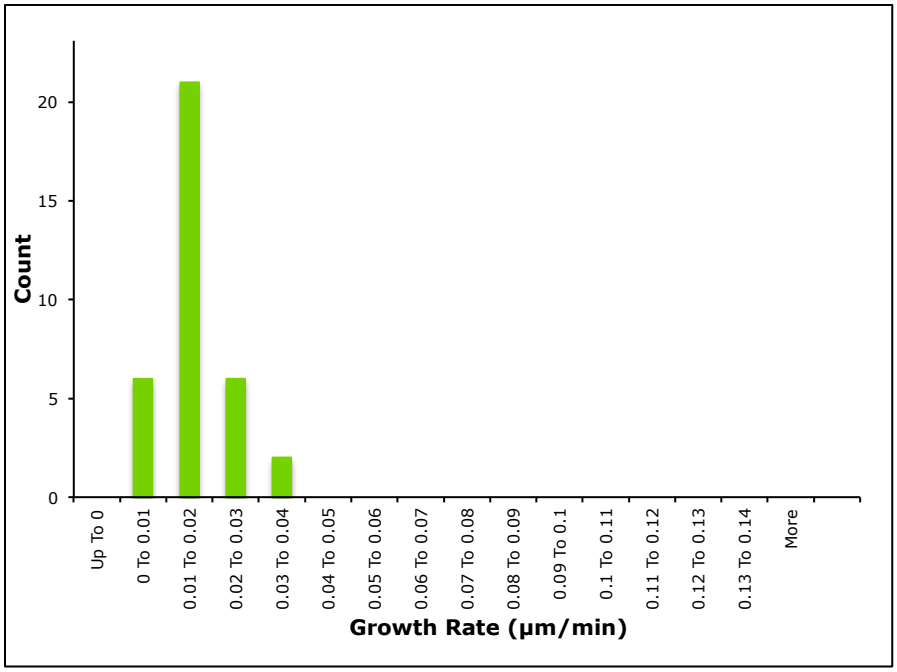

Figure 5-13 Growth rate dispersion of SUP α-lactose monohydrate at pH 3.59

It appears that the increase in ionic strength caused by the inorganic additives has a substantial influence on the behaviour of the lactose phosphate present, at low pH. The inhibitory effect is maintained, and a decrease in growth rate is observed, rather than a dramatic increase as found for the blank SUP system. The results obtained in the presence of sodium phosphate illustrate this clearly (Figure 5-15), with the size distribution decreasing as pH decreases.

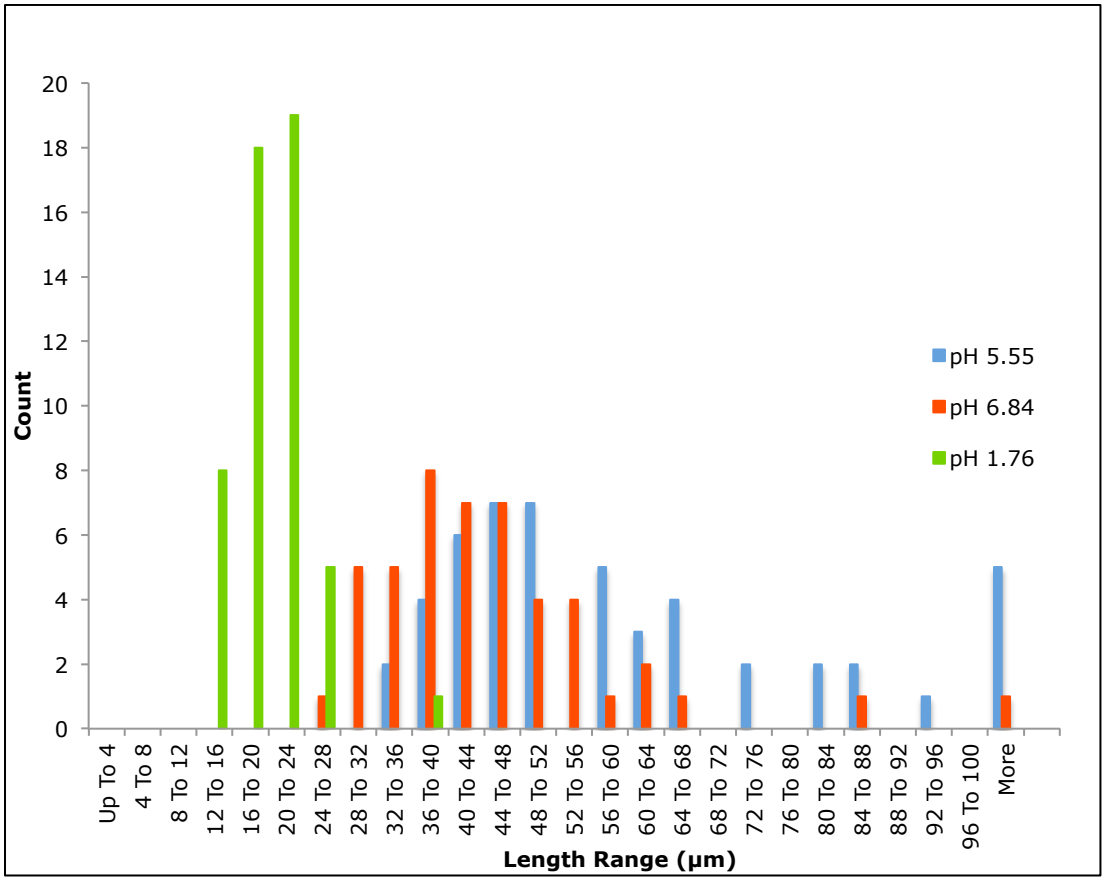

Figure 5-14 Initial seed size of SUP α-lactose grown in the presence of 1 mM Na_2HPO_4 at different pH values.

Given that growth rate dispersion reduced the clarity of the growth rate studies, the morphologies of the crystals produced in these experiments were examined, to try and better understand the unusual morphology observed in the presence of sodium phosphate. Considering first the hypothesis that the phosphate speciation might be critical, the morphologies of crystals produced in the presence of sodium phosphate at varying pH were studied. As demonstrated in Figure 5-16, 5-17 and 5-18 the broadened morphology of the crystals grown in the presence of 1 mM Na_2HPO_4, is maintained at pH values of 6.84, 5.55, and 1.76 (with severe inhibition at the latter pH). This suggests that phosphate speciation is not as critical as the presence of sodium and phosphate together in the solution. This hypothesis is supported by the results obtained in the presence of potassium phosphate at similar pH values, which show the more typical elongated morphology in all cases (Figure 5-15). It appears then, that the combination of sodium and phosphate is required to cause this unusual broadened morphology. The specific influence of an ion pair, as observed here,

might explain some of the inconsistencies reported in the literature concerning inorganic additives in lactose crystal growth.

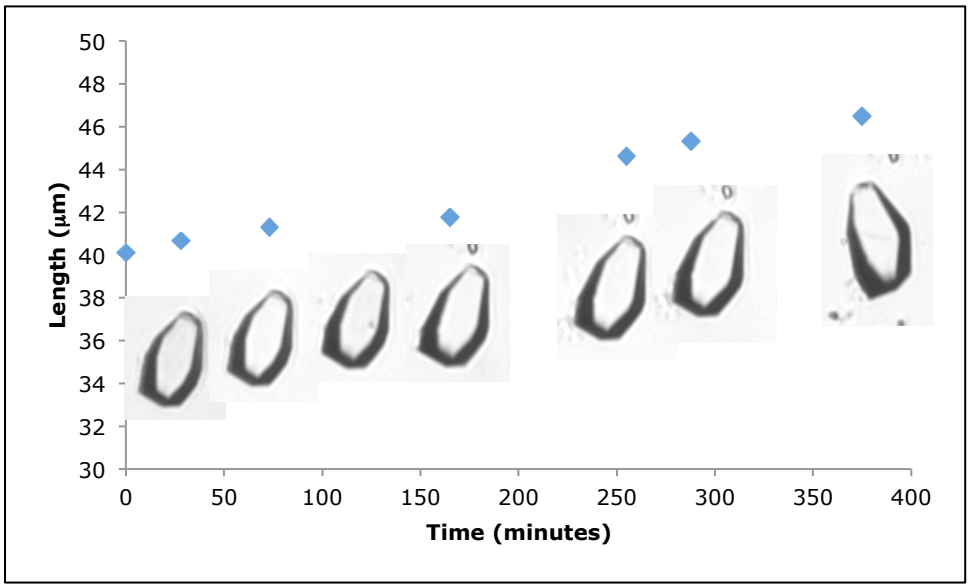

Figure 5-15 SUP + 1 mM KH_2PO_4 @ pH 6.89, growth rate 0.017 μm/min

It is acknowledged that the change in morphology caused by sodium phosphate does somewhat compromise the growth rate determination method used here. It is likely that the growth in width of these crystals is a substantial contributor to the overall growth, and hence measuring the length will underestimate the overall growth rate. Nevertheless, the comparison of the specific growth rate of the (010) face between systems remains valid, and it is clear that the system is significantly inhibited at low pH.

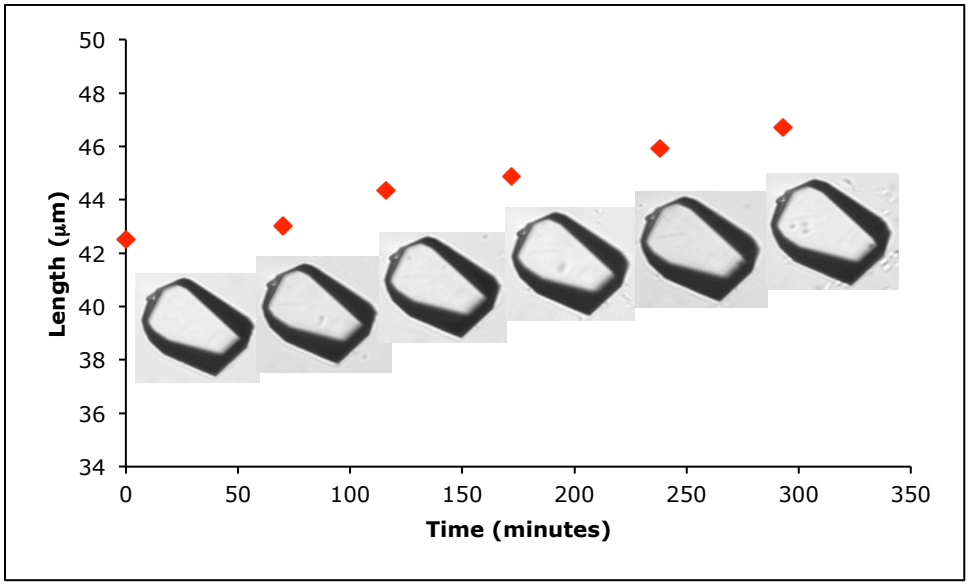

Figure 5-16 SUP + 1 mM Na_2HPO_4 @ pH 5.55, growth rate 0.015 µm/min

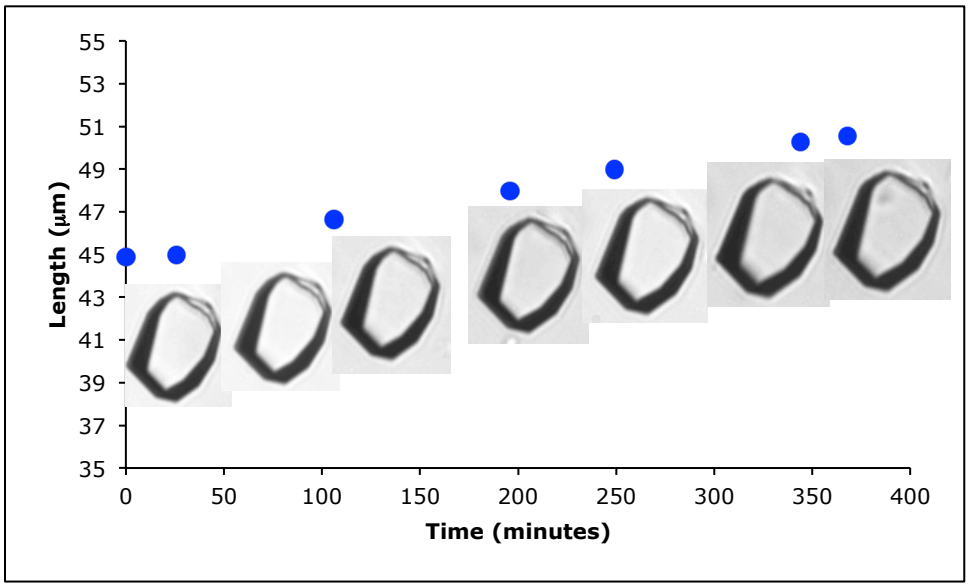

Figure 5-17 SUP + 1 mM Na_2HPO_4 @ pH 6.84, growth rate 0.016 µm/min

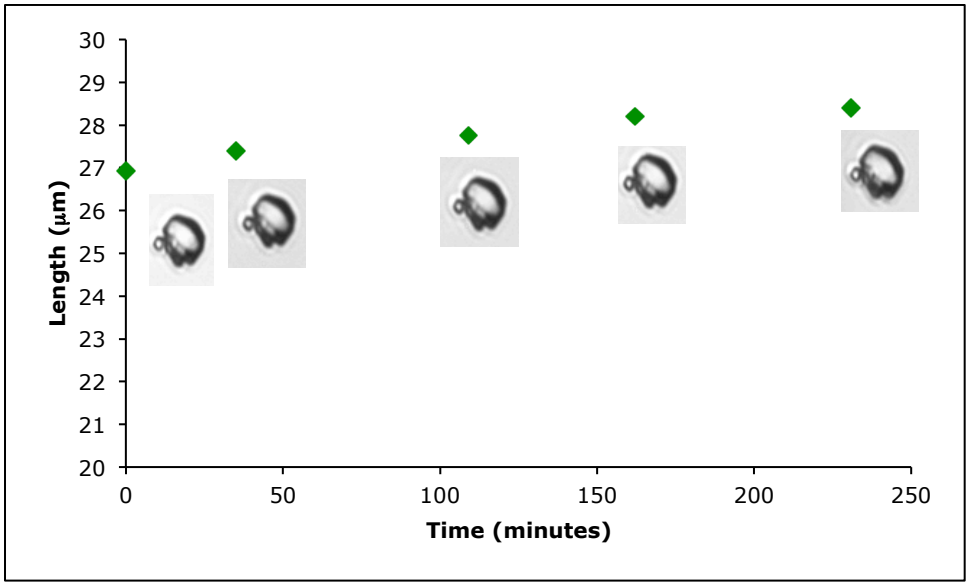

Figure 5-18 SUP + 1 mM Na_2HPO_4 @ pH 1.76, growth rate 0.006 µm/min

5.3.4 Impact on solubility

Additives may impact on crystal growth systems in different ways. So far, it has been assumed that the additives studied here are having an impact on the crystal growth processes by virtue of incorporation into or interaction with the crystal faces. It is also possible for the additive to change the solution-phase behaviour. Most importantly the additives may have an impact on the solubility of α-lactose monohydrate. This would result in changes in the starting supersaturation of the experiments described above. Supersaturation is a measure of expressing the driving force of both crystallization and nucleation (Visser, 1982).

The literature appears to have no common means of expressing lactose solubility. However, Visser (1982) has determined it most suitable to express lactose solubility as grams of anhydrous lactose per 100 g water.

The sodium phosphate additive exhibited the greatest impact on the morphology of the habit of α-lactose monohydrate, and hence the impact of this salt on the solubility of SUP α-lactose monohydrate was investigated. A bottle roller experiment was conducted at 30 ˚C. Samples were taken at intervals to determine the rate of lactose dissolution in an under-saturated solution and de-supersaturation in a supersaturated system, to ultimately

determine the equilibrium solubility. The anhydrous lactose concentrations were determined using HPLC. The density of SUP α-lactose at equilibrium solubility was determined using a density bottle and was calculated as 1.092 gmL^{-1}. Final solubility calculations were performed using the formula derived by Visser (1982), Equation 5-3.

S_{mh} = final solubility, expressed as grams lactose monohydrate per 100 g water

C_a = anhydrous lactose concentration, g/100g water

M_{mh} = molecular mass of lactose monohydrate

M_a = molecular mass of anhydrous lactose

$$C_a = (S_{mh} . M_a/M_{mh}) . (100/100 + S_{mh}(1-M_a/M_{mh})) \quad (1)$$

Such that; $$C_a = 0.95\, S_{mh} /(1 + 0.0005\, S_{mh}) \quad (2)$$

Finally; $$\mathbf{S_{mh} = 1/ (0.95/C_a) – 0.0005} \quad \mathbf{(3)}$$

Equation 5-1 Solubility calculation derived by Visser 1982

The equilibrium solubility for SUP α-lactose monohydrate, in the absence of any additives, in milliQ water at 30 ˚C was determined to be 25.87 ± 0.56 g α-lactose monohydrate per 100 g milliQ water. This was determined by calculating the mean solubility numbers from the final experimental period; where equilibrium appeared to have been well established (+10000 minutes), see Figure 5-20. This is comparable to the solubility determined by Visser (1982) of 26.5 g α-lactose monohydrate per 100 g water.

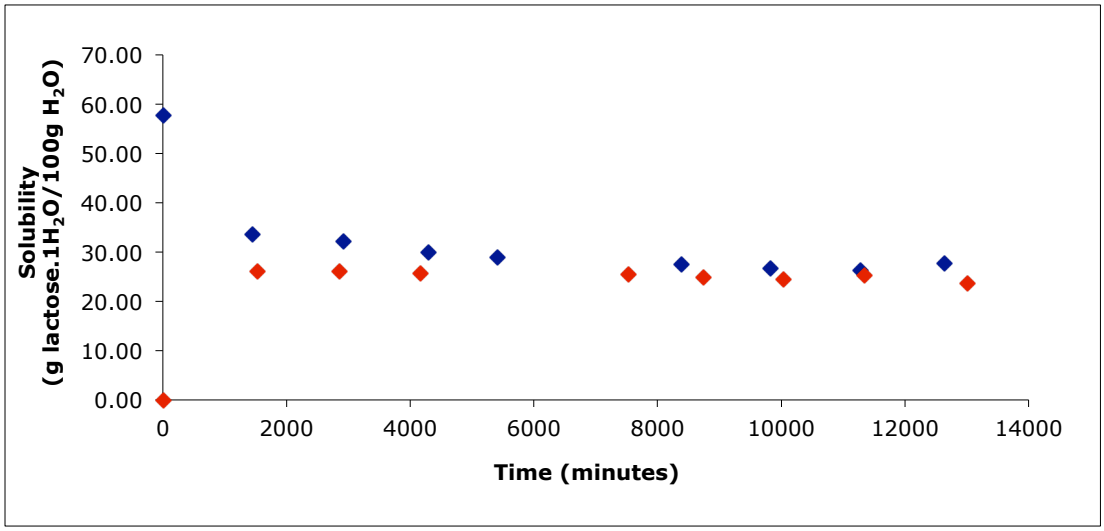

Figure 5-19 Saturation and de-supersaturation of SUP α-lactose monohydrate in milliQ water at 30 ˚C.

From Figure 5-19 it is observed that the de-supersaturation rate is somewhat slower than the saturation.

The same approach was applied to the SUP α-lactose monohydrate system spiked with 0.001M Na_2HPO_4. The equilibrium solubility was determined to be 25.33 ± 0.22 g α-lactose monohydrate per 100 g milliQ water (Figure 5-20). It would therefore appear that this low concentration of Na_2HPO_4 has no measureable impact upon the solubility of the SUP α-lactose monohydrate in milliQ water at 30 ˚C.

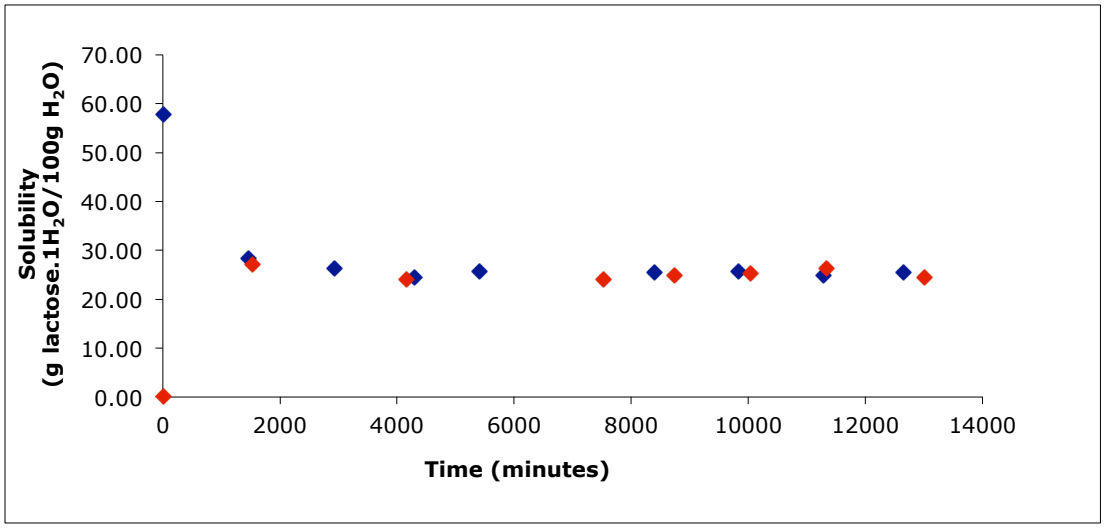

Figure 5-20 Saturation and de-supersaturation of SUP α-lactose monohydrate with 0.001M Na_2HPO_4 in milliQ water at 30 ˚C.

5.3.5 Bulk Crystallization Studies

Some of the experiments carried out using the Common History Seed method (CHS) method (Bronwen Butler,PhD thesis April 1998) proved to be poorly reproducible, in terms of the quantity of seed produced. Thus some experiments were carried out to determine the impact that ultrasonication has on nucleation and to determine if there is any secondary nucleation over time. Additive influence upon nucleation was also investigated.

These crystallization studies have been performed using the SUP α-lactose monohydrate as the blank, as there were inadequate quantities of the IEL α-lactose monohydrate to conduct these investigations. The impact of additives 0.001M Na_2HPO_4 and glucose 6-phosphate were also investigated.

5.3.5.1 SUP α-lactose monohydrate

Using the SUP α-lactose monohydrate with a constant supersaturation of 0.55, the impact of the 3 minutes of ultrasonication as prescribed by the 'Common History Seed method' (Bronwen Butler,PhD thesis April 1998) was examined.

Ultrasonication certainly has an impact on the induction period despite the system being stirred. The results clearly rule out the hypothesis that the impact of stirring may override the impact of sonication. Looking at the turbidity data (see Figure 5-21), the sonicated systems produce a change in turbidity after about 145 minutes, suggesting nucleation has commenced. Without sonication, incubation is lengthy and an equivalent rate change to the sonicated system does not occur until after 2850 minutes.

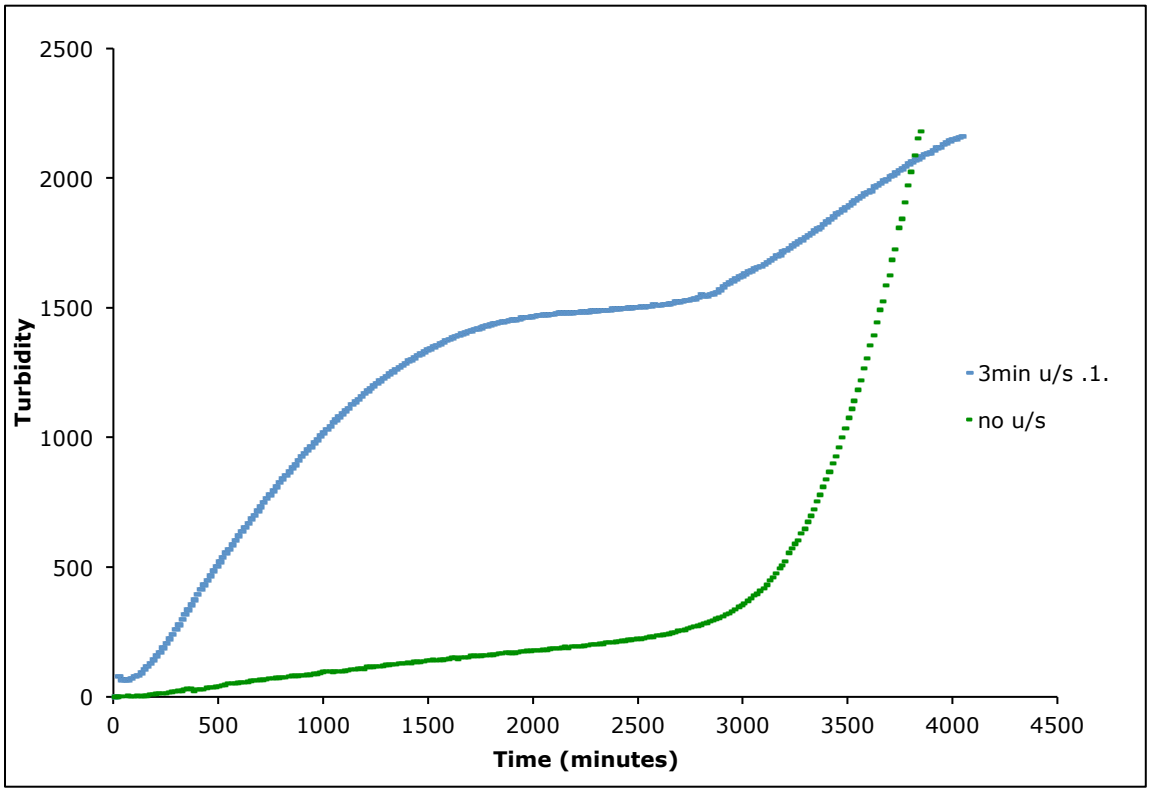

Figure 5-21 Turbidity of SUP α-lactose monohydrate with and without sonicated induced nucleation

For the sonicated runs it appears that there is minimal incubation time before nucleation commences followed by growth. After a plateau there appears to be some secondary nucleation and subsequent growth (2800 minutes). The first event initiates a more rapid increase in turbidity than the second, which is consistent with the second event occurring at a lower supersaturation. These results suggest that the CHS method successfully produced a batch of

nuclei over a short time period, but this does not prevent subsequent nucleation events taking place.

It is difficult to directly relate turbidity with crystal size and number, however, upon visually examining the crystals at intervals, there appears to be minimal breakage of the crystals and certainly growth followed by secondary nucleation at the aforementioned times. This suggests that there is secondary nucleation taking place independent of any crystal breakage caused by the stirring.

A replicate experiment (Figure 5-22) gave similar results in terms of the timing and number of nucleation events, but with some variation of the rates of increasing turbidity.

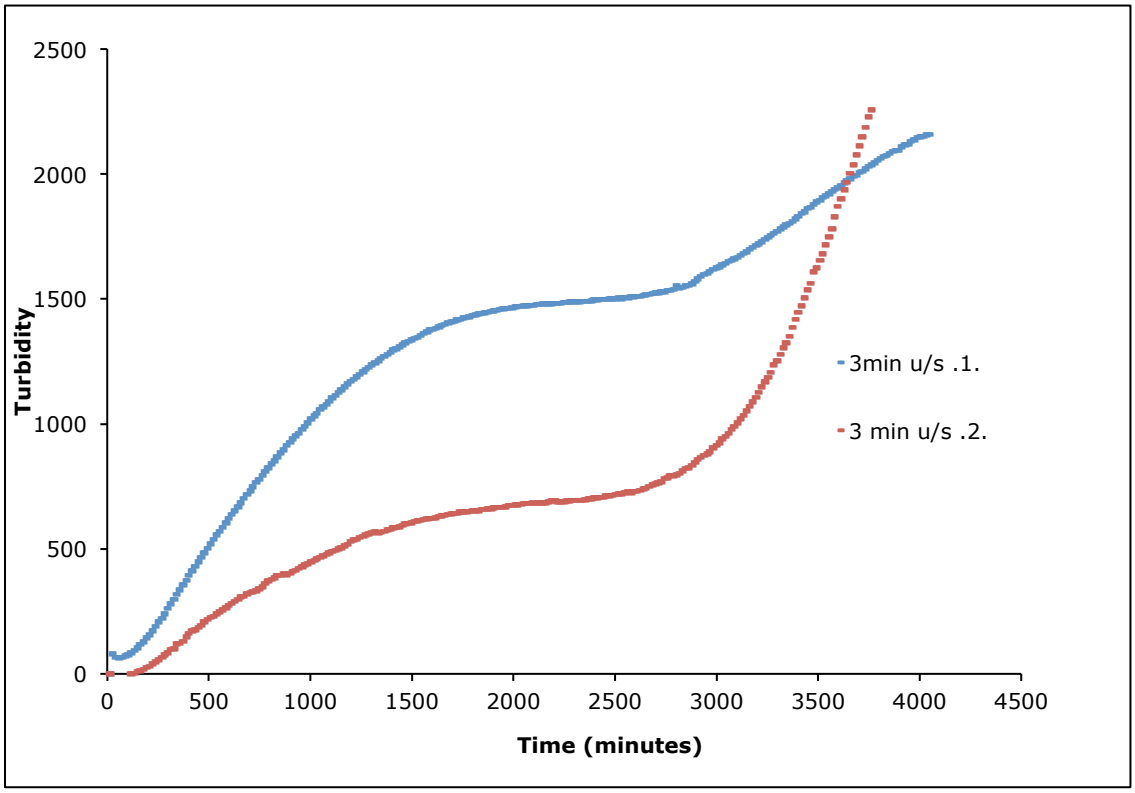

Figure 5-22 Replicate turbidity analysis of SUP α-lactose monohydrate under Common History Seed conditions.

These results suggest that the CHS method works so far as inducing nucleation but does not account for the problem of secondary nucleation, at least for longer term crystal growth experiments. Secondary nucleation is a significant issue when growing seed for measuring the growth rate using *in situ* optical microscopy, as during measurement the secondary nuclei crowd the seed of interest making it impossible to measure. The supersaturation of the liquor in the cell may also change too rapidly thereby producing invalid results for growth rate at a given supersaturation. It would be most suitable to grow and measure seed before secondary nucleation takes place, 25 hours being the most suitable total growth time to use. It is however not practical to apply this to every system as despite nucleation onset, if growth is slow then the crystals by this time may not have grown to a sufficient size for accurate measurements.

5.3.5.2 Na_2HPO_4

Sodium hydrogen phosphate was selected as the additive to test in bulk crystallization studies as it was found to have the most significant impact of the inorganic additives tested. Crystal size distribution (CSD) data has been gathered by measuring the crystals from 1mL samples taken at intervals and is shown in the figure (Figure 5-23) below.

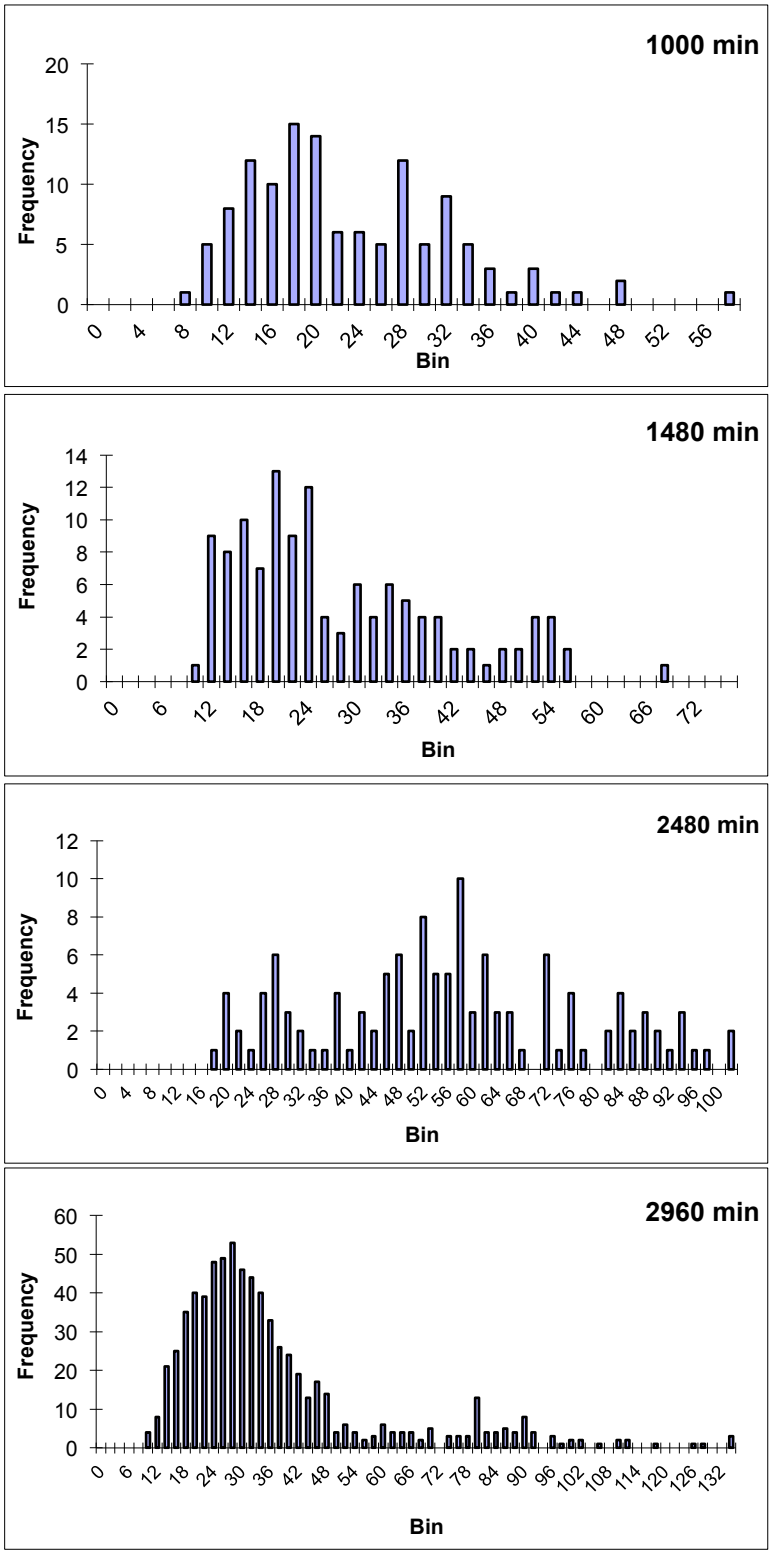

Figure 5-23 CSD of 0.001M Na_2HPO_4 in 0.55ss SUP α-lactose monohydrate, u/s 3 min, pH 6.38

This experiment was performed at the natural pH of the system pH 6.38 and with sonication for three minutes at the beginning of the experiment. As a rough estimate, the mean crystal length for the 1480 minutes (~24 hours) has been taken and the growth rate determined to be about 0.018 μm/minute, which matches the *in situ* growth rate studies of 0.018 μm/minute, which was measured after 20 hours of growth. From the above CSD graphs there appears to be a number of separate nucleation events. There does appear to be secondary nucleation happening at the 1480-minute mark, with a number of peaks and valleys becoming evident in the histogram and more exaggerated by 2480 minutes. By 2960 minutes there is a mass of smaller crystals; it may be that the larger crystals are not being sampled due to attrition in the crystallizer, or unrepresentative sampling of the largest crystals. The occurrence of secondary nucleation is, however, quite clearly revealed by examination of the crystals.

The morphology of the crystal continues to be different to that of an unmodified α-lactose monohydrate crystal and is illustrated in the table below (Table 5-3).

Table 5-3 Morphology and average crystal size of SUP α-lactose monohydrate grown in the presence of 0.001M Na_2HPO_4, pH 6.38

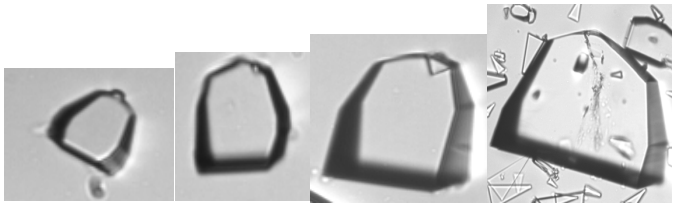

1000 mins	1480 mins	2480 mins	2960 mins
22.36 μm	26.77 μm	52.14 μm	35.80 μm

Changes in de-supersaturation rate are also consistent with the nucleation events. In the figure below (Figure 5-24), there would appear to be a steady

de-supersaturation, followed by a plateau and another decrease, highlighting two significant events.

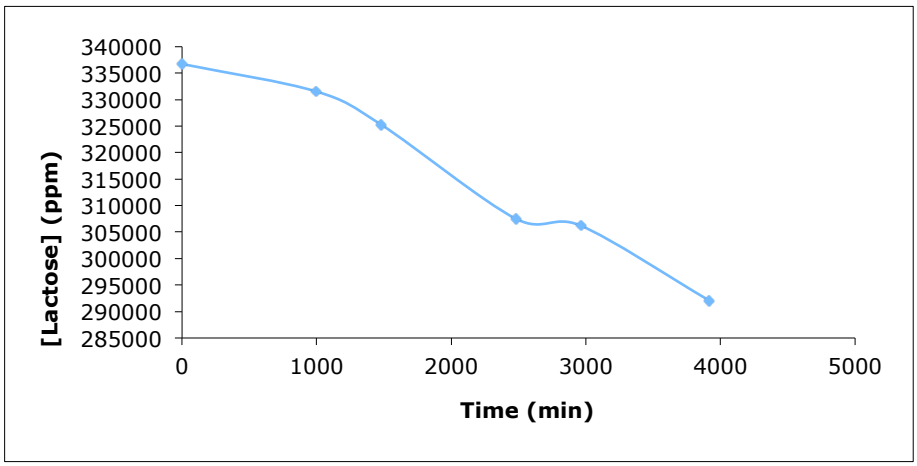

Figure 5-24 De-supersaturation of SUP α-lactose monohydrate, 0.55 ss, with 0.0001M Na_2HPO_4, pH 6.38

This experiment was repeated at a more neutral pH of 7.05. The slight change in pH appears to alter the nucleation and growth behaviour. When compared to the growth rate in earlier studies using *in situ* microscopy there is a discrepancy (0.013 μm/minute determined by *in situ* microscopy cf. 0.022 μm/minute from bulk crystallization). The estimated growth rate is also faster than that seen in the system at pH 6.38, 0.018 μm/minute. It should be noted that this method of estimating crystal growth rate from the bulk growth experiment is an approximation, and these differences may be due to experimental error.

With respect to the observed CSD, generally the average crystal size increases with time, unlike that seen in the previous experiment at pH 6.38, with a mass of crystals averaging 36 μm at 2960 minutes. At this pH of 7.05, the average crystal size at 2960 minutes is 44 μm. There is an onset of secondary nucleation by 1480 minutes, with a number of additional nucleation events happening as the experiment progresses. This is reflected in the de-supersaturation data (Figure 5-26), as the lactose concentration plateaus around 1000 minutes and continues to decrease about 1500 minutes.

Regardless of these variations with changing pH, it is notable that the unusual morphology of the crystals produced in the presence of sodium phosphate is maintained (Table 5-4)

Table 5-4 Morphology and average crystal size of SUP α-lactose monohydrate grown in the presence of 0.001M Na_2HPO_4, pH 7.05

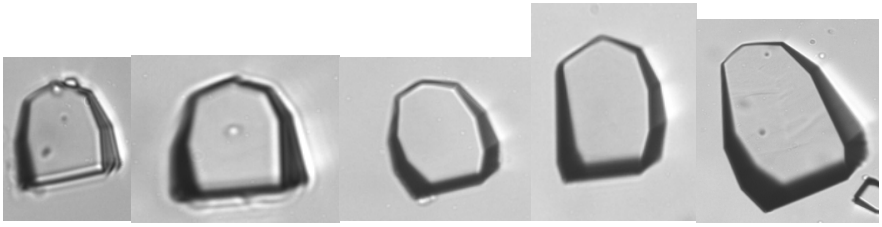

1000 mins	1480 mins	2480 mins	2960 mins	3800 mins
26.58 μm	32.72 μm	46.63 μm	43.94 μm	61.47 μm

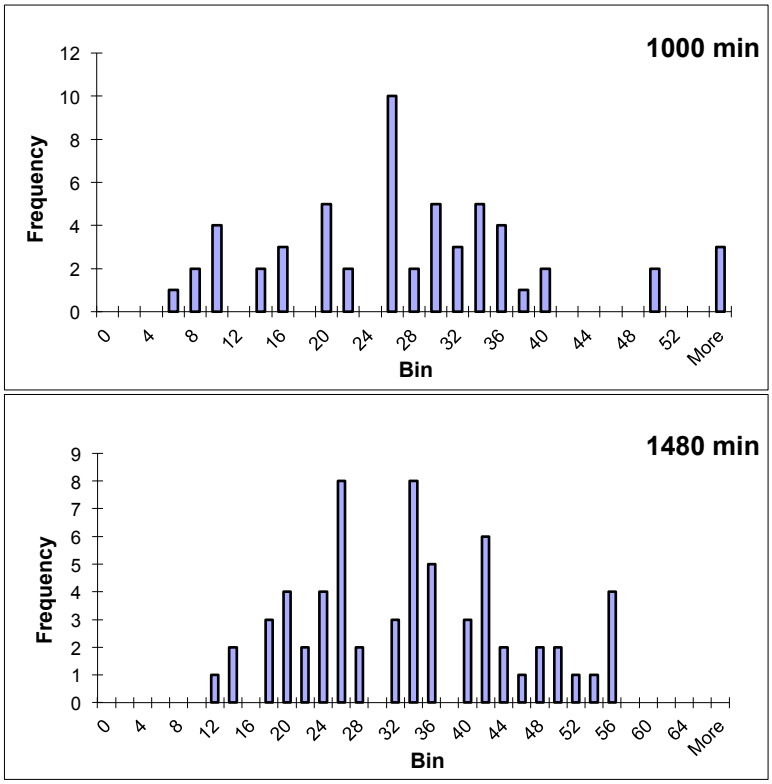

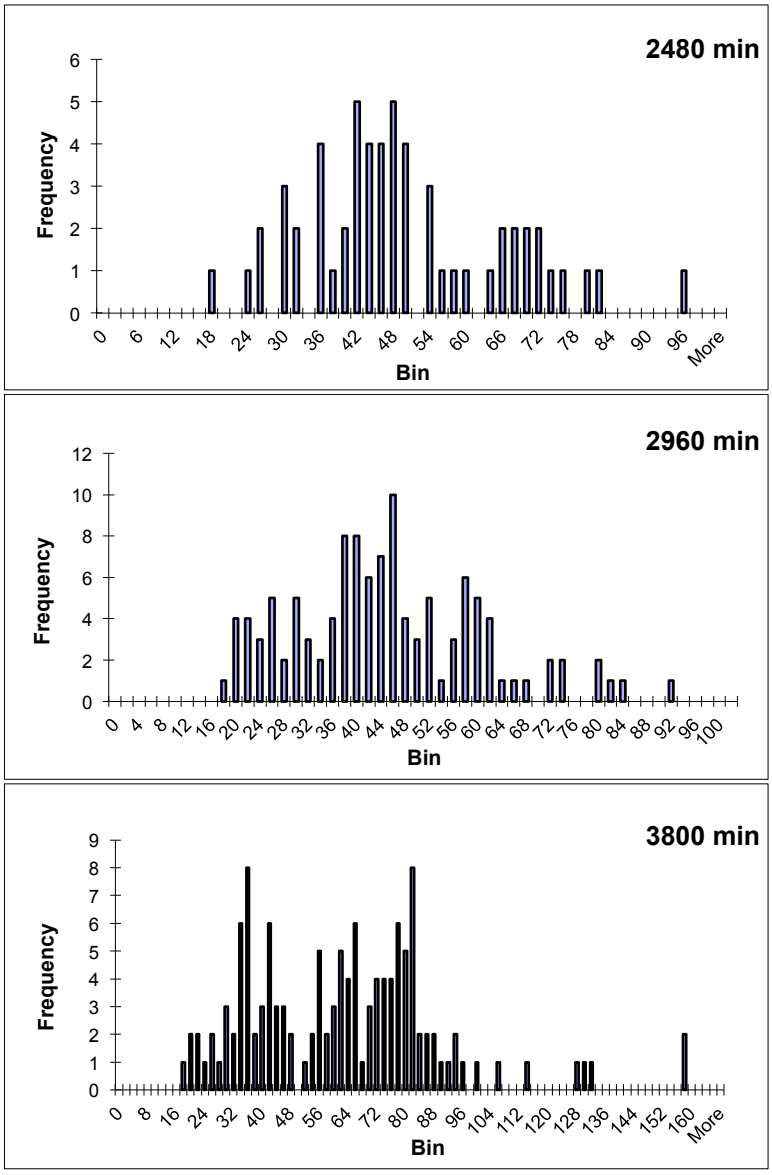

Figure 5-25 CSD of lactose crystals produced from a solution of 0.001M Na_2HPO_4 in 0.55 ss SUP α-lactose monohydrate, u/s 3 min, pH 7.05

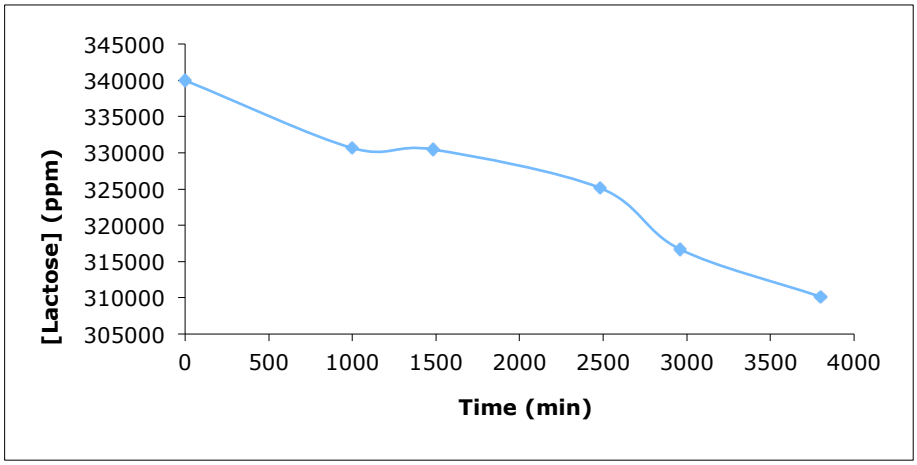

Figure 5-26 De-supersaturation of SUP α-lactose monohydrate, 0.55 ss, with 0.0001 M Na_2HPO_4, pH 7.05

5.4 CONCLUSIONS

The work reported here has shown that sugar phosphates with structural similarity to the intrinsic lactose phosphates present in lactose do have an impact on crystal growth. In the absence of other impurities, they clearly inhibit growth and alter morphology. When convoluted with the intrinsic lactose phosphates, the effects are not so clearly defined. The introduced sugar phosphates can actually increase the observed growth rate, perhaps by competing with the more effective lactose phosphates already present.

Inorganic additives were found in general to have a much smaller influence on growth rate. At low pH these additives do seem to allow the lactose phosphate inhibition to persist, whereas in the blank, low pH results in more rapid growth, presumably because the lactose phosphate is protonated. A particularly interesting observation was that sodium phosphate (but not potassium phosphate) has a very specific effect on the crystal morphology, inducing the formation of a much wider tomahawk shape. The fact that an ion pair has an impact, where the individual components do not, may explain some of the existing inconsistencies in the literature.

Bulk crystallisation studies indicated that ultrasound can be successfully used to initiate nucleation in a supersaturated lactose solution, but this does not prevent subsequent secondary nucleation on timescales that are relevant for

crystal growth studies. Similar behaviour is seen in the blank system and in the presence of sodium phosphate. This issue should be considered in any future work of this nature.

The remarkable impact of sodium phosphate, as an ion pair, on the morphology of lactose was consistent throughout these bulk crystallisation experiments. This is a significant result, as it shows that the cation and anion present in inorganic additives or impurities, may act synergistically with other components present in the liquor.

6 Conclusions and Recommendations

There were three aspects to this research program into the growth rate inhibition of lactose. Firstly, the purification of commercially available lactose, principally the removal of lactose monophosphates. Secondly, an extensive study of the growth rate of α-lactose monohydrate. Finally, an examination of the influence of inhibitors on the growth rate of α-lactose monohydrate.

To fully understand the impact of any growth retardation, the growth rate of pure lactose needed to be determined. The first step was to find a source of pure lactose. This is challenging, as there is currently no commercially available form of pure lactose. The commercially available material is always contaminated by lactose monophosphates, as current manufacturing techniques do not account for its removal. Hence purified lactose had to be prepared in-house, or supplied by a collaborator. Several techniques were evaluated for the purification of the purest form of commercially available α-lactose monohydrate.

Ion exchange chromatography was proven to be the most effective means of purifying the commercial α-lactose monohydrate. The total phosphate content of the SUP was reduced from 170.6 ppm to on average less than 4 ppm. However the technique is more suited to large-scale industrial processes for lactose purification.

Recrystallization methods were also investigated and attempts were made to refine the techniques undertaken by Visser to generate a pure lactose product, however they were very time-consuming. The reduction in organic phosphate concentration ranged from 10 – 30 ppm from the SUP blank of 128.5 ppm.

A novel approach using zirconium phosphonate modified surfaces as a means of removing organic phosphates was attempted. This proved to be surprisingly successful and significantly reduced the overall phosphate content of the SUP

α-lactose monohydrate. The inorganic phosphate content was reduced from 46 ppm in the SUP to 8.4 ppm and the organic phosphate content reduced from 128.5 ppm in the SUP to 4.6 ppm. Very little materials and handling were required for this method. This method of purification definitely warrants further investigation for future lab scale crystal growth studies.

Crystal growth rate studies of the purified lactose samples clearly demonstrated that the growth rate of α-lactose monohydrate can be greatly enhanced by removal of the lactose phosphate impurities.

As previously discussed, ion exchange chromatography can produce highly purified α-lactose monohydrate with growth rates from 0.12 μm/min to 0.14 μm/min. However, the inefficiency of the process in lab scale production prevented production of sufficient quantities of purified lactose and a supplementary source was investigated and found at the University of Western Sydney. This lactose was produced on a pilot plant scale using ion exclusion. The purified samples (IEL) were found to have faster growth rates than the SUP, growing on average 0.034 μm/min compared to 0.013 μm/min.

The SUP when in solution at ss 0.55 and 30 ˚C has a pH of 3.59, compared to the equivalent solution of the purified lactose of pH 6.5. The acidity of the SUP is due to the presence of the organic phosphate contaminants. It was found that at this pH the SUP growth rate is effectively inhibited, however, increasing or decreasing the pH of the SUP system enhances the growth rate.

Lactose phosphates are known adsorb to crystal surfaces during the preliminary stages of lactose crystallisation. The pH of the system has a significant effect on the lactose phosphate speciation. At the lower pH the phosphate species present in solution are protonated and may have less affinity with the crystal surface as a neutral species. At the higher pH the more prevalent dianion species may be less surface active, perhaps due to the lack of an H-bond donor. These tentative hypotheses may explain why the lactose crystal growth rate increases when the pH is changed to higher or lower values.

The impact of pH on the purified lactose product was also investigated. This lactose product grew at a significantly enhanced rate compared to the SUP. At close to neutral pH, ss 0.55 at 30 ˚C the growth of the (010) face was determined to be 0.034 μm/min. At the lower pH 3.21 the growth was doubled to 0.067 μm/min and then diminished at pH 1.95 to 0.009 μm/min. It is proposed that this reduction in growth rate is a result of the rapid growth of the (010) face when nucleated at such a low pH, such that the face grows out of the morphology entirely. Once this face is absent, the crystal grows at a significantly reduced rate.

Much of the work reported in the literature involves impure lactose systems. There is very little literature on the impact of pH on pure lactose systems, specifically on the growth rate of α-lactose monohydrate. The literature reviewed in Chapter 2 demonstrates some conflicting results into the impact of pH, which may be a result of the complexities of the pH and lactose phosphate impurities. The work undertaken in this study shows that pH has a significant impact on the growth rate of α-lactose monohydrate when examined as a pure system.

Finally, studies were undertaken to examine the influence of several inhibitors. These inhibitors were selected based on structural similarity to lactose, and inorganic salts present in lactose production and by-products.

The impacts of additives that are structurally similar to the lactose phosphates found in lactose were initially investigated. In the absence of other impurities they inhibit growth and alter morphology. However, when convoluted with the intrinsic impurities the impact is not so evident. The sugar phosphate additives can even increase the observed growth rate of the impure system, perhaps as they are competing with the more effective inherent lactose phosphates for surface absorption.

Inorganic additives appeared to have a lesser impact on growth rate. At low pH the additives appear to have no effect on the persistent inhibition resulting

from the lactose phosphates. The morphology of the α-lactose monohydrate crystal was, however, significantly changed by the presence of sodium phosphate, whereby a much broader tomahawk morphology was observed. This was not observed in the potassium phosphate additive system. It would appear that the ion pair has a significant impact upon the crystal growth, where the individual components do not. This observation may explain some of the inconsistencies in the literature.

Bulk crystallization studies confirmed that ultrasound can induce nucleation in a supersaturate lactose solution. However, subsequent secondary nucleation events cannot be avoided within the time parameters that are required for the crystal growth studies carried out in this study. Additional studies into the impact of ultrasonic induced nucleation should be undertaken to further explore this methodology.

The most significant observation made in this study was the impact of the sodium phosphate. At a relatively low concentration, the ion pair appears to have a substantial influence on the morphology of the α-lactose monohydrate crystal. This suggests that the cations and anions present in additives or impurities may behave synergistically with other components present, complicating any prediction of the effect of impurities on the crystal growth of lactose.

7 References

Alderighi, L., Gans, P., Ienco, A., Peters, D., Sabatini, A., Vacca, A. (1999). "Hyperquad simulation and speciation (HySS): a utility program for the investigation of equilibria involving soluble and partially soluble species." Coordination Chemistry Reviews **184**: 311-318.

Allen, F. H. (2002). "The Cambridge Structural Database: a quarter of a million crystal structures and rising." Acta Crystallographica **B58**: 380-388.

Beever, C. A., Hansen, H.N (1971). "The structre of alpha lactose monohydrate." Acta Crystallographica Section B **27**(7): 1323-1325.

Berdholdt, A., Overgaard, J., Colding, A. (1993). "Separation of D-galactonic and D-gluconic acids by capillary zone electrophoresis." Journal of Chromatography A **644**: 412-415.

Berenblum, I., Chain, I. (1938). "An Improved Method for the Colourimetric Determination of Phosphate." Biochemical Journal **32**(2): 295-298.

Bernabe, I., Di Martino, P., Joiris, E., Berneron, C., Guyot-Hermann, A.M., Conflant, P., Drache, M. (1995). "Compression Ability Improvement of Lactose by Recrystallization. Influence of Lactose Phosphate Content." Il Farmaco **50**(11): 801 - 809.

Bhargava, A., Jelen, P. (1996). "Lactose Solubility and Crystal Growth as Affected by Mineral Impurities." Journal of Food Science **61**(1): 180-184.

Breg, J., Visser, R.A., Haasnoot , C.A.G. (1988). "Characterisation of Four Lactose Monophosphates by Application of ^{31}P-, ^{13}C-, and ^{1}H-N.M.R. Spectroscopy." Carbohydrate Research **174**: 23-36.

Brons, C., Oliman, C. (1983). "Study of the High Performance Liquid Chromatographic Separation of Reducing Sugars, Applied to the Determination of Lactose in Milk." Journal of Chromatography **259**: 79-86.

Burma, T. J., Wiegers, G.A. (1967). "X-Ray powder patterns of lactose and unit cell dimensions of beta lactose." Netherlands Milk Dairy **21**: 208-213.

Butler, B. (1998). Modelling Industrial Lactose Crystallization. Department of Chemical Engineering. Brisbane, The University of Queensland. **Doctor of Philosophy**.

Caron, V., Lefebvre, J., Wilart, J.F., Lefort, R., Affouard, F., Danede, F. (2005). "Structure determination of the 1/1 α/β mixed lactose by X-ray powder diffraction." Acta Crystallographica Section B **64**: 455-463.

Carvalho, L. H. M., De Koe, T., Tavares, P.B. (1998). "An improved molybdenum blue method for simultaneous determination of inorganic phosphate and arsenate." Ecotoxicology and Environmental Restoration 1 **1**: 13-19.

Chaplan, M. F., Kennedy, J.F. (1994). Carbohydrate Analysis: A Practical Approach. Oxford, Oxford University Press.

Chifflet, S., Torriglia, A., Chiesa, R., Tolosa, S. (1986). "A method for the determination of inorganic phosphate in the presence of labile organic phosphate and high concentrations of protein: Application to Lens ATPases." Analytical Biochemistry **168**: 1-4.

Christian, G. D. (2004). Liquid Chromatography. Analytical Chemistry. D. Brennan. Washington, John Wiley and Sons Inc.

Clydesdale, G., Roberts, K.J., Telfer, G.B., Grant, D.J.W. (1997). "Modelling the Crystal Morphology of α-Lactose Monohydrate." Journal of Pharmaceutical Sciences **86**(1): 135-141.

Cook, W. J., Bugg, C.E. (1973). "A Lactose-Calcium Chloride Heptahydrate Complex." Acta Crystallographica **B29**: 907-909.

Dickman, S. R., Bray, R.H. (1940). "Colourimetric Determination of Phosphate." Industrial and Engineering Chemistry, Analytical Edition **12**(11): 665-668.

Dincer, D. T., Parkinson, G.M., Rohl, A.L., Ogden, M.I. (1999). "Crystallisation of α-lactose monohydrate from dimethyl sulfoxide (DMSO) solutions: influence of β-lactose." Journal of Crystal Growth(205): 368-374.

Dincer, T. D. (2000). Mechanisms of Lactose Crystallisation. School of Applied Chemistry. Perth, Curtin University of Technology. **Doctor of Philosophy**.

Doble, P., Hahhad P.R. (1999). "Indirect photometric detection of anions in capillary electrophoresis." Journal of Chromatography A **834**: 189-212.

Dong, J., Zhou, H., Wu, R., Ye, M., Zou, H, (2007). "Specific capture of phosphopeptides by Zr^{4+}-modified monolithic capillary column." Separation Science **30**: 2917-2923.

El-Mahdaoui, L., Neault, J.F., Tajmir-Riahi, H.A. (1997). "Carbohydrate-Nucleotide Interaction. The Effects of Mono- and Disaccharides on the Solution Structure of AMP, dAMP, ATP, GMP, dGMP, and GTP Studies by FTIR Difference Spectroscopy." Journal of Inorganic Biochemistry: 123-131.

Etienne, M., Walcarius, A. (2002). "Analytical investigation of the chemical reactivity and stability of aminopropyl-grafted silica in aqueous medium." Talanta **59**: 1173-1188.

Ferro, V., Li, C., Fewings, K., Palmero, M.C., Linhardt, R.J., Toida, T. (2002). "Determination of the composition of the oligosaccharide phosphate fraction of *Pichia (Hansenula) holstii* NRRL Y-2448 phosphomannan by capillary electrophoresis and HPLC." Carbohydrate Research **337**: 139-146.

Feurle, J., Jomaa, H., Wilhem, M., Gutsche, B., Herderich, M. (1998). "Analysis of phosphorylated carbohydrates by high-performance liquid chromatography-electrospray ionization tandem mass spectrometry utilising a beta-cyclodextrin bonded stationary phase." Journal of Chromatography A **803**: 111-119.

Freij, A. J. (2006). Crystallization of Lactose from Whey and Permeate. Department of Applied Chemistry. Perth, Curtin University of Technology. **Doctor of Philosophy**.

Fries, D. C., Rao, S.T., Sundaralingam, M. (1971). "Structural chemistry of carbohydrates. III. Crystal and molecular structure of 4-O-β-$_D$-galactopyranosyl-α-$_D$-glucopyranose monohydrate (α-lactose monohydrate)." Acta Crystallographica Section B **27**(2): 994-1005.

Garnier, S., Petit, S., Coquerel, G. (2002). "Dehydration Mechanism and Crystallisation Behaviour of Lactose." Journal of Thermal Analysis and Calorimetry **68**: 489-502.

Garnier, S., Petit, S., Coquerel, G. (2002). "Influence of supersaturation and structurally related additives on the crystal growth of α-lactose monohydrate." Journal of Crystal Growth **234**: 207-219.

Goodhart, F. W. (1994). Handbook of Pharmaceutical Excipients. London, The Pharmaceutical Press.

Grases, F., Garcia-Ferragut, L., Cost-Bauza, A., Prieto, R., March, J.G. (1994). "Determination of escin based on its inhibitory action on lactose crystallization." Analytica Chimica Acta **288**: 265-269.

Gurney, R. W., Kurimoto, M., Subramony, J.A., Bastin, L.D., Kahr, B. (2001). Optical Probes for Crystal Growth Mechanisms: Intersectoral Zoning. Anisotropic Organic Materials. R. Glasser and P. Kaszynski, American Chemical Society. **798:** 143-156.

Guu, M. Y. K., Zall, R.R. (1991). "Lactose Crystallization: Effects of Minerals and Seeding." Process Biochemistry **26**: 167-172.

Haase, G., Nickerson, A. (1966a). "Kinetic reactions of α- and β- lactose, I Mutarotation." Journal of Dairy Science(49): 127-132.

Haase, G., Nickerson, A. (1966b). "Kinetic reactions of α- and β- lactose, II Crystallization." Journal of Dairy Science(49): 757-761.

Harper, W. J. (1992). Lactose and Lactose Derivatives. Whey and Lactose Processing, Elsevier Applied Science**:** 317- 360.

Hartel, R. W., Shastry, A.V. (1991). "Sugar Crystallization in Food Products." Critical Reviews in Food Science and Nutrition **30**(1): 49-112.

Heiger, D. (2000). An Introduction - High performance capillary electrophoresis. Germany, Agilent Technologies.

Hendriksen, B. A., Grant, D.J.W., Meenan, P., Green, D.A. (1998). "Crystallization of paracetamol (acetaminophen) in the presence of structurally related additives." Journal of Crystal Growth **183**: 629-640.

Herrington, B. L. (1934). "Some physiochemical properties of lactose." Journal of Dairy Science(17): 533-542.

Hodges, G. E., Lowe, E.K., Paterson, A.H.J (1993). "A mathematical model for lactose dissolution." The Chemical Engineering Journal **53**: B25-B33.

Hoffstetter-Kuhn, S., Paulus, A., Gassmann, E., Widmer, H. M. (1991). "Influence of Borate Complexation on the Electrophoretic Behaviour of Carbohydrates in Capillary Electrophoresis." Analytical Chemistry **63**: 1541-1547.

Holsinger, V. H. (1988). Lactose. Fundamentals of dairy chemistry. W. P. Wong. New York, Van Nostrand Reihold Co.

Holsinger, V. H. (1997). Physical and Chemical Properties of Lactose. Advanced Dairy Chemistry, Volume 3, Lactose, Water, Salts and Vitamins. P. F. Fox. London, Chapman & Hall.

Hunziker, O. F., Nissen, B.H. (1924). Lactose Solubility and Lactose Crystal Formation. Chicago, Illinois, Blue Valley Research Laboratories.

Jager, A. V., Tonin, F.G., Tavare, F.M.M. (2007). "Comparative evaluation of extraction procedure and method validation for determination of carbohydrates in cereals and dairy products by capillary electrophoresis." Journal of Separation Science **30**: 586-594.

Jelen, P., Coulter, S.T (1973). "Effects of Certain Salts and other Whey Substances on the Growth of Lactose Crystals." Journal of Food Science **38**: 1186-1189.

Jelen, P., Coulter, S.T. (1973). "Effects of supersaturation and temperature on the growth of lactose crystals." Journal of Food Science(38): 1182-1185.

Jencks, W. P., Regenstein, J. (2010). Ionization Constants of Acids and Bases Handbook of Biochemistry and Molecular Biology. R. L. Lundblad and F. M. MacDonald, CRC Press 595–635.

Jennes, R., Sloan, R.E. (1970). "The composition of milks in various species: A review." Dairy Science Abstracts **32**: 599-612.

Kahr, B., Gurney, R.W. (2001). "Dyeing Crystals." Chemical Reviews **101**: 893-951.

Katz, H. E., Schilling, M.L., Chidsey, C.E.D., Putvinski, T.M., Hutton, R.S. (1991). "Quaterthiophendiphosphonic acid (QDP): A Rigid Electron-Rich Building Block for Zirconium-Based Multilayers." Chemistry Materials **3**: 699-703.

Kauter, M. D. (2003). The Effects of Impurities on Lactose Crystallization. Division of Chemical Engineering. Brisbane, The University of Queensland. **Doctor of Philosophy**.

Khanjin, N. A., Montero, J.L. (2002). "Synthesis of mannose-6-phosphate analogs: large-scale preparation of isoteric mannose-6-phosphonate via cyclic sulfate precursor." Tetrahedron Letters **43**: 4017-4020.

Klockow, A., Paulus, A., Figueiredo, V., Amado, R., Widmer, H. M. (1994). "Determination of carbohydrates in fruit juices by capillary electrophoresis and high performance liquid chromatography." Journal of Chromatography A **680**: 187-200.

Koichi, I., Michio, U. (1965). "A new micromethod for the colourimetric determination of inorganic phosphate." Clinica Chemica Acta **14**: 361-366.

Koketsu, M., Linhardt, R. J. (2000). "Electrophoresis of Acidic Oligosaccharides." Analytical Biochemistry **283**: 136-145.

Kougoulos, E., Marziano, I., Miller, P.R. (2010). "Lactose particle engineering: Influence of ultrasound and anti-solvent on crystal habit and particle size." Journal of Crystal Growth **312**: 3509-3520.

Kubota, N., Yokota, M., Mullin, J.W. (2000). "The combined influence of superaturation and impurity concentration on crystal growth." Journal of Crystal Growth **212**: 480-488.

Landers, J. P. (1997). Handbook of Capillary Electrophoresis. New York, CRC Press.

Lane, S. M., Monot, J., Petit, M., Bujoli, B., Talham, D.R. (2007). "XPS Investigation of DNA binding to zircomium-phosphonate surfaces." Colloids and Surfaces B: Biointerfaces **58**: 34-38.

Lifran, E. V., Vu, T.L.L, Durham, R.J., Hourigan, J.A., Sleigh, R.W. (2006). "Crystallisation kinetics of lactose in the presence of lactose phosphate." Powder Technology **179**: 43-54.

Lowry, O. H., Lopex, J.A. (1945). "The Determination of Inorganic Phosphate in the Presence of Labile Phosphate Esters." The Journal of Biological Chemistry 421-428.

Lowry, O. H., Roberts, N.R., Leiner, K.Y., Wu, M., Farr, L. (1953). "The Quantitative Histochemistry of Brain, Chemical Methods." The Journal of Biological Chemistry **207**(1): 1-18.

Massari, A. M., Gurnwy R.W., Wightman M.D., Huang CH.K., Nguyen SB.T., Hipp J.T. (2002). "Ultrathin micropatterned porphyrin films assembled via zirconium phosphonate chemistry." Polyhderon **22**: 3065-3072.

Mazzobre, M. F., Aguilera, J.M., Buera, M.P. (2003). "Microscopy and calorimetry as complementary techniques to analyze sugar crystallization from amorphous systems." Carbohydrate Research **338**: 541-548.

McCommins, D. B., Bernhard, R.A., Nickerson, T.A. (1980). "Recovery of Lactose from Aqueous Solutions: Precipitation with Calcium Hydroxide and Sodium Hydroxide." Journal of Food Science **45**: 362-366.

McLeod, J., Paterson, A.H.J., Jones, J.R., Bronlund, J.E. (2011). "Primary nucleation of α-lactose monohydrate: The effect of supersaturation and temperature." International Dairy Journal **21**: 455-461.

McLeod, J. S., Paterson, A.H.J., Bronlund, J.E., Jones, J.R. (2010). "Nucleation of α-lactose monohydrate induced using flow through a venturi orifice." Journal of Crystal Growth **312**: 800-807.

McSweeney, P. L. H., Fox, P.F. (1997). Advanced Dairy Chemistry, Volume 3, Lactose, Water, Salts and Minor Constituents. New York, Springer.

Michaels, A. S., Van Kreveld, A. (1966). "Influences of Additives on Growth Rates in Lactose Crystals." Netherlands Milk and Dairy Journal **20**: 163-181.

Modler, H. W., Lefkovitch, L.P. (1986). "Influence of pH, Casein, and Whey Protein Denaturation on the Composition of Crystal Size, and Yield of Lactose from Condensed Whey." Journal of Dairy Science **69**: 684-697.

Mullin, J. W. (1997). Crystallization. Oxford, Reed Educational and Professional Publishing Ltd.

Murphy, J., Riley, J.P. (1962). "A modified single solution method for the determination of phosphate in natural waters." Analytica Chimica Acta **27**: 31-36.

Neuman, R. P., Rudge, S.R., Ladisch, M.R. (1987). "Sulfuric Acid-Sugar Separation by Ion Exclusion." Reactive Polymers **5**: 55-61.

Nickerson, T. A. (1979). "Lactose Chemistry." Journal of Agricultural Food Chemistry **27**(4): 672-677.

Nickerson, T. A., Moore, E.E. (1973). "α-Lactose crystallization rate." Journal of Dairy Science(57): 160-164.

Noordik, J. H., Beuskens, P.T., Bennema, P., Visser, R.A., Gould, R.O. (1984). "Crystal structure, polarity and morphology of 4-O-β-$_D$-galactopyranosyl-α-$_D$-glucopyranose monohydrate (α-lactose monohydrate): a redetermination." Zeitschrift fur Kristallographie - Crystalline Materials **168**(1-4): 59-65.

Oefner, P. J., Vorndran, A. E., Grill, E., Huber, C., Bonn, G. K. (1992). "Capillary Zone Electrophoretic Analysis of Carbohydrates by Direct and Indirect UV Detection." Chromatographia **34**(5-8): 308-316.

Pate, S. R., Murthy, Z.V.P. (2011). "Effect of process parameters on crystal size and morphology of lactose in ultrasound-assisted crystallization." Crystal Research and Technology **46**(3): 243-248.

Platteau, C., Lefebvre, J., Affouard, F., Derollez, P. (2004). "*Ab initio* structure determination of the hygroscopic anhydrous form of α-lactose by powder X-ray diffraction." Acta Crystallographica Section B **60**: 453-460.

Playne, M. J., Crittenden, R.G. (1997). Galacto-oligosaccharides and Other Products Derived from Lactose. Advanced Dairy Chemistry, Lactose, Water, Salts and Minor Constituents. P. L. H. McSweeney and P. F. Fox. New York, Springer. **3**.

Raghavan, S. L., Ristic, R.I., Sheen, D.B., Sherwood, J.N., Trowbridge, L., York, P. (2000). "Morphology of Crystals of α-Lactose Hydrate Grown from Aqueous Solution." Journal of Physical Chemistry B(104): 12256-12262.

Rassi, Z. E. (1999). "Recent Developments in capillary electrophoresis and capillary electrochromatography of carbohydrate species." Electrophoresis **20**: 3134-3144.

Rauls, M., Bartosch, K., Kind, M., Kuch, St., Lacmann, R., Mersmann, A. (2000). "The influence of impurities on crystallization kinetics - a case study on ammonium sulfate." Journal of Crystal Growth **213**: 166-128.

Sano, C., Kashiwagi, T., Nagashima, N., Kawakita, T. (1997). "Effects of additives on the crystal growth of L-glutamic acid crystals (beta-form)." Journal of Crystal Growth **178**: 568-574.

Schneider, I. C., Rhamy, P.J., Fink-Winter, R.J., Reilly, P.J. (1999). "High-performance anion-exchange chromatography of sugar and glycerol phosphates on quaternary ammonium resins." Carbohydrate Research **322**: 128-134.

Shi, Y., Hartel, W., Liang, B. (1989). "Formation and growth phenomena of lactose nuclei under contact nucleation conditions." Journal of Dairy Science **72**(11): 2906-2915.

Smart, J. B. (1988). "Effect of Whey Components on the Rate of Crystallization and Solubility of alpha-Lactose Monohydrate." New Zealand Journal of Dairy Science and Technology **23**: 275-289.

Smith, J. H., Dann, S.E., Elsegood, M.R.J., Blatchford, C.G. (2005). "α-Lactose monohydrate: a redetermination at 150K." Acta Crystallographica Section E **61**(8): 2499-2501.

Soga, T., Imaizumi, M. (2001). "Capillary electrophoresis method for the analysis of inorganic anions, organic acids, amino acids, nucleotides, carbohydrates and other anionic compounds." Electrophoresis **22**: 3418-3425.

Springfield, R. M., Hester, R.D. (1999). "Continuous Ion-Exclusion Chromatography System for Acid/Sugar Separation." Separation Science and Technology **34**(6): 1217-1241.

Stick, R. V. (2001). Carbohydrates: The Sweet Molecules of Life. London, Academic Press.

Swartz, M. L., Bernhard, R.A., Nickerson, T.A. (1978). "Interactions of Metal Ions with Lactose." Journal of Food Science **43**: 93-97.

Thurlby, J. A. (1976). "Crystallization Kinetics of α-Lactose." Journal of Food Science **41**: 38-42.

Van Kreveld, A. (1969). "Growth rates of lactose crystals in solution of stable anhydrous α-lactose." Netherlands Milk and Dairy Journal(23): 258.

Visser, R. A. (1980). "A natural crystal growth retarder in lactose." Netherlands Milk and Dairy Journal **34**: 255-275.

Visser, R. A. (1982). "Growth of non-ionic lactose at various temperatures and supersaturations." Netherlands Milk and Dairy Journal **36**: 167-193.

Visser, R. A. (1982). "Supersaturation of α-lactose in aqueous solutions in mutarotation equilibrium." Netherlands Milk and Dairy Journal **36**: 89-101.

Visser, R. A. (1984). "Experiments for tracing growth retarders in lactose." Netherlands Milk and Dairy Journal **38**: 107-133.

Visser, R. A. (1988). "Crystal growth retarding of α-lactose by sugar phosphates; a continued study." Netherlands Milk and Dairy Journal **42**: 449-468.

Visser, R. A., Bennema, P. (1983). "Interpretation of morphology of α-lactose hydrate." Netherlands Milk and Dairy Journal(37): 109-137.

Vorndran, A. E., Oefner, P. J., Scherz, H., Bonn, G. K. (1992). "Indirect UV Detection of Carbohydrates in Capillary Zone Electrophoresis." Chromatographia **33**(3/4): 163 - 168.

Walstra, P., Jennes, R. (1984). Carbohydrates. Dairy Chemistry and Physics, John Wiley and Sons Publications**:** 27-40.

Wang, H. C., Kurimoto, M., Kahr, B., Chimielewski, J. (2001). "α-Lactose Monohydrate Single Crystals as Hosts for Matrix Isolation of Guest Biopolymers." Bioorganic & Medicinal Chemistry **9**: 2279-2283.

Wang, S., Cheng, C., Tzou, Y., Liaw, R., Chang, T., Chen, J. (2007). "Phosphate removal from water using lithium intercalated gibbsite." Journal of Hazardous Materials(147): 205-212.

Wong, S. Y., Bun, R.K., Connelly, R.K., Hartel, R.W. (2011). "Determination of the dynamic metastable limit for α-lactose monohydrate crystallization." International Dairy Journal **21**: 839-846.

Woo, M. W., Fu, N., Moo, F.T., Chen, X.D. (2012). "Unveiling the Mechanism of in situ Crystallization in the Spray Drying of Sugars." Industrial & Engineering Chemical Research **51**: 11791-11802.

Yangzhen, C., Lindsey, J.S. (1998). "Analysis of sugar phosphate and related compounds using capillary zone electrophoresis with indirect UV detection." Journal of Chromatography A **816**: 251-259.

Zadow, J. G. (1984). "Lactose : Properties and Uses." Journal of Dairy Science **67**: 2654-2679.

"Every reasonable effort has been made to acknowledge the owners of copyright material. I would be pleased to hear from any copyright owner who has been omitted or incorrectly acknowledged."

8 Appendix

Table A-1 Growth measurements of SUP ss 0.55, 30 ˚C, pH 3.59

	Measurement time (min)							
	0	50	115	176	254	319		
Crystal #	Length of (010) face (μm)						GR (μm/min)	RSQ
1	19.6770	20.3410	21.1950	21.9690	23.4040	24.0590	0.0141	0.9954
2	61.7950	62.0640	63.0650	64.7970	65.3440	67.0680	0.0168	0.9706
3	44.9510	45.2950	45.4980	46.6320	47.2870	47.2870	0.0083	0.9355
4	71.9260	72.6310	73.9360	74.6780	75.9470	77.3200	0.0166	0.9957
5	73.5650	74.2770	75.4250	76.0480	77.0600	77.7030	0.0130	0.9957
6	65.6720	66.1760	67.0740	67.3960	68.8050	69.6710	0.0125	0.9854
7	33.6750	34.2650	34.8260	35.9900	36.2780	37.1780	0.0108	0.9785
8	37.6710	38.2000	34.6120	35.5940	36.1560	37.1890	0.0115	0.9820
9	50.7200	52.7500	53.1170	53.6010	55.1750	56.1730	0.0154	0.9481
10	45.0650	45.8700	46.1490	47.5970	48.4690	48.7680	0.0122	0.9655
11	62.4280	63.0380	64.1650	65.8990	66.4880	68.7890	0.0194	0.9723
12	70.8390	71.5530	73.2060	74.3560	75.0000	76.0820	0.0165	0.9773
13	31.7740	31.7740	33.6090	33.8670	36.4790	37.1340	0.0183	0.9550
14	38.9670	39.1070	39.6040	40.4660	40.7820	41.4940	0.0082	0.9760
15	49.2270	50.1140	51.5440	53.2080	53.5310	54.7380	0.0173	0.9667
16	58.7540	59.3090	59.9700	60.0730	62.8180	63.3750	0.0151	0.9175
17	46.9440	47.1610	48.4600	50.4000	51.0090	52.2310	0.0176	0.9703
18	75.9180	76.6500	77.9570	79.5500	80.1190	80.1660	0.0145	0.9233
19	34.4260	34.5240	34.6350	35.0950	35.6670	35.7740	0.0047	0.9484
20	53.3410	54.6620	54.7940	54.8050	55.4550	56.6170	0.0082	0.8663
21	36.9020	37.4350	38.5100	39.3540	40.2250	40.3690	0.0116	0.9671
Average	50.6780	51.2950	51.9691	52.9226	53.8809	54.7231	0.0135	0.9615

Table A- 2 Growth measurements of SUP ss 0.55, 30 ˚C, pH 1.68

	Measurement time (min)						
	0	75	133	210	280		
Crystal #	Length of (010) face (μm)					GR (μm/min)	RSQ
1	32.1780	35.4560	36.4100	37.8690	38.2200	0.0209	0.8964
2	25.0810	29.9970	32.4370	35.0480	37.2350	0.0422	0.9711
3	19.4850	21.9220	22.3480	22.6380	23.5260	0.0127	0.8456
4	18.0320	20.5080	21.6490	22.1290	22.2200	0.0143	0.8133
5	31.8560	37.5780	42.7960	48.0940	51.6020	0.0718	0.9911
6	27.5710	33.5570	42.7960	45.6960	48.3530	0.0769	0.9656
7	108.3510	113.6740	116.7320	120.5550	122.4160	0.0503	0.9743
8	15.7040	20.5370	24.8430	29.3270	32.2970	0.0603	0.9917
9	26.7060	31.1220	32.5790	35.0550	37.7730	0.0376	0.9798
10	16.8290	20.2600	24.2960	26.1990	27.6030	0.0393	0.9499
11	28.6600	34.6870	40.0000	43.4020	48.1250	0.0684	0.9863
12	34.1800	39.8870	44.7260	49.9810	53.4410	0.0698	0.9922
13	30.0580	35.8630	39.3580	45.1070	48.0190	0.0650	0.9913
14	29.1120	33.6590	35.9410	36.3160	37.8650	0.0289	0.8698
15	50.2810	60.0940	68.6500	81.3800	75.2670	0.1022	0.8347
16	14.9520	15.4410	16.4580	17.2120	17.3430	0.0094	0.9443
17	16.5470	22.3240	26.9240	31.7740	33.4810	0.0622	0.9700
18	22.2410	27.7600	32.9660	36.5870	51.4760	0.0969	0.9266
19	17.5190	20.6050	23.2190	26.7320	28.0730	0.0391	0.9852
20	32.9320	40.2850	44.3560	49.1600	52.0000	0.0676	0.9745
21	22.7250	24.0620	24.2400	25.9000	26.0980	0.0124	0.9481
22	33.4950	38.8790	38.9860	40.5360	40.6630	0.0231	0.7544
23	22.6260	28.4320	33.5560	37.4950	40.7740	0.0651	0.9821
24	34.3060	40.3350	43.6280	48.3220	49.6950	0.0557	0.9641
25	26.3680	27.8390	31.6730	34.3260	35.4300	0.0352	0.9586
26	20.8090	21.3980	21.4290	23.1310	23.7850	0.0111	0.9229
27	17.9320	22.1290	25.7980	30.9410	32.7970	0.0554	0.9852
28	19.2730	19.7760	20.1860	21.0270	21.9010	0.0094	0.9801
29	27.7410	30.9210	33.5930	36.7740	38.6190	0.0397	0.9921
30	28.9520	31.6280	30.2900	33.0680	35.2850	0.0206	0.8508
31	44.3890	63.9460	70.2820	76.4820	80.1190	0.1208	0.8892
32	19.6370	22.9150	26.3680	30.7200	33.8440	0.0521	0.9972
33	26.3680	27.2520	28.2260	29.4260	29.4260	0.0119	0.9444
34	16.2430	20.3720	23.5420	28.8560	31.3130	0.0556	0.9926
35	17.5190	19.3040	18.8350	19.7230	21.4610	0.0121	0.8602
36	32.7140	39.3220	42.2290	47.2240	49.9650	0.0611	0.9816
37	33.2950	37.9420	41.9350	46.0780	49.4820	0.0582	0.9959
38	17.5480	22.1290	26.0890	28.9720	30.0880	0.0457	0.9492
39	26.5980	32.3980	35.8400	40.4680	43.3580	0.0598	0.9885
40	31.2430	35.3180	38.8210	43.3730	44.5140	0.0497	0.9737
41	21.5440	21.5440	22.0300	23.6680	25.0120	0.0131	0.8831
42	36.4910	36.6690	38.1620	39.6770	41.1210	0.0176	0.9537
43	35.2090	40.7450	44.6670	50.9980	54.1010	0.0691	0.9930
44	25.5150	27.1600	28.6550	32.4550	34.8220	0.0345	0.9772
45	36.9790	42.2910	44.0610	49.6020	53.4360	0.0581	0.9917
46	22.6260	27.7830	28.1530	28.1530	30.5600	0.0253	0.8335
47	24.4110	29.0050	31.9280	35.6920	38.6150	0.0505	0.9948
Average	28.1028	32.4832	35.3763	38.7946	40.9068	0.0459	0.9445

Table A- 3 Growth measurements of SUP ss 0.55, 30 ˚C, pH6.86

	Measurement time (min)							
	0	60	119	175	237	334		
Crystal #	Length of (010) face (μm)						GR (μm/min)	RSQ
1	44.1800	44.5560	44.7780	45.5200	45.7910	45.8900	0.0056	0.9177
2	51.6910	53.0060	53.6270	54.6620	55.5210	56.4220	0.0141	0.9816
3	48.2030	52.0520	54.1120	56.1820	60.0260	65.5940	0.0504	0.9910
4	28.8510	28.8520	29.6410	30.5600	31.1660	31.4170	0.0090	0.9273
5	72.8310	73.9100	74.5680	75.3400	76.2350	77.7960	0.0145	0.9969
6	41.0050	41.2880	41.6470	42.4240	42.3810	43.0150	0.0062	0.9525
7	38.1040	38.9910	39.9930	43.3430	45.1120	47.8020	0.0311	0.9704
8	81.3790	81.8160	83.1710	84.3120	84.8830	86.0450	0.0148	0.9770
9	36.1340	37.2440	37.7380	38.1480	38.6050	39.8870	0.0103	0.9764
10	48.0780	48.4640	48.5580	48.5580	49.0410	50.0120	0.0052	0.8825
11	86.3390	90.3760	93.2730	96.3480	100.8310	103.7050	0.0532	0.9854
12	42.7550	46.7430	47.9340	48.6010	50.0700	50.0700	0.0202	0.8012
13	37.1520	37.5570	37.7890	37.8890	38.2270	40.2010	0.0081	0.8286
14	44.6100	45.6640	46.9940	47.0470	47.2760	47.5660	0.0084	0.7988
15	36.4670	37.8670	37.9420	38.6070	39.2000	40.7670	0.0117	0.9611
16	32.9710	33.9200	34.4240	35.4380	35.7600	36.5940	0.0108	0.9742
17	48.8250	48.9000	50.6170	50.7650	51.6460	53.0840	0.0132	0.9606
18	41.0120	41.1240	41.8970	43.0880	43.4020	43.5420	0.0089	0.8870
19	44.6770	44.7320	46.1440	46.8220	47.0280	48.8550	0.0127	0.9561
20	58.6950	59.1290	61.3180	61.7550	61.7550	64.3860	0.0164	0.9296
21	69.8930	70.5420	72.6230	73.4390	74.9000	76.5770	0.0209	0.9864
22	44.3350	45.4980	44.6130	45.6640	45.6640	46.4690	0.0055	0.7238
23	31.4410	31.9310	33.8920	36.1780	40.1810	47.2700	0.0481	0.9334
24	44.8270	45.6210	45.9280	46.2470	46.5760	47.8730	0.0083	0.9632
25	66.2160	67.0580	67.8930	69.2020	68.3260	69.6810	0.0098	0.8404
26	51.8370	53.0460	54.0200	55.2320	56.0830	58.0750	0.0184	0.9979
27	58.7230	55.7830	60.0420	61.9010	62.4410	63.8370	0.0207	0.7443
28	53.4980	53.6940	55.6540	56.9500	57.8840	59.4070	0.0191	0.9725
29	36.4720	37.0190	38.2450	38.8730	39.4490	40.5510	0.0125	0.9853
30	51.2870	51.2870	51.7280	53.1200	53.5560	55.0980	0.0122	0.9419
31	44.7890	45.9790	47.2990	47.8720	48.8510	49.9330	0.0153	0.9805
32	42.0550	43.1100	43.6840	43.7710	44.3440	45.0120	0.0082	0.9457
33	54.9290	55.0310	55.5010	56.0730	57.1260	58.2730	0.0106	0.9529
34	51.6630	52.9980	53.3160	54.1460	55.4930	56.8300	0.0152	0.9845
35	46.2880	46.4930	47.9680	48.4640	48.8000	50.6440	0.0130	0.9629
36	42.8280	43.8080	44.6130	44.6780	45.9450	45.9450	0.0093	0.9304
37	52.4210	52.5540	53.4070	53.8240	55.2490	55.4080	0.0103	0.9312
38	46.0020	46.0780	46.7430	48.0730	48.6670	48.7390	0.0098	0.8905
39	34.6870	34.6800	35.8440	36.0080	36.4620	36.9010	0.0072	0.9233
40	55.5280	60.1190	63.1340	65.4040	67.6330	71.1110	0.0450	0.9739
41	43.0060	43.5350	43.8080	44.3070	44.8470	44.9270	0.0061	0.9436
42	53.3410	54.0780	55.5200	56.3970	57.6560	59.4970	0.0188	0.9963
43	75.7210	79.2970	82.1430	83.1710	84.0880	85.7620	0.0285	0.9004
44	65.0050	66.1160	68.1560	68.9000	69.2650	71.1180	0.0179	0.9596
45	78.4250	81.9540	84.1450	86.0280	88.3380	89.2200	0.0325	0.9381
46	42.4220	42.8190	42.9820	42.4220	42.9820	43.7120	0.0030	0.5866
47	43.1540	43.3810	45.0690	45.0690	45.8000	46.2580	0.0099	0.9035
48	52.8440	53.4070	55.4080	55.0150	55.9300	57.7820	0.0142	0.9337
49	45.5530	45.9360	47.0840	47.8310	48.0940	48.2100	0.0088	0.8729
50	40.9880	42.3010	43.0720	43.6160	43.6160	45.7070	0.0126	0.9410

51	37.4900	39.3420	40.9030	40.9790	41.7140	43.3440	0.0161	0.9366
Average	49.4437	50.4056	51.5804	52.4365	53.3317	54.7416	0.0159	0.9242

Table A- 4 Growth measurements of IEL ss 0.55, 30 ˚C, pH 3.21

	Measurement time (min)							
	0	59	123	187	254	322		
Crystal #	Length of (010) face (μm)						GR (μm/min)	RSQ
1	48.3430	49.3800	49.6660	50.1720	50.1720	50.4360	0.0059	0.8524
2	53.6410	54.9670	55.5250	56.0330	56.3060	56.6050	0.0085	0.8932
3	61.5930	62.2690	62.7140	62.8180	64.2440	65.5630	0.0115	0.9203
4	80.2090	81.0710	81.3260	81.5380	82.9860	82.2480	0.0071	0.7987
5	30.7660	36.0330	42.1860	48.2550	54.5880	62.7950	0.0983	0.9977
6	31.2290	31.2470	31.0880	32.7660	32.4550	33.2770	0.0069	0.7873
7	50.3290	50.6500	50.0000	50.2560	50.9300	51.2240	0.0025	0.4383
8	33.2910	38.9930	46.1440	54.5040	63.1140	71.8540	0.1212	0.9974
9	60.9480	60.4790	59.9210	60.5760	61.4570	60.8010	0.0013	0.0952
10	56.6050	57.8850	58.4110	59.7410	59.9940	59.7410	0.0102	0.8526
11	99.0060	105.8850	112.9580	119.7210	126.1560	134.7890	0.1091	0.9988
12	111.9110	118.3310	124.0810	131.1660	138.7410	146.4740	0.1068	0.9987
13	56.2890	57.7920	58.2070	58.5760	58.8490	58.8490	0.0071	0.7873
14	101.0080	106.7440	114.6610	121.0440	128.2690	136.4830	0.1100	0.9991
15	94.4490	99.3790	103.1950	106.4240	106.6680	107.6870	0.0401	0.8778
16	96.8530	101.3490	106.7260	111.4830	116.2510	121.5650	0.0766	0.9995
17	58.4110	62.5470	66.5040	70.8750	74.5670	77.3720	0.0598	0.9933
18	78.7430	80.8920	83.4740	86.2690	88.9400	92.3300	0.0420	0.9980
19	225.1400	225.2320	228.1100	229.1400	231.7360	232.6020	0.0256	0.9656
20	35.8700	36.3570	36.3150	36.2830	36.9530	36.9310	0.0031	0.8133
21	68.3080	68.8680	69.6690	69.5350	69.5350	70.7560	0.0062	0.8328
22	52.0000	55.8300	56.8880	59.4950	60.0760	60.9790	0.0265	0.9114
23	97.6720	100.0860	101.9330	104.0580	106.4460	107.7730	0.0317	0.9930
24	118.8370	125.6670	133.4200	141.0560	149.7260	157.8270	0.1217	0.9998
25	36.9120	37.4390	37.4390	37.2310	37.1650	38.3110	0.0027	0.4468
26	56.0770	61.7650	68.8480	75.9320	78.5890	80.3600	0.0789	0.9471
27	310.7720	318.4500	326.4860	331.7160	341.0290	349.2220	0.1174	0.9969
28	72.4680	76.0010	78.2670	82.1140	86.3910	88.0920	0.0500	0.9892
29	71.5920	71.4710	71.6510	71.1440	73.0730	73.0730	0.0053	0.5587
30	41.0150	44.5900	49.2060	53.1830	59.5720	68.7890	0.0834	0.9743
31	183.5310	189.4680	194.2820	198.0630	202.9470	208.8080	0.0755	0.9951
32	35.3250	42.0000	49.6400	55.9530	64.3080		0.1131	0.9990
33	61.4040	67.4460	75.0000	81.5140	88.5400	97.3510	0.1105	0.9988
34	79.0270	80.4740	85.4830	91.3290	95.0420	100.8770	0.0704	0.9860
35	46.5930	50.9250	55.5350	59.9200	64.3040	68.0210	0.0671	0.9976
36	84.8490	90.8450	95.8320	101.3380	106.8930	115.9710	0.0927	0.9923
37	179.3530	183.4740	188.3220	194.0080	197.5140	202.5750	0.0725	0.9968
38	316.7840	321.5230	323.3270	324.1630	324.8030	328.8070	0.0312	0.9005
39	153.9550	157.2770	160.7830	164.2290	167.7160	171.7240	0.0547	0.9998
40	73.0140	75.9560	78.3880	81.4450	84.0190	83.5030	0.0351	0.9364
41	67.2470	72.0860	78.0200	80.9490	85.1870	84.4810	0.0565	0.9209
42	86.8210	88.3930	90.4120	90.3900	92.5420	95.2110	0.0241	0.9582
43	41.8020	45.3920	50.1810	50.9660	51.7640	51.7640	0.0305	0.8041
44	81.2610	82.0310	81.2500	82.3930	82.4940	83.3980	0.0059	0.7516
45	84.2850	87.8070	90.2860	93.4540	94.3360	95.0970	0.0338	0.9293
46	312.8070	318.9930	325.3480	333.8900	341.7120	351.1360	0.1189	0.9968

47	46.4990	47.6030	47.6030	48.1910	47.3250	48.7560	0.0049	0.5827
48	78.1440	81.5900	83.4350	85.3810	86.5500	91.4960	0.0370	0.9613
49	88.6380	91.3410	94.0470	96.3140	100.0820	103.4140	0.0454	0.9961
50	54.3100	55.3190	54.4370	56.0640	56.4530	55.6780	0.0052	0.5280
Average	90.9187	94.1518	97.3326	100.4612	103.5902	107.6097	0.0492	0.8789

Table A- 5 Growth measurements of IEL ss 0.55, 30 ˚C, pH 6.50

	Measurement time (min)							
	0	54	151	293	338	392		
Crystal #	Length of (010) face (μm)						GR (μm/min)	RSQ
1	55.7310	56.8450	57.1980	57.7120	57.7120	59.1140	0.0064	0.8504
2	69.4160	73.0300	78.7530	84.8430	86.7940	88.5990	0.0486	0.9912
3	36.2900	36.8100	36.5910	37.5960	38.8730	38.7280	0.0064	0.8550
4	142.9720	147.7070	153.7610	163.3490	166.8850	170.2320	0.0687	0.9989
5	75.4760	77.3310	79.9900	84.7080	86.3520	88.5130	0.0327	0.9977
6	40.3380	40.4260	41.2220	41.6910	41.6770	43.2700	0.0061	0.8386
7	36.3820	37.3110	35.5020	38.8570	38.3280	39.5390	0.0076	0.6298
8	160.5920	166.0960	173.0190	182.3730	186.3020	189.1640	0.0719	0.9965
9	111.8780	114.8220	115.5760	116.0270	116.5210	116.3530	0.0092	0.7229
10	62.7070	64.7530	64.7220	67.3300	66.1690	67.0640	0.0099	0.8280
11	84.8510	85.7900	86.9810	86.4510	86.7580	87.0190	0.0043	0.6511
12	64.8110	64.8110	67.0770	67.0480	66.3530	67.2380	0.0057	0.6564
13	111.3560	113.6900	118.6570	128.2380	129.8330	132.1800	0.0555	0.9949
14	48.1900	49.6550	50.6410	51.8370	51.9780	51.8370	0.0090	0.9013
15	36.0080	36.4910	36.8850	38.1740	37.7870	37.9540	0.0053	0.9109
16	59.8090	63.5110	67.9630	73.6500	75.8480	77.6120	0.0445	0.9940
17	44.6670	44.7980	45.9360	46.4380	46.4380	47.4550	0.0065	0.9340
18	102.7430	106.1970	111.1470	119.6610	120.8560	124.4590	0.0547	0.9976
19	99.5800	102.5380	108.0450	116.6230	120.9500	124.0450	0.0627	0.9965
20	117.8180	120.9040	126.5670	135.1650	137.6550	140.4660	0.0584	0.9997
21	60.7040	61.2520	61.2470	63.2970	66.1760	67.0740	0.0159	0.8625
22	130.6220	134.1620	140.3810	151.9340	154.6670	157.2110	0.0703	0.9966
23	67.2050	68.3110	68.0940	71.5050	74.5990	77.2320	0.0236	0.8739
24	150.2310	152.0970	159.3340	170.2430	175.1850	176.8930	0.0727	0.9919
25	109.2720	112.5710	116.7410	124.1070	125.8540	129.2980	0.0497	0.9982
26	61.9920	64.6650	62.6510	64.2580	65.0650	65.5890	0.0066	0.5574
27	82.8230	84.4230	87.6070	93.3670	93.2980	97.2080	0.0353	0.9849
28	121.7290	124.5370	128.5160	137.1900	136.9160	140.7330	0.0481	0.9890
29	85.0550	86.7860	90.7240	96.3860	98.1310	100.7360	0.0399	0.9989
30	68.8680	70.0030	74.9130	80.8340		85.1140	0.0426	0.9964
31	106.2900	107.9340	112.5250	118.9660	120.8850	122.8810	0.0436	0.9985
32	127.8930	132.4270	133.3240		153.2460	156.9120	0.0756	0.9599
33	145.3820	148.2480	155.2530	163.9610	167.6980	171.4140	0.0666	0.9987
34	38.6050	39.0770	39.8570	40.2950	40.2950	41.2540	0.0057	0.9303
35	71.0080	72.5060	73.5170	74.5400	74.0270	75.0540	0.0087	0.8813
36	170.9250	175.4500	179.8670	191.4010	192.7390	197.6000	0.0667	0.9934
37	88.5030	91.6840	96.8450	104.9290	106.6290	110.2040	0.0547	0.9991
38	39.9060	42.3010	40.6200	41.9440	41.9520	43.0470	0.0050	0.4836
39	68.4870	69.2950	70.0850	71.1410	71.9440	72.2100	0.0092	0.9884
40	118.5420	118.8980	118.4390	120.1400	120.1360	120.1570	0.0047	0.8078
41	84.8940	86.8410	91.8910	98.4540	100.8480	103.6330	0.0481	0.9990
42	151.6550	156.8310	163.9050	173.4410	176.8070	178.8540	0.0697	0.9945
43	57.7890	58.1820	57.9720	59.9980	60.0500	61.0140	0.0081	0.9050

Average	87.6743	89.8139	92.5707	96.4310	99.4575	100.9805	0.0336	0.9055

Table A- 6 Growth measurements of IEL ss 0.55, 30 ˚C, pH 1.95

	Measurement time (min)						
	0	65	123	182	253		
Crystal #	Length of (010) face (μm)					GR (μm/min)	RSQ
1	179.8080	180.0530	180.5860	181.2420	181.3650	0.0091	0.8962
2	96.7260	97.0830	97.2090	97.4100	97.7580	0.0035	0.9746
3	54.0020	54.6110	55.1820	55.2790	55.4000	0.0056	0.9186
4	42.4790	42.7380	42.7580	43.2820	43.2820	0.0048	0.8598
5	92.7880	92.9820	93.3610	93.5530	94.2280	0.0071	0.9180
6	130.0990	143.7180	150.7190	156.4230	163.8180	0.1286	0.9690
7	25.1330	25.5150	25.9100	25.9890	26.4670	0.0051	0.9744
8	37.0120	37.4560	38.1180	38.3280	39.2250	0.0085	0.9781
9	26.1500	26.2270	26.3210	26.4320	26.8930	0.0027	0.8554
10	168.8090	185.9940	199.8750	210.1250	222.6540	0.2113	0.9896
11	35.6920	35.8860	36.5360	36.7200	37.3460	0.0067	0.9686
12	52.9670	53.1580	53.3560	54.4600	54.6340	0.0074	0.8883
13	39.5120	39.5120	40.1600	40.6620	40.7340	0.0057	0.8974
14	29.6410	30.7740	31.3470	31.3540	31.9590	0.0084	0.8914
15	25.1800	24.7280	25.2960	25.4290	25.8640	0.0033	0.6319
16	106.3940	106.8120	106.9370	109.1180	108.9460	0.0118	0.8160
17	41.4270	42.2770	42.3140		44.8020	0.0131	0.9344
18	67.9960	68.6520	69.1900	69.3090	70.2130	0.0082	0.9678
19	55.0370	55.0370	55.7170	56.3790	57.0590	0.0086	0.9405
20		48.3410		49.3740	50.0650	0.0091	0.9993
21	73.5700	73.8030	74.2880	74.4160	74.6540	0.0044	0.9588
22	66.6040	67.2730	67.3630	67.8250	68.7000	0.0077	0.9511
23	30.2880	30.5190	30.8400	31.3980	31.5050	0.0053	0.9543
24	54.1340	69.7020	84.7480	95.1980	110.5760	0.2220	0.9964
25	98.8280	99.3390	99.4590	99.9620	100.0900	0.0050	0.9524
26	32.5250	32.5250	32.7960	32.8370	33.0950	0.0023	0.9204
27	21.3070	22.7680	22.7680	22.7680	24.2300	0.0095	0.8236
28	80.6390	82.6490	82.7140	83.3500	84.5640	0.0138	0.9128
29	49.6290	50.3390	50.4370	51.0800	51.2670	0.0064	0.9457
30	25.0730	25.6080	25.8220	27.2410	27.1490	0.0092	0.8801
31	105.9880	106.9380	108.2810	111.1440	115.7950	0.0066	0.9182
32	24.1610	24.7280	25.1800	25.4290	26.0890	0.0073	0.9894
33	48.7820	49.1130	49.2180	49.4250	49.6850	0.0034	0.9842
34	88.3140	90.5850	91.1530	92.0550	93.3080	0.0184	0.9550
35	41.4400	41.6120	41.7140	42.1180	44.0900	0.0095	0.7374
36	63.1804	64.5444	66.4021	67.8563	68.7860	0.0228	0.9185

Table A- 7 Growth measurements of IEL ss 0.55, 30 ˚C, 0.001 M Glucose-6-Phosphate, pH 3.61

	Measurement time (min)						
	0	52	117	167	226		
Crystal #	Length of (010) face (μm)					GR (μm/min)	RSQ
1	149.8950	151.7350	154.9530	158.0730	158.3650	0.0410	0.9558
2	106.3390	106.5000	112.6910	114.6430	119.8590	0.0624	0.9531

3	51.2490	51.6940	51.7050	54.7840	55.1890	0.0191	0.8185
4	36.9420	37.0330	37.0330	37.7710	38.4800	0.0067	0.8107
5	284.4640	286.6430	290.0620	293.2140	293.2660	0.0426	0.9458
6	62.9700	63.2900	63.5880	63.7470	64.0850	0.0047	0.9917
7	30.6430	30.6430	31.7990	31.8200	32.9750	0.0104	0.9129
8	19.9160	19.9300	20.7680	21.2390	21.3150	0.0073	0.9169
9	17.3410	17.9190	18.1190	18.5090	18.5250	0.0052	0.9060
10	21.2060	23.2490	22.3480	23.2490	23.9010	0.0093	0.6394
11	56.6770	56.9560	57.8240	57.8660	58.2890	0.0073	0.9481
12	35.0750	35.0750	35.2590	36.3150		0.0068	0.6949
13	84.7880	85.5420	85.7910	86.4500	87.2350	0.0102	0.9696
14	115.7530	115.8920	120.0850	123.0130	125.7850	0.0481	0.9612
15	41.7260	41.8020	42.1370	42.2040	43.8500	0.0082	0.7240
16	28.6550	28.9100	29.3760	30.1050	31.4410	0.0119	0.9112
17	12.5390	13.5340	13.5640	14.0190	14.6630	0.0083	0.9145
18	52.1740	52.5910	53.0430	53.0880	53.9550	0.0072	0.9386
19	28.7110	28.7110	29.1080	29.6370	29.6370	0.0049	0.8960
20	23.8500	24.3350	24.3350	24.4930	25.0390	0.0044	0.8748
21	204.7040	205.3890	207.8380	211.0010	213.4090	0.0406	0.9652
22	159.7250	160.6740	161.8190	162.4270	162.1210	0.0116	0.8478
23	90.4610	91.4560	91.6200	91.6870	92.0720	0.0061	0.8164
24	30.5950	31.4410	31.8040	32.9200	33.7610	0.0137	0.9719
25	35.8440	35.8630	36.4410	37.0920	39.3060	0.0144	0.8096
26	32.3770	32.4330	32.4810	33.5330	34.1630	0.0082	0.8222
27	71.0420	71.9230	72.2830	72.3880	74.6220	0.0134	0.8297
28	49.3070	49.9060	49.9410	50.7050	52.0650	0.0111	0.8742
29	85.2760	85.7840	85.7840	85.7840	86.4410	0.0041	0.7867
30	37.5850	38.3510	38.9980	39.6770	40.1470	0.0114	0.9915
31	72.2040	73.2930	74.0620	74.0860	74.8570	0.0108	0.9295
32	83.4740	83.6900	84.0720	84.8580	85.0320	0.0075	0.9469
33	78.2390	78.8710	82.3060	83.3030	85.2280	0.0327	0.9720
Average	69.4468	70.0321	71.0011	71.9303	74.0337	0.0155	0.8863

Table A- 8 Growth measurements of SUP ss 0.55, 30 ˚C, 0.001 M Glucose-6-Phosphate, pH 3.90

	Measurement time (min)							
	0	79	121	175	264	319		
Crystal #	Length of (010) face (μm)						GR (μm/min)	RSQ
1	55.5560	56.0690	56.0690	56.1060	56.1060	56.6830	0.0026	0.7597
2	25.4930	25.7490	26.3030	27.1140	27.3490	27.3530	0.0066	0.8948
3	29.1410	29.7330	29.8060	29.8900	31.0670	31.2170	0.0067	0.9390
4	141.7540	145.0600	146.4200	147.2030	149.1830	151.1940	0.0274	0.9747
5	63.7700	63.9960	64.8760	65.3190	65.6580	67.8450	0.0116	0.8651
6	30.7980	31.6720	32.2420	32.9190	33.2300	33.9530	0.0095	0.9705
7	51.8770	52.4260	53.2080	53.0970	52.9010	53.9800	0.0052	0.7400
8	21.9760	21.9650	22.5430	22.5530	22.5530	23.1210	0.0033	0.8071
9	19.5400	19.6770	20.8370	20.8780	21.6010	22.3350	0.0089	0.9372
10	25.9190	25.9190	26.0290	26.4850	27.1490	27.8130	0.0062	0.8914
11	41.9580	42.2680	43.4070	44.7890	44.9240	45.1170	0.0111	0.8713
12	31.9410	32.4550	32.9710	33.2770	34.0080	34.1020	0.0071	0.9801
13	32.8120	32.8120	32.9290	33.2810	34.1910	34.9990	0.0071	0.8653
14	62.1240	63.4430	64.5080	64.5090	65.8380	66.4010	0.0130	0.9662
15	24.8650	24.8920	25.4420	25.5130	26.0460	26.7250	0.0058	0.9239

16	64.0920	64.7350	64.8330	66.1670	67.7360	68.9480	0.0158	0.9539
17	39.2900	40.0150	40.7470	40.9290	41.3920	42.0400	0.0081	0.9637
18	40.9880	46.1550	46.6210	47.0590	47.1880	47.7540	0.0047	0.9590
19	74.0980	74.5830	74.7140	75.3360	75.7230	76.9050	0.0082	0.9326
20	32.9670	33.1510	33.5250	34.2620	34.6430	34.6430	0.0061	0.9230
21	42.2680	42.7270	43.6550	43.9770	44.1150	45.0120	0.0081	0.9253
22	76.2580	79.7240	81.4650	81.5500	83.7770	84.2560	0.0237	0.9193
23	29.5050	30.6270	31.0010	31.2750	31.2750	33.0450	0.0090	0.8498
24	28.4510	29.5840	29.7510	30.2470	30.4140	31.5840	0.0084	0.9246
25	45.4100	46.9870	47.5210	47.8630	48.8510	49.4190	0.0118	0.9675
26	39.3300	39.3420	39.6040	39.9490	39.9950	39.9950	0.0025	0.8404
27	26.2320	26.3340	26.9450	27.0010	27.6680	27.7350	0.0052	0.9429
28	106.0070	106.4310	107.3120	109.0730	109.4960	110.0570	0.0139	0.9299
29	96.9710	99.8530	100.9050	101.1140	102.3870	102.7760	0.0167	0.8878
30	22.0820	20.8900	21.3880	22.0820	22.3950	23.9320	0.0064	0.5357
31	38.0870	39.1490	39.7370	40.2380	41.4050	41.4050	0.0108	0.9714
32	56.3060	56.6100	56.6500	57.1790	57.5210	57.7830	0.0048	0.9739
33	42.2980	42.4240	42.9880	43.2010	43.9370	45.6050	0.0096	0.8646
34	32.3950	32.9320	33.1980	33.7180	35.0430	36.9090	0.0134	0.9054
35	151.0860	155.3140	155.8470	158.8630	162.9930	166.5030	0.0470	0.9897
36	49.7000	50.0290	50.4370	50.5600	50.8950	50.9550	0.0040	0.9500
37	38.3510	38.9910	39.5470	39.6530	41.5050	41.8640	0.0116	0.9584
38	36.0640	36.9140	37.2910	37.3820	38.2450	38.3620	0.0071	0.9651
39	32.6270	32.7690	33.7340	34.0870	34.0870	34.9410	0.0070	0.8858
40	69.6520	69.6520	70.2340	71.9730	71.9790	73.7140	0.0129	0.8792
41	82.5050	82.7320	83.5820	83.6370	83.7780	84.2300	0.0052	0.8783
42	69.6810	70.5290	71.3930	71.4230	71.8730	71.8730	0.0067	0.8485
43	122.4530	124.0540	125.9370	127.0550	128.9050	129.1140	0.0220	0.9629
44	177.8220	181.2580	183.4840	185.6320	189.8310	194.4340	0.0503	0.9877
45	157.1470	160.8760	162.2090	164.0600	168.5610	170.7050	0.0423	0.9964
46	146.5530	151.0780	151.7890	153.8790	156.2020	159.3340	0.0370	0.9788
47	38.5450	40.3720	40.3720	41.1790	41.2540	42.5110	0.0105	0.8942
48	108.4310	109.6120	109.8690	110.3500	111.0900	111.2000	0.0085	0.9559
49	49.0230	49.2320	49.4560	50.8920	51.4820	51.7000	0.0097	0.9135
	59.6367	60.6898	61.3333	61.9547	62.8458	63.7568	0.0123	0.9102

Table A- 9 Growth measurements of IEL ss 0.55, 30 ˚C, 0.001 M Lactose-1-Phosphate, pH 3.7

	Measurement time (min)					
	0	50	85	133		
Crystal #	Length of (010) face (μm)				GR (μm/min)	RSQ
1	63.0600	64.0190	64.2390	64.3100	0.0092	0.8059
2	44.0050	45.0280	45.6890	47.3400	0.0246	0.9768
3	44.5360	44.6000	44.6710	45.1000	0.0041	0.8070
4	38.2450	39.0120	38.8730	39.9350	0.0116	0.8735
5	20.3450	25.6660	28.3440	30.2550	0.0748	0.9522
6	31.2980	31.8540	32.7960	35.6400	0.0322	0.8746
7	47.6510	49.4040	51.5570	54.0140	0.0487	0.9882
8	61.5230	63.4620	64.0310	65.1520	0.0266	0.9688
9	63.2100	64.3960	64.8380	65.9040	0.0198	0.9906
10	30.8820	31.8870	33.6590	34.2450	0.0269	0.9448
11	36.5870	37.2640	37.5500		0.0115	0.9835
12	27.6030	35.5790	42.5130		0.1743	0.9963

13	47.2090	47.2090	47.8310	48.2100	0.0082	0.8642
14	25.9310	27.7350		29.1000	0.0231	0.9515
15	24.3900	24.9590		25.8470	0.0109	0.9997
16	51.0260	51.4630		50.2940	-0.0064	0.5252
17	32.8720	33.6370		34.2480	0.0100	0.9578
18	75.0100	78.3840		81.6430	0.0488	0.9770
19	63.1380	65.5090		72.2040	0.0694	0.9841
20	158.7450	165.0900	167.7390	173.4130	0.1081	0.9934
21	42.7430	43.2280		43.3990	0.0046	0.8397
22	32.3880	33.4380	34.5440	34.6800	0.0182	0.9098
23	73.4520	77.4970	79.3540	81.6920	0.0615	0.9815
24	33.4470	33.5930	34.2190	35.1250	0.0129	0.9026
25	56.5000	56.9390	59.1290	59.6240	0.0260	0.8794
26	17.9640	21.5440	24.5270	27.7070	0.0740	0.9981
27	44.7430	45.3080	46.7360	46.9640	0.0183	0.8989
28	70.1140	71.0640	73.5060		0.0385	0.8823
29	26.5870	27.3970	29.0290		0.0279	0.9163
30	20.2670	20.9480	22.0980		0.0210	0.9396
31	68.8100	70.2250	70.5170	72.3980	0.0257	0.9593
32	20.3410	21.5080	21.0920	26.8920	0.0450	0.7132
33	28.4040	28.7690	29.7510		0.0153	0.8759
34	57.3450	58.3430	59.6600		0.0267	0.9676
Average	46.4815	48.1164	49.9441	48.0547	0.0339	0.9141

Table A- 10 Growth measurements of SUP ss 0.55, 30 ˚C, 0.001 M Lactose-1-Phosphate, pH 3.88

	Measurement time (min)						
	0	50	151	237	289		
Crystal #	Length of (010) face (μm)					GR (μm/min)	RSQ
1	42.0460	40.3270	43.4930	44.3770	44.7850	0.0131	0.7649
2	55.7550	59.1430	60.9720	63.8870	66.4310	0.0335	0.9691
3	25.9100	25.9890	26.9480	26.9480	27.4340	0.0053	0.9254
4	64.0350	64.7700	67.0840	70.4790	70.6220	0.0250	0.9712
5	24.9400	28.4000	31.0070	32.8360	33.0680	0.0269	0.9197
6	29.9610	30.7830		32.6010	34.3630	0.0186	0.9983
7	53.4000	53.6910	56.8830	57.7570	58.9310	0.0200	0.9685
8	29.9890	31.8670	31.3430	32.1500	32.6510	0.0069	0.6804
9	43.1370	43.7800	50.9670	56.3140	56.5180	0.0525	0.9662
10	41.2100	43.3600	44.2720	48.2060	50.8950	0.0311	0.9417
11	57.1200	58.4610	60.6790	63.8530	63.9700	0.0252	0.9784
12	48.5420	50.4710	51.7280	52.8650	56.3970	0.0229	0.9026
13	50.6500	50.4390	53.2220	56.5660	56.8330	0.0247	0.9500
14	31.6990	32.1200	33.4700	35.2040	35.8360	0.0149	0.9877
15	49.3190	51.0800	54.6620	57.5490	59.2300	0.0344	0.9997
16	22.4280	22.7880	23.6680	24.0940	24.5390	0.0072	0.9930
17	21.6110	23.6680	23.7320	28.0720	29.7970	0.0267	0.9068
18	46.6870	48.8420	51.7940	52.7150	53.8210	0.0236	0.9570
19	59.6550	61.8310	65.5930	68.6420	68.6420	0.0327	0.9699
20	76.3310	78.4240	79.2550	80.9750	81.3940	0.0163	0.9446
21	19.6460	21.2640	22.0510	22.3130	22.6260	0.0090	0.8364
22	57.5490	60.0150	63.2840	64.2000	65.6410	0.0265	0.9556
23	55.7100	57.5830	58.6320	60.2920	61.3930	0.0181	0.9730

24	29.6100	31.6760	34.6210	37.4560	40.1050	0.0347	0.9928
25	45.2660	46.4540	49.7940	50.7800	52.5760	0.0247	0.9806
26	67.6650	68.8930	68.9190	71.8400	72.0020	0.0151	0.8922
27	43.4150	43.8140	45.3190	45.6890	45.6890	0.0086	0.9165
28	57.4230	57.7010	60.7240	63.2170	65.3170	0.0279	0.9797
29	55.6540	58.3410	60.1270	61.0530	62.0700	0.0200	0.9271
30	28.3360	28.5880	29.2190	30.2180	30.9210	0.0088	0.9686
31	34.1630	35.9390	38.1740	40.0250	41.7050	0.0248	0.9938
32	37.3820	39.1970	43.2980	47.5080	51.0040	0.0463	0.9904
33	37.1470	39.3570	40.1050	40.7750	41.6990	0.0134	0.8898
34	55.0980	55.3860	61.9020	65.9350	70.4080	0.0540	0.9756
35	55.4080	56.1340	58.7180	59.2370	60.3460	0.0170	0.9680
36	27.9030	28.0040	31.0070	33.0130	33.6370	0.0219	0.9764
37	43.8140	45.9220	48.6970	49.0740	50.7690	0.0220	0.9428
38	35.0950	35.3260	38.0550	39.5860	40.7340	0.0205	0.9856
39	36.6960	37.9660	40.1260	41.1240	41.9300	0.0178	0.9821
40	48.0190	48.2060	49.7520	50.3290	50.3290	0.0090	0.9370
41	30.0000	30.7450	31.0620	32.4870	33.8150	0.0120	0.9185
42	17.9640	18.4900	18.6010	19.3040	20.1960	0.0067	0.8918
43	36.1950	37.4030	38.7800	39.1560	39.2340	0.0102	0.8920
44	55.4070	55.8120	59.2040	61.2260	61.3110	0.0187	0.9116
45	44.4150	47.5970	48.1750	50.5120	52.5300	0.0243	0.9272
Average	42.8757	44.1344	46.5709	48.0542	49.2032	0.0216	0.9400

Table A- 11 Morphology Studies using SUP

0.001 M $CaCl_2$, *pH 4.9*			**0.001 M KCl, *pH 4.65***			**0.001 M NaCl, *pH 6.36***		
Length (μm)	Width (μm)	W:L	Length (μm)	Width (μm)	W:L	Length (μm)	Width (μm)	W:L
54.202	24.285	0.4480	87.128	75.473	0.8662	63.003	25.215	0.4002
80.623	35.082	0.4351	106.820	45.412	0.4251	94.229	43.359	0.4601
59.503	32.286	0.5426	90.382	38.323	0.4240	84.118	42.926	0.5103
86.603	35.288	0.4075	88.914	35.741	0.4020	84.402	27.380	0.3244
61.283	27.374	0.4467	98.157	43.689	0.4451	89.257	33.785	0.3785
71.396	27.375	0.3834	83.617	38.053	0.4551	93.476	42.635	0.4561
76.469	34.185	0.4470	99.476	45.378	0.4562	89.109	40.608	0.4557
51.365	26.941	0.5245	96.224	33.101	0.3440	62.798	31.392	0.4999
48.800	20.191	0.4138	94.420	37.708	0.3994	85.898	49.859	0.5804
54.683	26.663	0.4876	83.976	52.006	0.6193	75.600	41.848	0.5535
90.142	39.089	0.4336	96.821	41.552	0.4292	81.881	30.653	0.3744
86.361	34.166	0.3956	64.178	18.868	0.2940	88.365	38.175	0.4320
63.852	33.744	0.5285	77.981	30.650	0.3930	70.817	26.037	0.3677
44.625	23.424	0.5249	81.704	27.592	0.3377	90.708	44.504	0.4906
94.854	43.101	0.4544	65.352	25.449	0.3894	90.413	31.305	0.3462
76.579	26.726	0.3490	73.090	36.101	0.4939	90.547	40.918	0.4519
51.227	20.880	0.4076	84.651	33.256	0.3929	98.263	40.326	0.4104
66.566	47.041	0.7067	103.830	65.428	0.6301	84.964	36.340	0.4277
77.963	38.046	0.4880	103.390	44.191	0.4274	89.987	41.149	0.4573
84.308	30.705	0.3642	77.943	37.661	0.4832	51.408	38.330	0.7456
69.563	30.898	0.4442	70.130	30.451	0.4342	65.047	32.723	0.5031
79.544	34.536	0.4342	95.833	37.429	0.3906	87.351	29.816	0.3413
62.493	26.662	0.4266	82.830	42.487	0.5129	92.252	34.991	0.3793
60.157	29.160	0.4847	84.806	35.397	0.4174	95.315	38.873	0.4078
88.673	38.113	0.4298	91.691	41.036	0.4475	72.059	42.893	0.5952
57.282	24.635	0.4301	82.182	35.960	0.4376	98.474	38.337	0.3893

66.627	32.915	0.4940	77.250	32.875	0.4256	86.359	35.328	0.4091
49.235	28.739	0.5837	80.141	32.660	0.4075	88.490	29.036	0.3281
72.694	29.700	0.4086	93.910	43.831	0.4667	94.327	44.318	0.4698
88.180	42.571	0.4828	78.948	29.770	0.3771	100.030	47.339	0.4732
63.041	25.400	0.4029	99.013	47.129	0.4760	103.890	42.426	0.4084
89.556	53.032	0.5922				88.117	37.522	0.4258
49.822	22.403	0.4497				99.100	47.360	0.4779
						95.370	40.482	0.4245
						57.786	28.618	0.4952
						75.828	36.352	0.4794
						80.595	34.953	0.4337
						95.418	33.682	0.3530
						107.430	41.301	0.3844
						92.366	46.129	0.4994
						89.590	40.549	0.4526
						71.393	24.908	0.3489
						77.624	26.490	0.3413
						104.050	41.634	0.4001
						91.665	40.772	0.4448
						104.700	40.632	0.3881
						80.704	34.245	0.4243
						97.773	46.550	0.4761
Average								
Length (μm)	Width (μm)	W:L	Length (μm)	Width (μm)	W:L	Length (μm)	Width (μm)	W:L
73	31.68	0.4622	78.5	39.18	0.4484	76.6	37.6	0.4391

0.001 M KH_2PO_4, *pH 5.67*			**0.001 M Na_2HPO_4, *pH 6.39***		
Length (μm)	Width (μm)	W:L	Length (μm)	Width (μm)	W:L
94.854	37.515	0.3955	79.672	48.881	0.6135
89.447	45.833	0.5124	88.227	46.154	0.5231
106.530	62.158	0.5835	82.006	53.395	0.6511
67.172	24.643	0.3669	65.193	35.693	0.5475
148.500	91.171	0.6139	78.160	37.366	0.4781
71.803	32.070	0.4466	79.697	37.251	0.4674
90.330	47.773	0.5289	78.206	55.611	0.7111
95.253	47.420	0.4978	81.629	51.237	0.6277
69.936	26.455	0.3783	67.074	41.385	0.6170
101.150	38.808	0.3837	111.870	61.939	0.5537
86.278	46.215	0.5357	76.107	48.961	0.6433
97.210	73.552	0.7566	78.099	45.002	0.5762
71.121	29.587	0.4160	77.414	44.462	0.5743
68.631	27.660	0.4030	65.728	38.380	0.5839
104.700	53.822	0.5141	67.358	46.114	0.6846
104.080	52.937	0.5086	75.102	54.134	0.7208
63.884	27.620	0.4323	94.147	64.111	0.6810
59.304	29.452	0.4966	112.360	61.609	0.5483
85.602	38.981	0.4554	119.210	68.942	0.5783
77.727	28.347	0.3647	82.176	45.767	0.5569
78.730	38.487	0.4888	71.376	43.359	0.6075
98.032	45.949	0.4687	88.757	49.149	0.5537
94.637	39.739	0.4199	98.596	56.406	0.5721
91.743	42.014	0.4580	104.880	61.110	0.5827
97.582	27.685	0.2837	92.656	50.522	0.5453
134.810	44.934	0.3333	105.560	67.488	0.6393
66.579	24.255	0.3643	65.263	34.162	0.5235

87.832	39.263	0.4470	86.952	57.756	0.6642
99.240	64.772	0.6527	88.532	49.722	0.5616
94.890	74.355	0.7836	62.765	31.598	0.5034
86.790	45.040	0.5190	76.862	46.031	0.5989
84.175	44.501	0.5287	91.459	49.582	0.5421
92.852	49.964	0.5381	90.723	82.935	0.9142
			77.076	44.922	0.5828
			100.170	59.215	0.5911
			82.064	55.336	0.6743
			119.220	81.124	0.6805
Average					
Length (μm)	Width (μm)	W:L	Length (μm)	Width (μm)	W:L
71.9	43.73	0.4811	84.6	51.54	0.602

SUP, *pH 4.5*			**Non-ionic SUP, *pH 6.9***		
Length (μm)	Width (μm)	W:L	Length (μm)	Width (μm)	W:L
97.301	42.317	0.4349	127.950	57.405	0.4487
121.430	73.743	0.6073	149.560	59.001	0.3945
119.310	77.337	0.6482	181.490	65.706	0.3620
77.639	35.114	0.4523	114.350	53.253	0.4657
83.531	57.526	0.6887	48.410	23.450	0.4844
106.470	54.163	0.5087	103.770	47.649	0.4592
106.930	54.949	0.5139	54.656	32.915	0.6022
63.342	31.081	0.4907	37.896	34.760	0.9172
60.193	24.820	0.4123	298.130	82.432	0.2765
77.020	35.673	0.4632	126.440	49.627	0.3925
60.725	25.012	0.4119	97.823	44.607	0.4560
64.658	29.029	0.4490	87.043	31.511	0.3620
103.330	52.623	0.5093	75.155	39.155	0.5210
105.970	49.766	0.4696	108.590	48.234	0.4442
50.250	30.389	0.6048	158.380	56.930	0.3595
77.503	41.106	0.5304	138.970	60.208	0.4332
71.367	36.494	0.5114	123.900	60.789	0.4906
56.804	23.697	0.4172	106.170	58.669	0.5526
102.830	41.760	0.4061	88.379	35.767	0.4047
82.616	36.466	0.4414	71.160	40.039	0.5627
94.550	45.835	0.4848	102.460	50.358	0.4915
61.116	33.454	0.5474	119.050	43.019	0.3614
120.330	78.000	0.6482	299.590	83.218	0.2778
123.630	74.714	0.6043	104.210	48.141	0.4620
56.880	22.821	0.4012	151.000	61.533	0.4075
117.780	76.447	0.6491	84.591	37.429	0.4425
93.877	41.988	0.4473	162.020	62.617	0.3865
116.990	61.026	0.5216	119.980	47.715	0.3977
81.402	34.240	0.4206	203.770	71.794	0.3523
126.800	60.228	0.4750	127.350	57.903	0.4547
106.320	48.603	0.4571	151.250	59.445	0.3930
66.007	28.108	0.4258	182.000	68.942	0.3788
109.870	56.508	0.5143	112.470	54.145	0.4814
102.620	35.673	0.3476	204.550	71.380	0.3490
77.893	28.375	0.3643	113.320	55.537	0.4901
90.777	48.407	0.5333	152.630	58.740	0.3849
100.600	57.874	0.5753	64.160	39.388	0.6139
113.770	42.770	0.3759	77.390	39.548	0.5110
130.530	48.155	0.3689	174.340	65.428	0.3753
99.053	46.114	0.4655	202.880	64.131	0.3161
92.308	33.059	0.3581	148.420	60.549	0.4080

114.340	43.431	0.3798	71.116	36.389	0.5117
			246.550	77.821	0.3156
			96.211	43.786	0.4551
			91.381	48.316	0.5287
			192.510	69.537	0.3612
			70.361	36.481	0.5185
			118.680	58.842	0.4958
			135.510	59.328	0.4378
			101.220	49.118	0.4853
			104.220	49.698	0.4769
			136.960	59.328	0.4332
			118.740	59.627	0.5022
			203.090	62.006	0.3053
			118.740	54.119	0.4558
			68.995	37.224	0.5395
			177.070	64.993	0.3670
			194.280	61.597	0.3171
			167.380	59.082	0.3530
			101.950	45.110	0.4425
			241.210	81.605	0.3383
			136.050	64.460	0.4738
			122.520	58.114	0.4743
			75.296	33.105	0.4397
			97.975	47.861	0.4885
			106.060	52.723	0.4971
			88.551	35.208	0.3976
			77.900	35.501	0.4557
			90.671	33.538	0.3699
			145.090	57.747	0.3980
			150.180	64.294	0.4281
			76.576	33.736	0.4406
			123.980	58.764	0.4740
			118.290	51.177	0.4326
			74.456	46.825	0.6289
			84.654	46.757	0.5523
			97.763	43.918	0.4492
			126.160	48.620	0.3854
			327.110	73.138	0.2236
			86.278	39.043	0.4525
			155.240	70.589	0.4547
			167.010	73.930	0.4427
			94.066	51.383	0.5462
			154.380	63.249	0.4097
			133.230	51.265	0.3848
			152.940	67.844	0.4436
Average					
Length (μm)	Width (μm)	W:L	Length (μm)	Width (μm)	W:L
85.7	45.21	0.4842	150.5	53.49	0.4361

Table A- 12 Growth measurements of SUP ss 0.55, 30 ˚C, 0.001 M NaCl

	0.001 M NaCl, *pH 3.27*			**0.001 M NaCl, *pH 6.88***		
Crystal #	Initial Length (010) (μm)	GR (μm/min)	RSQ	Initial Length (010) (μm)	GR (μm/min)	RSQ
1	42.64	0.0133	0.8961	83.44	0.0243	0.9986
2	26.18	0.0043	0.7881	64.25	0.0200	0.9676
3	38.47	0.0085	0.8379	63.10	0.0204	0.9801
4	26.15	0.0112	0.9162	62.69	0.0045	0.8913

5	27.74	0.0080	0.9388	77.34	0.0237	0.9744
6	23.71	0.0077	0.9549	58.91	0.0161	0.9359
7	31.17	0.0043	0.6172	78.24	0.0276	0.9635
8	25.27	0.0081	0.7269	47.04	0.0232	0.9905
9	22.79	0.0084	0.7460	61.64	0.0166	0.9204
10	44.32	0.0074	0.8053	67.48	0.0269	0.9879
11	29.49	0.0092	0.8010	56.42	0.0157	0.9644
12	22.47	0.0097	0.9309	49.67	0.0100	0.9861
13	25.57	0.0106	0.9566	47.89	0.0058	0.7179
14	104.55	0.0042	0.4381	27.82	0.0068	0.8054
15	127.70	0.0079	0.9426	72.71	0.0182	0.9659
16	27.58	0.0106	0.8273	87.45	0.0199	0.9721
17	25.07	0.0084	0.7337	79.41	0.0235	0.9843
18	40.15	0.0155	0.8260	79.27	0.0169	0.9529
19	77.02	0.0080	0.8898	55.55	0.0236	0.9453
20	61.76	0.0088	0.9435	77.56	0.0184	0.9192
21	35.29	0.0127	0.9363	71.92	0.0097	0.8678
22	33.78	0.0084	0.8760	69.04	0.0180	0.9724
23	24.69	0.0095	0.8644	77.97	0.0198	0.9914
24	67.40	0.0084	0.8761	49.86	0.0092	0.9325
25	54.44	0.0072	0.8344	58.09	0.0108	0.8841
26	41.63	0.0141	0.9381	46.72	0.0169	0.9351
27	108.72	0.0051	0.6854	62.98	0.0149	0.9871
28	33.96	0.0101	0.9507	62.23	0.0195	0.9530
29	37.87	0.0117	0.9028	69.26	0.0192	0.9890
30	72.72	0.0042	0.7251	50.42	0.0166	0.9966
31	26.32	0.0079	0.9841	62.62	0.0160	0.9759
32	37.66	0.0038	0.5049	57.46	0.0208	0.9934
33	31.15	0.0050	0.7906	65.26	0.0210	0.9798
34	47.42	0.0077	0.9480	84.80	0.0210	0.9783
35	25.65	0.0090	0.9318	83.52	0.0214	0.9761
36	41.59	0.0140	0.9779	69.80	0.0206	0.9789
37	43.56	0.0116	0.8916	51.25	0.0173	0.9698
38	64.51	0.0115	0.8610	53.46	0.0148	0.8476
39				62.76	0.0040	0.5353
40				73.57	0.0255	0.9661
41				47.40	0.0157	0.8988
42				61.52	0.0153	0.9504
43				49.56	0.0218	0.8921
44				131.28	0.0371	0.9740
45				62.83	0.0175	0.9413
46				74.06	0.0153	0.9226
47				64.15	0.0213	0.9138
48				60.94	0.0150	0.9833
49				49.69	0.0191	0.9606
50				48.25	0.0263	0.9830
51				72.45	0.0293	0.9773
52				60.16	0.0177	0.9773
Average	44.16	0.0088	0.8420	64.68	0.0183	0.9405

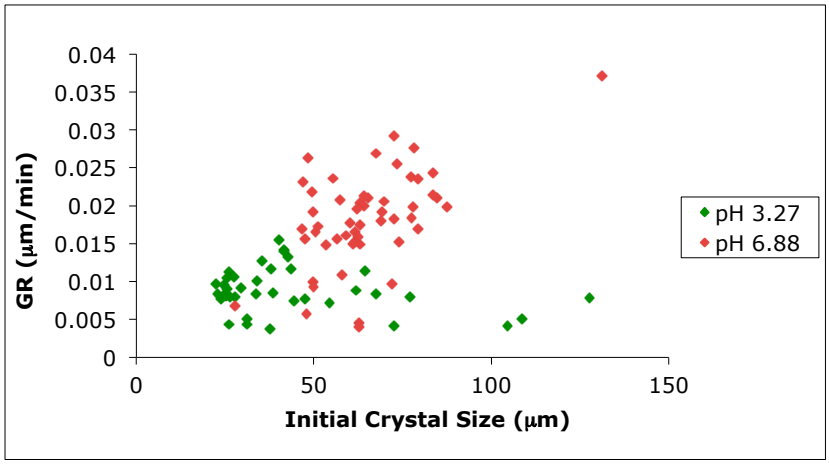

Figure A- 1 Growth Rate Distribution of SUP ss 0.55, 30 ˚C, 0.001 M NaCl

Table A- 13 Growth measurements of SUP ss 0.55, 30 ˚C, 0.001 M KCl

	0.001 M KCl, *pH 3.20*			**0.001 M KCl, *pH 6.63***		
Crystal #	Initial Length (010) (μm)	GR (μm/min)	RSQ	Initial Length (010) (μm)	GR (μm/min)	RSQ
1	44.28	0.0103	0.9399	48.42	0.0386	0.9616
2	29.83	0.0094	0.9202	65.59	0.0264	0.9586
3	42.76	0.0106	0.9778	57.67	0.0293	0.8699
4	28.68	0.0046	0.9563	38.09	0.0080	0.8895
5	26.12	0.0105	0.9642	59.29	0.0099	0.9180
6	34.42	0.0140	0.8983	47.60	0.0099	0.9017
7	26.86	0.0088	0.7658	49.79	0.0141	0.8953
8	32.40	0.0133	0.9738	52.26	0.0151	0.9210
9	24.90	0.0053	0.8265	70.62	0.0093	0.9040
10	44.73	0.0152	0.9713	43.82	0.0210	0.8647
11	25.58	0.0070	0.9759	49.75	0.0120	0.9246
12	24.87	0.0096	0.9625	53.69	0.0118	0.9289
13	38.92	0.0125	0.9671	56.11	0.0191	0.9465
14	52.63	0.0153	0.9700	48.35	0.0049	0.6859
15	42.82	0.0098	0.9634	56.26	0.0076	0.7472
16	36.26	0.0103	0.9528	48.68	0.0116	0.9322
17	35.69	0.0090	0.8932	50.09	0.0120	0.9371
18	25.93	0.0107	0.9431	54.75	0.0148	0.7948
19	30.00	0.0097	0.9844	82.97	0.0251	0.9728
20	31.38	0.0132	0.9827	45.39	0.0132	0.8129
21	28.32	0.0111	0.9337	50.16	0.0100	0.7602
22	31.34	0.0121	0.9815	59.11	0.0175	0.8851
23	33.90	0.0103	0.8254	50.78	0.0216	0.8703
24	33.90	0.0098	0.9228	50.82	0.0116	0.8752
25	38.16	0.0169	0.9413	41.89	0.0086	0.6008
26	27.16	0.0080	0.6909	79.23	0.0191	0.9284
27	27.04	0.0119	0.8824	44.45	0.0198	0.9061
28	31.57	0.0125	0.8759	51.76	0.0081	0.8452
29	40.55	0.0123	0.9689	51.96	0.0091	0.8654
30	29.73	0.0046	0.5476	46.52	0.0085	0.7234
31	47.32	0.0104	0.8835	53.45	0.0068	0.8224
32	58.44	0.0214	0.8934	57.41	0.0155	0.9556
33	30.82	0.0122	0.8769	37.24	0.0173	0.9225
34	30.64	0.0085	0.8971	52.11	0.0170	0.7581

35	39.87	0.0061	0.6429	51.17	0.0076	0.7581
36	29.78	0.0101	0.9819	42.29	0.0082	0.8370
37	32.71	0.0143	0.9633	42.89	0.0488	0.9488
38	40.11	0.0100	0.8562	64.71	0.0430	0.9342
39	46.50	0.0214	0.9927	77.80	0.0165	0.9258
40				36.52	0.0091	0.9357
41				45.11	0.0101	0.9379
42				68.75	0.0394	0.8713
43				60.13	0.0201	0.9488
44				45.68	0.0108	0.8455
45				57.05	0.0148	0.9577
46				46.05	0.0098	0.7463
47				67.70	0.0163	0.9780
48				43.94	0.0120	0.8464
49				59.15	0.0140	0.9158
50				51.87	0.0059	0.7709
Average	34.79	0.0111	0.9063	53.34	0.0158	0.8729

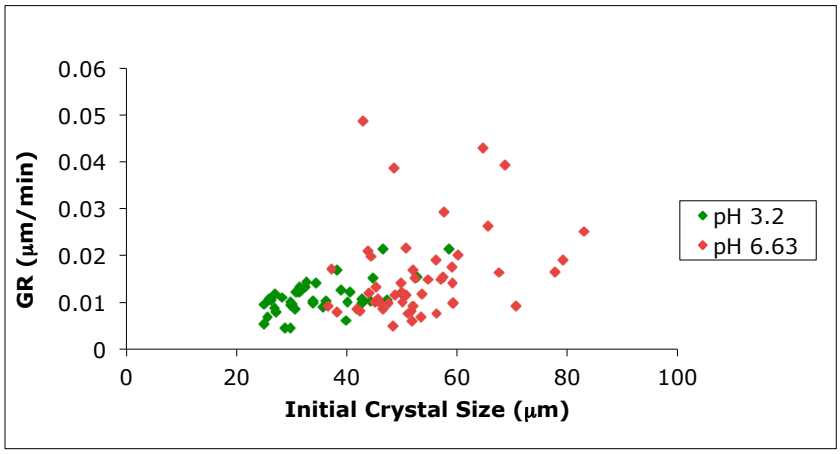

Figure A- 2 Growth Rate Distribution of SUP ss 0.55, 30 ˚C, 0.001 M KCl

Table A- 14 Growth measurements of SUP ss 0.55, 30 ˚C, 0.001 M $CaCl_2$

	0.001 M $CaCl_2$, *pH 3.32*			**0.001 M $CaCl_2$, *pH 6.94***		
Crystal #	Initial Length (010) (μm)	GR (μm/min)	RSQ	Initial Length (010) (μm)	GR (μm/min)	RSQ
1	40.36	0.0115	0.9268	45.59	0.0134	0.9943
2	49.47	0.0154	0.8709	67.40	0.0216	0.9816
3	22.94	0.0086	0.7313	38.62	0.0097	0.9642
4	26.45	0.0105	0.9458	38.62	0.0097	0.9642
5	22.70	0.0083	0.9522	38.62	0.0097	0.9642
6	35.57	0.0110	0.9709	71.88	0.0032	0.4970
7	46.43	0.0125	0.9056	36.27	0.0063	0.7370
8	29.23	0.0085	0.9253	36.90	0.0095	0.6273
9	24.46	0.0125	0.9202	35.80	0.0053	0.7859
10	24.13	0.0163	0.8319	35.64	0.0156	0.9051
11	24.17	0.0117	0.9410	34.16	0.0122	0.9357
12	42.29	0.0139	0.9149	80.35	0.0271	0.9573
13	29.90	0.0133	0.9841	25.51	0.0075	0.8415
14	28.79	0.0059	0.7978	47.70	0.0205	0.9159
15	31.80	0.0141	0.9751	29.78	0.0124	0.9182
16	25.58	0.0100	0.8413	37.23	0.0091	0.9164

17	21.80	0.0089	0.9379	35.80	0.0057	0.7964
18	32.80	0.0086	0.7657	56.15	0.0132	0.9059
19	30.29	0.0107	0.9912	30.99	0.0068	0.7455
20	30.00	0.0095	0.9671	28.34	0.0088	0.8782
21	37.67	0.0097	0.8719	51.97	0.0098	0.8224
22	37.86	0.0091	0.8959	52.67	0.0349	0.9682
23	27.78	0.0113	0.9256	59.80	0.0378	0.9729
24	27.94	0.0100	0.7634	35.29	0.0146	0.9818
25	33.96	0.0132	0.9796	58.37	0.0159	0.9863
26	28.57	0.0069	0.7157	49.92	0.0219	0.9226
27	27.23	0.0058	0.6655	26.99	0.0100	0.9472
28	29.73	0.0095	0.9506	52.42	0.0073	0.8951
29	29.81	0.0090	0.8230	62.51	0.0070	0.9342
30	36.26	0.0106	0.9431	53.79	0.0138	0.9446
31	33.96	0.0103	0.7212	27.78	0.0037	0.7585
32	25.99	0.0059	0.7594	38.77	0.0125	0.9277
33	27.43	0.0105	0.9746	35.31	0.0108	0.9427
34	29.68	0.0104	0.9571	70.87	0.0116	0.9839
35	36.36	0.0058	0.7293	38.39	0.0139	0.8949
36	30.62	0.0118	0.9248	35.80	0.0078	0.8220
37	32.03	0.0109	0.9345	53.61	0.0090	0.8135
38	35.80	0.0088	0.7692	52.18	0.0135	0.9581
39	40.94	0.0132	0.9107	33.87	0.0054	0.6930
40	23.64	0.0081	0.9272	40.96	0.0167	0.9221
41	27.24	0.0112	0.9173	40.69	0.0109	0.8686
42	25.05	0.0063	0.7692	29.90	0.0079	0.8313
43	30.40	0.0117	0.8513	35.13	0.0152	0.9677
44	60.95	0.0095	0.8775	30.49	0.0051	0.8614
45	26.85	0.0066	0.7572	59.57	0.0146	0.9861
46	25.67	0.0084	0.8861	33.76	0.0142	0.8436
47	27.67	0.0084	0.8419	49.16	0.0271	0.9563
48	26.07	0.0088	0.9117	64.74	0.0069	0.8325
49	28.48	0.0066	0.8944			
50	34.79	0.0140	0.9936			
51	30.75	0.0110	0.9569			
52	41.57	0.0120	0.8380			
Average	31.50	0.0101	0.8795	44.29	0.0126	0.8848

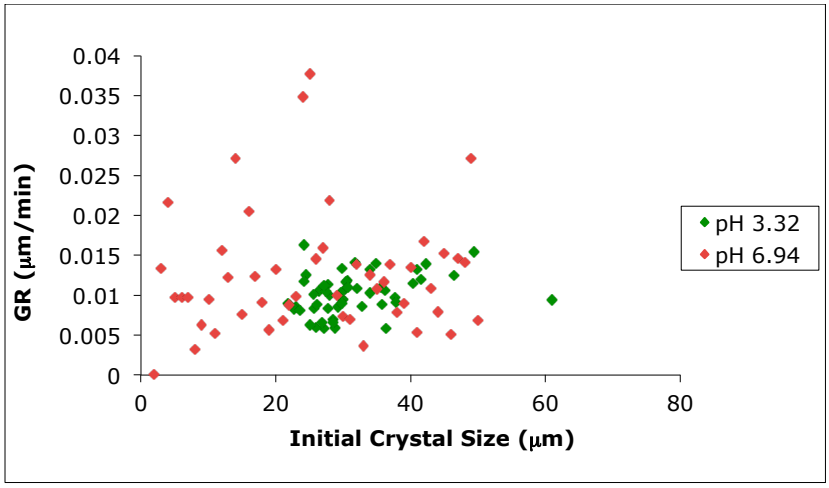

Figure A- 3 Growth Rate Distribution of SUP ss 0.55, 30 ˚C, 0.001 M $CaCl_2$

Table A- 15 Growth measurements of SUP ss 0.55, 30 ˚C, 0.001 M KH_2PO_4

	0.001 M KH_2PO_4, *pH 3.63*			**0.001 M KH_2PO_4, *pH 6.89***		
Crystal #	Initial Length (010) (μm)	GR (μm/min)	RSQ	Initial Length (010) (μm)	GR (μm/min)	RSQ
1	33.27	0.0138	0.9849	L	GR	RSQ
2	32.02	0.0122	0.9118	65.58	0.0179	0.9720
3	16.51	0.0094	0.9326	53.34	0.0187	0.9468
4	31.19	0.0104	0.9737	58.21	0.0182	0.9615
5	20.84	0.0107	0.9185	120.78	0.0261	0.9580
6	25.70	0.0110	0.9664	40.96	0.0168	0.9623
7	35.64	0.0136	0.9901	52.27	0.0181	0.9661
8	24.16	0.0115	0.8654	26.95	0.0113	0.9698
9	28.38	0.0105	0.8487	55.58	0.0116	0.9738
10	23.36	0.0087	0.8917	40.10	0.0174	0.9651
11	23.22	0.0146	0.8625	45.06	0.0148	0.9795
12	23.28	0.0066	0.8040	42.41	0.0160	0.8749
13	23.25	0.0153	0.9829	41.96	0.0114	0.9731
14	37.08	0.0146	0.9838	46.83	0.0147	0.9441
15	27.08	0.0164	0.9769	31.22	0.0117	0.9303
16	21.24	0.0102	0.9853	48.72	0.0147	0.9567
17	26.03	0.0123	0.8823	64.77	0.0118	0.8322
18	18.00	0.0129	0.9724	39.90	0.0093	0.9663
19	32.77	0.0145	0.9394	42.52	0.0110	0.9007
20	28.43	0.0110	0.9533	54.27	0.0111	0.9383
21	24.62	0.0134	0.9703	35.13	0.0099	0.9347
22	19.08	0.0125	0.9773	48.89	0.0123	0.9142
23	28.40	0.0168	0.9096	55.41	0.0187	0.9817
24	21.67	0.0090	0.9678	44.67	0.0175	0.9535
25	32.63	0.0124	0.9752	39.60	0.0116	0.9785
26	32.77	0.0129	0.9321	38.99	0.0120	0.9624
27	37.82	0.0182	0.9763	51.49	0.0203	0.9732
28	26.20	0.0111	0.9794	75.58	0.0256	0.9680
29	31.17	0.0162	0.9654	62.20	0.0148	0.8980
30	29.90	0.0109	0.9782	63.71	0.0381	0.9310
31	26.37	0.0161	0.9706	51.88	0.0132	0.8909
32	24.89	0.0240	0.9229	34.82	0.0179	0.9705
33	22.77	0.0109	0.9722	44.85	0.0172	0.9710
34	31.12	0.0153	0.9633	54.82	0.0156	0.9204
35	34.27	0.0174	0.9655	50.49	0.0173	0.9869
36	32.37	0.0138	0.9310	40.63	0.0190	0.9389
37	30.75	0.0156	0.9238	46.57	0.0170	0.9023
38	33.60	0.0110	0.9503	47.70	0.0141	0.8860
39	33.56	0.0136	0.9811	54.38	0.0234	0.9596
40	35.50	0.0126	0.9201	37.80	0.0169	0.9362
41	27.66	0.0121	0.9826	38.23	0.0131	0.9264
42	30.62	0.0186	0.9903	49.79	0.0159	0.9316
43	29.40	0.0133	0.9617	74.14	0.0213	0.9816
				46.42	0.0141	0.9453
				46.53	0.0123	0.9189
				39.86	0.0174	0.9660
				33.03	0.0175	0.9584
				52.46	0.0151	0.9536
				39.33	0.0225	0.9849
Average	28.11	0.0132	0.9464	49.39	0.0163	0.9458

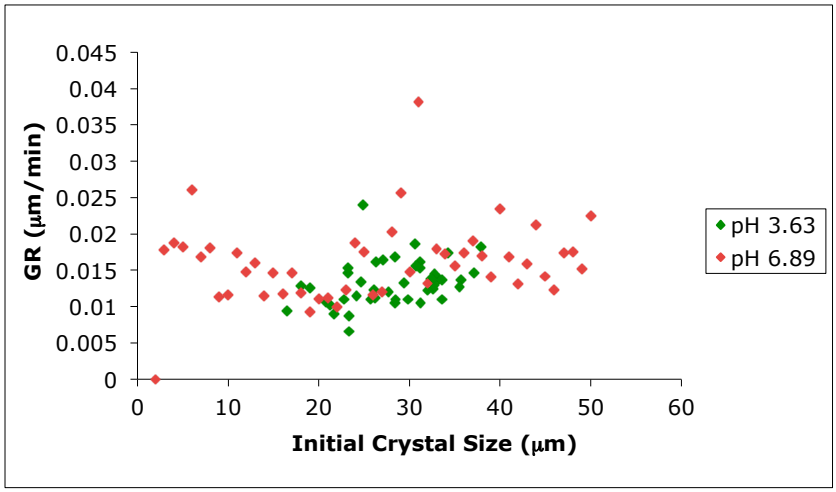

Figure A- 4 Growth Rate Distribution of SUP ss 0.55, 30 ˚C, 0.001 M KH_2PO_4

Table A- 16 Growth measurements of SUP ss 0.55, 30 ˚C, 0.001 M Na_2HPO_4

	0.001 M Na_2HPO_4, *pH 1.76*			**0.001 M Na_2HPO_4, *pH 5.55***			**0.001 M Na_2HPO_4, *pH 6.84***		
Crystal #	Initial Length (010) (μm)	GR (μm/min)	RSQ	Initial Length (010) (μm)	GR (μm/min)	RSQ	Initial Length (010) (μm)	GR (μm/min)	RSQ
1	24.09	0.1186	0.9142	40.86	0.0566	0.9278	106.53	0.0000	0.7999
2	16.28	0.1268	0.8315	43.99	0.0618	0.9682	54.75	0.0849	0.9729
3	15.47	0.1018	0.9495	45.80	0.0646	0.9495	28.10	0.0516	0.8802
4	15.05	0.0894	0.7166	57.18	0.0766	0.9471	38.31	0.0932	0.9605
5	22.42	0.1681	0.9054	45.84	0.0647	0.9645	43.54	0.1041	0.9166
6	19.54	0.1997	0.4256	34.81	0.0459	0.9463	33.09	0.0733	0.9028
7	19.16	0.1963	0.6937	45.31	0.0639	0.9916	35.46	0.0831	0.9774
8	19.84	0.2012	0.8622	46.19	0.0652	0.9277	30.52	0.0621	0.8973
9	19.88	0.2013	0.8512	63.62	0.0777	0.9619	32.43	0.0705	0.8951
10	20.14	0.2014	0.7772	130.61	0.0025	0.9920	37.05	0.0890	0.9290
11	20.61	0.1994	0.7214	44.29	0.0623	0.8486	28.48	0.0532	0.9601
12	18.94	0.1936	0.9364	42.53	0.0594	0.9748	38.23	0.0930	0.8671
13	17.91	0.1736	0.9202	37.67	0.0510	0.9747	29.55	0.0579	0.9626
14	19.26	0.1974	0.7777	45.81	0.0646	0.9775	51.42	0.0960	0.8631
15	17.69	0.1679	0.6576	62.83	0.0778	0.9762	44.86	0.1048	0.9926
16	21.70	0.1845	0.8709	42.20	0.0589	0.9272	55.22	0.0831	0.9695
17	17.52	0.1635	0.8946	41.77	0.0581	0.9184	51.84	0.0948	0.7414
18	25.37	0.0804	0.9774	57.36	0.0767	0.8751	48.17	0.1029	0.9418
19	20.24	0.2013	0.8988	36.75	0.0493	0.9823	42.06	0.1022	0.9522
20	20.03	0.2015	0.9751	80.89	0.0599	0.9705	43.23	0.1038	0.9150
21	20.95	0.1963	0.9274	67.23	0.0762	0.9782	51.25	0.0965	0.9610
22	18.06	0.1770	0.6632	82.44	0.0573	0.9794	45.49	0.1049	0.9438
23	37.23	0.0000	0.8147	122.38	0.0055	0.9936	61.21	0.0575	0.9884
24	22.64	0.1622	0.8370	57.07	0.0766	0.9193	58.17	0.0708	0.9508
25	21.51	0.1881	0.5792	60.44	0.0777	0.9796	47.13	0.1041	0.9937
26	15.38	0.0992	0.9063	47.51	0.0671	0.9751	43.18	0.1037	0.9075
27	20.06	0.2015	0.9129	152.85	0.0002	0.9665	67.23	0.0334	0.9540
28	22.85	0.1562	0.9237	50.25	0.0706	0.9293	47.51	0.1037	0.8511
29	17.55	0.1643	0.7479	36.93	0.0497	0.9213	37.51	0.0906	0.9855
30	15.96	0.1168	0.8408	50.57	0.0710	0.9448	54.67	0.0852	0.9745
31	19.22	0.1970	0.7399	67.56	0.0760	0.9847	39.83	0.0976	0.8740
32	20.32	0.2010	0.9860	56.06	0.0760	0.8947	44.45	0.1047	0.9287
33	23.25	0.1446	0.9860	86.50	0.0501	0.9560	26.43	0.0447	0.9388

34	25.58	0.0747	0.9115	85.47	0.0520	0.8895	35.84	0.0846	0.4242
35	26.94	0.0432	0.9573	92.96	0.0386	0.9778	41.93	0.1020	0.9335
36	24.72	0.0993	0.9569	66.43	0.0767	0.8263	43.86	0.1044	0.9424
37	17.71	0.1684	0.8638	39.64	0.0545	0.9671	31.86	0.0680	0.9943
38	13.93	0.0596	0.9090	49.94	0.0702	0.9525	38.43	0.0936	0.8988
39	21.91	0.1802	0.8524	66.31	0.0767	0.8491	36.31	0.0863	0.7867
40	23.25	0.1446	0.9389	51.72	0.0723	0.9682	41.68	0.1016	0.8572
41	21.67	0.1851	0.7789	35.84	0.0477	0.9113	45.60	0.1049	0.8766
42	18.83	0.1919	0.7768	114.65	0.0103	0.9583	33.19	0.0738	0.9146
43	20.17	0.2014	0.9087	56.87	0.0765	0.9124	53.48	0.0895	0.9901
44	16.78	0.1422	0.7832	74.45	0.0694	0.9847	63.01	0.0498	0.9769
45	15.44	0.1009	0.9056	108.09	0.0165	0.9701	39.87	0.0977	0.7280
46	20.54	0.2000	0.5965	41.43	0.0576	0.9408	44.87	0.1048	0.4859
47	23.80	0.1277	0.8296	73.58	0.0705	0.7731	84.03	0.0029	0.9011
48	17.52	0.1636	0.9433	50.30	0.0707	0.8029			
49	16.64	0.1381	0.7398	49.66	0.0699	0.9797			
50	15.81	0.1122	0.9376	50.81	0.0713	0.9142			
51	15.42	0.1003	0.7183						
Average	20.05	0.1530	0.8378	61.84	0.0591	0.9400	45.34	0.0822	0.8991

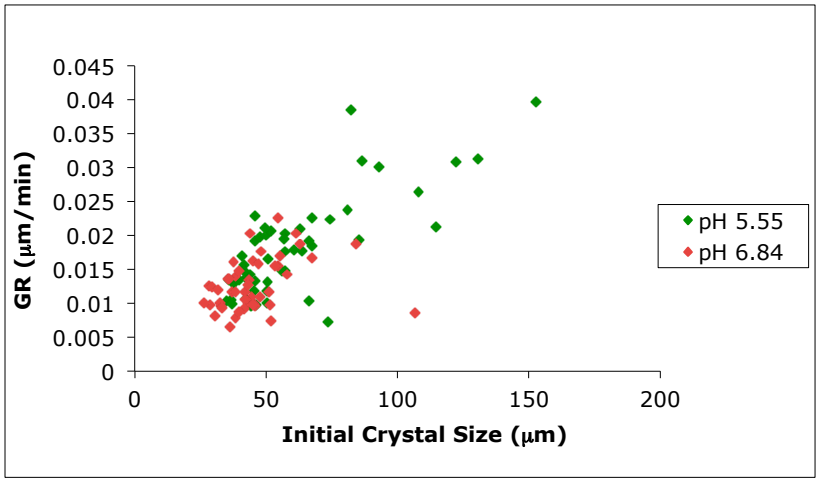

Figure A- 5 Growth Rate Distribution of SUP ss 0.55, 30 ˚C, 0.001 M Na_2HPO4

Table A- 17 Growth measurements of IEL ss 0.55, 30 ˚C, 0.001 M Na_2HPO_4

	0.001 M Na_2HPO_4, *pH 1.79*			**0.001 M Na_2HPO_4, *pH 2.66***			**0.001 M Na_2HPO_4, *pH 7.69***		
Crystal #	Initial Length (010) (µm)	GR (µm/min)	RSQ	Initial Length (010) (µm)	GR (µm/min)	RSQ	Initial Length (010) (µm)	GR (µm/min)	RSQ
1	131.66	0.0105	0.8476	36.67	0.0056	0.8800	73.16	0.0866	0.9995
2	50.14	0.0078	0.8656	57.02	0.0069	0.9279	41.41	0.0056	0.8905
3	19.84	0.0060	0.9738	24.49	0.0044	0.8599	52.81	0.0846	0.9951
4	26.02	0.0097	0.9979	30.52	0.0036	0.9452	46.06	0.0099	0.8411
5	102.25	0.0172	0.8329	97.09	0.0041	0.9627	66.61	0.0879	0.9981
6	133.61	0.0112	0.9781	23.36	0.0031	0.8275	38.04	0.0718	0.8910
7	104.59	0.0094	0.9307	48.47	0.0041	0.8383	51.65	0.0136	0.8404
8	33.68	0.0046	0.8073	26.13	0.0050	0.8882	55.25	0.0087	0.9293
9	57.10	0.0113	0.8912	38.17	0.0066	0.8575	15.90	0.0031	0.9087
10	58.41	0.0054	0.8661	66.64	0.0069	0.8052	29.73	0.0041	0.8040
11	22.95	0.0121	0.8839	46.37	0.0068	0.9375	54.14	0.0225	0.9827
12	26.13	0.0050	0.8524	110.03	0.0067	0.9464	285.47	0.1098	0.9910

13	15.71	0.0071	0.8952	144.15	0.0126	0.9568	62.42	0.0073	0.9231
14	29.54	0.0065	0.9156	42.66	0.0036	0.8857	73.49	0.0061	0.9512
15	58.98	0.0110	0.9504	26.37	0.0046	0.9659	20.81	0.0067	0.8859
16	20.23	0.0078	0.9752	181.39	0.0269	0.9840	28.14	0.0131	0.8731
17	78.92	0.0050	0.9031	20.80	0.0038	0.9163	36.59	0.0796	0.9956
18	76.38	0.0074	0.9515	17.57	0.0042	0.8127	273.59	0.1150	0.9139
19	108.71	0.0471	0.9533	22.16	0.0026	0.8795	28.89	0.0051	0.9888
20	96.76	0.0041	0.9328	50.37	0.0028	0.8239	28.77	0.0049	0.9520
21	32.66	0.0053	0.9593	110.06	0.0064	0.8550	27.73	0.0131	0.9891
22	30.54	0.0146	0.9129	22.83	0.0051	0.8874	68.29	0.0910	0.9984
23	27.44	0.0039	0.9022	33.39	0.0029	0.9293	42.99	0.0038	0.9626
24	31.64	0.0031	0.8554	52.51	0.0080	5.4604	29.22	0.0890	0.9851
25	52.61	0.0127	0.9413	106.39	0.0081	5.3960	116.80	0.1063	0.9993
26	57.09	0.0098	0.9378	39.32	0.0046	5.5715	177.87	0.0631	0.9889
27	34.11	0.0100	0.8686	42.44	0.0080	5.4527	245.91	0.0770	0.9856
28	70.50	0.0075	0.9211	48.08	0.0051	5.7444	34.84	0.0073	0.9441
29	100.81	0.0164	0.9663	64.15	0.0053	5.7953	37.97	0.0079	0.9590
30	44.11	0.0171	0.9503	39.36	0.0076	5.6096	32.63	0.0788	0.9971
31	21.26	0.0086	0.8374	36.95	0.0045	5.5102	28.23	0.0035	0.9434
32	33.49	0.0290	0.8485	40.08	0.0039	5.2268			
33	22.85	0.0056	0.9151	45.11	0.0058	5.8843			
34	47.97	0.0056	0.9592	34.85	0.0191	0.1089			
35				32.43	0.0047	5.6023			
36				45.94	0.0024	4.2325			
37				30.30	0.0045	5.5133			
38				43.01	0.0033	4.8790			
Average	54.67	0.0104	0.9112	52.04	0.0062	2.5410	71.14	0.0415	0.9454

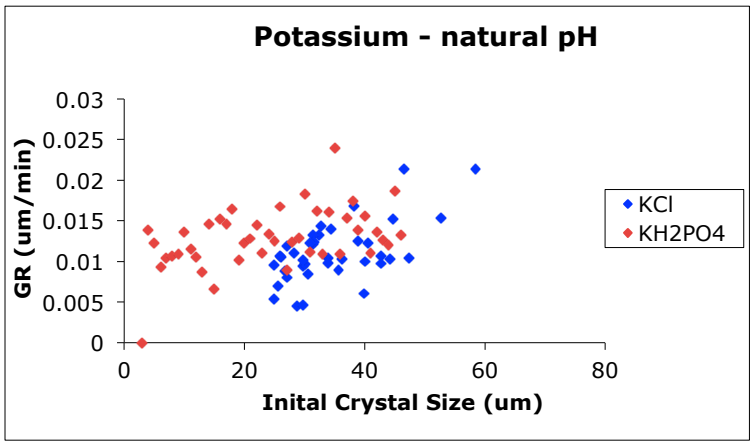

Figure A- 6 Growth rate observations of SUP ss 0.55, 30 ˚C, 0.001 M KCl and KH_2PO_4 at the natural pH

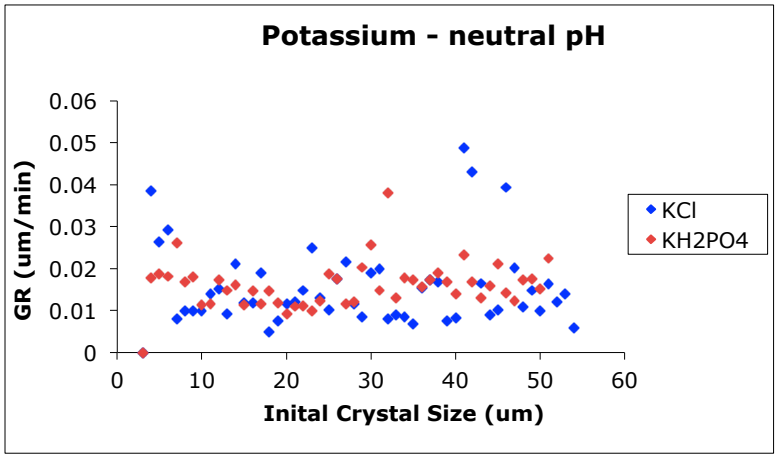

Figure A- 7 Growth rate observations of SUP ss 0.55, 30 ˚C, 0.001 M KCl and KH_2PO_4 at the neutral pH

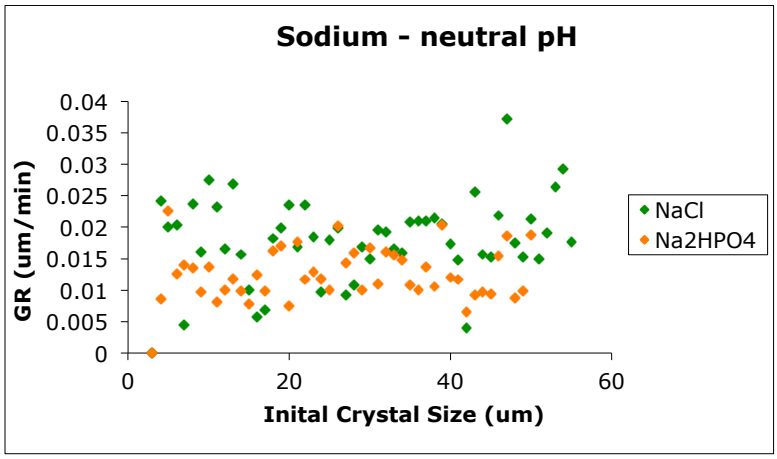

Figure A- 8 Growth rate observations of SUP ss 0.55, 30 ˚C, 0.001 M NaCl and Na_2HPO_4 at the neutral pH

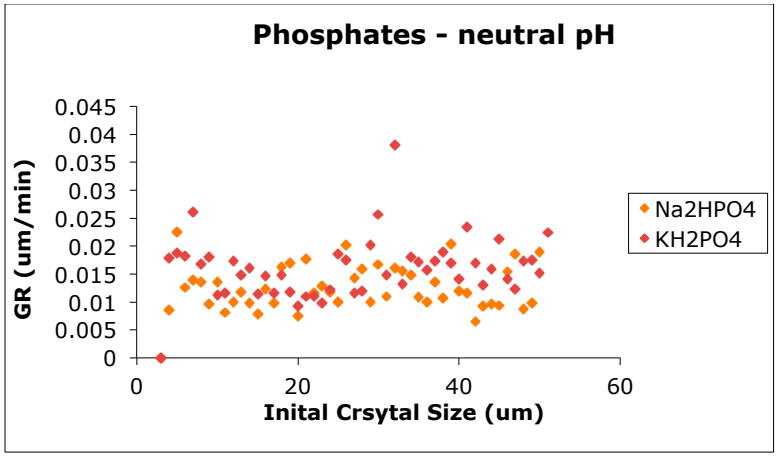

Figure A- 9 Growth rate observations of SUP ss 0.55, 30 ˚C, 0.001 M KH_2PO_4 and Na_2HPO_4 at the neutral pH

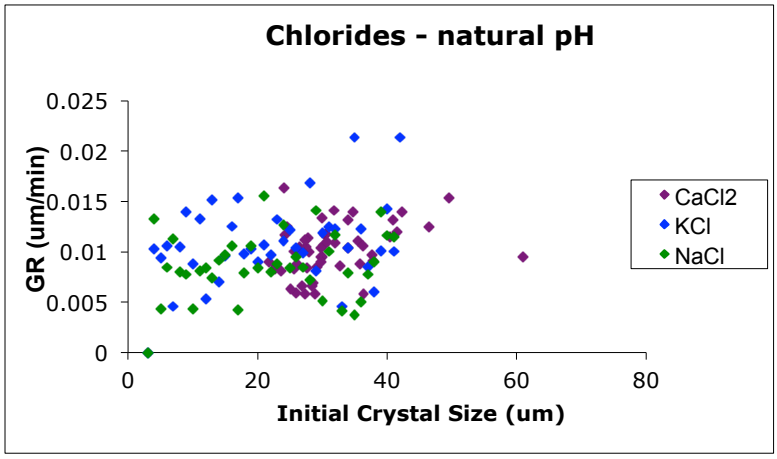

Figure A- 10 Growth rate observations of SUP ss 0.55, 30 ˚C, 0.001 M $CaCl_2$, KCl and NaCl at the natural pH

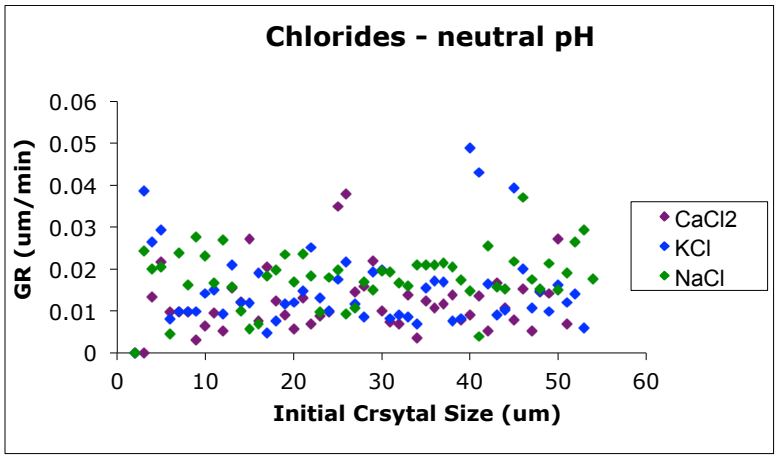

Figure A- 11 Growth rate observations of SUP ss 0.55, 30 ˚C, 0.001 M $CaCl_2$, KCl and NaCl at the neutral pH

Table A- 18 Solubility Determination of SUP at 30 ˚C

De-supersaturation					
Time (min)	% lactose	g.lactose/ 100 g solution	100 g solution	100 g water	g.lactose.1H2O/ 100 g H20
0	38.00	34.80	65.20	53.37	57.81
1450	26.07	23.87	76.13	31.36	33.56
2920	25.27	23.14	76.86	30.10	32.20
4290	23.87	21.86	78.14	27.97	29.89
5415	23.30	21.34	78.66	27.13	28.97
8390	22.33	20.45	79.55	25.70	27.42
9830	21.78	19.95	80.05	24.92	26.57
11285	21.64	19.82	80.18	24.71	26.36
12640	22.56	20.66	79.34	26.04	27.79
Equilibrium	22.08	20.22	79.78	25.34	27.03
Saturation					
0	0	0	100	0	0
1530	21.41	19.61	80.39	24.39	26.01
2850	21.51	19.70	80.30	24.53	26.16
4160	21.14	19.36	80.64	24.01	25.60
7525	21.01	19.24	80.76	23.83	25.40
8735	20.65	18.91	81.09	23.32	24.85
10030	20.40	18.68	81.32	22.97	24.48
11340	20.89	19.13	80.87	23.65	25.21
13010	19.85	18.18	81.82	22.22	23.67

Table A- 19 Solubility Determination of SUP dosed with 0.001 M Na_2HPO_4 at 30 ˚C

De-supersaturation					
Time (min)	% lactose	g.lactose/ 100 g solution	100 g solution	100 g water	g.lactose.1H2O/ 100 g H20
0	38.00	34.80	65.20	53.37	57.81
1460	22.94	21.00	79.00	26.59	28.38
2930	21.69	19.86	80.14	24.79	26.44
4300	20.43	18.70	81.30	23.01	24.52
5420	21.23	19.44	80.56	24.13	25.72
8400	21.07	19.29	80.71	23.90	25.48
9835	21.21	19.42	80.58	24.10	25.69
11290	20.66	18.92	81.08	23.34	24.87
12645	21.08	19.31	80.69	23.93	25.51
Equilibrium	21.00	19.23	80.77	23.82	25.39
Saturation					
0	0	0	100	0	0
1530	22.08	20.22	79.78	25.34	27.04
4160	20.22	18.51	81.49	22.72	24.20
7525	20.21	18.51	81.49	22.71	24.19
8735	20.58	18.85	81.15	23.23	24.75
10030	20.88	19.12	80.88	23.64	25.19
11340	21.54	19.73	80.27	24.58	26.21
13010	20.36	18.64	81.36	22.92	24.42